E-ISSN 2228-8082
Volume 78, Number 5, May 2026

PMAC
PRINCE MAHIDOL AWARD CONFERENCE 2026

SMJ

Siriraj Medical Journal

The world-leading biomedical science of Thailand

MONTHLY

ORIGINAL ARTICLE REVIEW ARTICLE

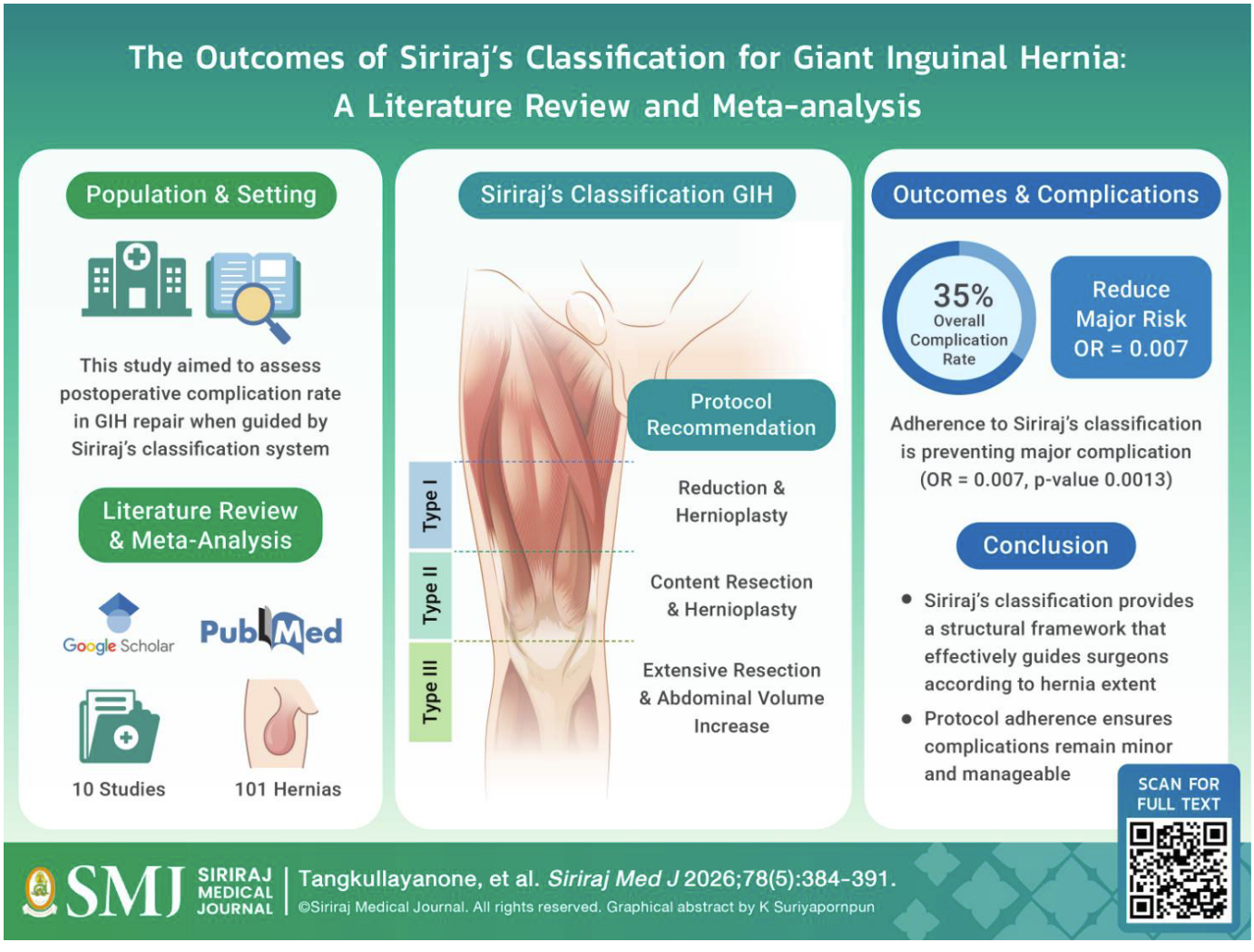

Indexed by
Scopus
DOAJ
EBSCO
MESDA
https://he02.tci-thaijo.org/index.php/sirirajmedj/index
E-mail: sijournal92@gmail.com

SMJ
Siriraj Medical Journal
The world-leading biomedical science of Thailand
Volume 78 Number 5
May 2026

ORIGINAL ARTICLE

332 Clinical Outcomes and Predictive Factors in Acute Tandem Occlusion: A Single Center Experience
Ritthikrai Wichianrat, Boonrerk Sangpetngam, Thaweesak Aurboonyawat, Ekawut Chankaew, Anchalee Churojana, Pattarawit Withayasuk

350 Intraoperative Cerebral Angiography in the Surgical Resection of Brain Arteriovenous Malformations
Kan Tapunya, Thaweesak Aurboonyawat

359 Long-Term Refractive Outcomes Following Pediatric Cataract Surgery with Primary IOL Implantation
Arnan Limmahachai, Thammanoon Surachatkumtonekul

367 Digital Reference Frame Anchored to the Pedicle Screw–rod Construct for O-arm–Assisted Pedicle Screw Insertion: A Pilot Study
Korawish Mekariya, Chonlatid Ruangsangthong, Dollaporn Anopas, Chatupon Chotigavanichaya, Ekkapoj Korwutthikulrangsri, Sirichai Wilartratsami, Werasak Sutipornpalangkul, Panya Luksanapruksa, Monchai Ruangchainikom

377 Is Erythema Toxicum Neonatorum in Neonates Associated with Atopic Diseases?
Suthida Chaithirayanon, Napat Chaimongkol, Nyda Yotsaranphorn Songkiatkul, Siripa Satianvatidkul, Suphatsorn Charoenkitmongkol Arpanun Nitayamekin, Arucha Treesirichod, Vorasith Siripornpanich

384 The Outcomes of Siriraj's Classification for Giant Inguinal Hernia: A Literature Review and Metaanalysis
Watsaphon Tangkullayanone, Chawisa Nampoolsuksan, Thikamporn Tawantanakorn, Tharathorn Suwatthanarak, Nicha Sriworanan, Voraboot Taweerutchana, Thammawat Parakonthun, Chinarong Phalanusitthepha, Jirawat Swangsri, Thawatchai Akaraviputh, Asada Methasate, Vitoon Chinswangwattanakul, Atthaphorn Trakarnsanga

REVIEW ARTICLE

392 Bispecific Protein Engager-Armed T Cells (BATs): Next-Generation Platforms for Precision Cancer Immunotherapy
Pa-thai Yenchitsomanus

SIRIRAJ MEDICAL JOURNAL

https://he02.tci-thaijo.org/index.php/sirirajmedj/index

Executive Editor:
Professor Apichat Asavamongkolkul, Mahidol University, Thailand

Editorial Director:
Professor Aasis Unnanuntana, Mahidol University, Thailand

Associate Editors
Assistant Professor Adisorn Ratanayotha, Mahidol University, Thailand
Pieter Dijkstra, University of Groningen, Netherlands
Professor Phunchai Charatcharoenwitthaya, Mahidol University, Thailand
Professor Varut Lohsiriwat, Mahidol University, Thailand

Editor-in-Chief:
Professor Thawatchai Akaraviputh,
Mahidol University, Thailand

International Editorial Board Members

Allen Finley, Delhousie University, Canada
Christopher Khor, Singapore General Hospital, Singapore
Ciro Isidoro, University of Novara, Italy
David S. Sheps, University of Florida, USA
David Wayne Ussery, University of Arkansas for Medical Sciences, USA
Dennis J. Janisse, Medical College of Wisconsin, USA
Dong-Wan Seo, University of Ulsan College of Medicine, Republic of Korea
Folker Meyer, Argonne National Laboratory, USA
Frans Laurens Moll, University Medical Center Ultrecht, Netherlands
George S. Baillie, University of Glasgow, United Kingdom
Gustavo Saposnik, Unity Health Toronto, St. Micheal Hospital, Canada
Harland Winter, Harvard Medical School, USA
Hidemi Goto, Nagoya University Graduate School of Medicine, Japan
Ichizo Nishino, National Institute of Neuroscience NCNP, Japan
Intawat Nookaew, University of Arkansas for Medical Sciences, USA
James P. Doland, Oregon Health & Science University, USA
John Hunter, Oregon Health & Science University, USA
Karl Thomas Moritz, Swedish University of Agricultural Sciences, Sweden
Kazuo Hara, Aichi Cancer Center Hospital, Japan
Keiichi Akita, Institute of Science Toko, Japan
Kyoichi Takaori, Kyoto University Hospital, Japan
Marcela Hermoso Ramello, University of Chile, Chile
Marianne Hokland, University of Aarhus, Denmark
Matthew S. Dunne, Institute of Food, Nutrition, and Health, Switzerland
Mazakayu Yamamoto, Tokyo Women's Medical University, Japan
Mitsuhiro Kida, Kitasato University & Hospital, Japan
Moses Rodriguez, Mayo Clinic, USA
Nam H. CHO, Ajou University School of Medicine and Hospital, Republic of Korea
Nima Rezaei, Tehran University of Medical Sciences, Iran
Noritaka Isogai, Kinki University, Japan
Philip A. Brunell, State University of New York At Buffalo, USA
Philip Board, Australian National University, Australia
Ramanuj Dasgupta, Genome Institution of Singapore
Richard J. Deckelbaum, Columbia University, USA
Robert W. Mann, University of Hawaii, USA
Robin CN Williamson, Royal Postgraduate Medical School, United Kingdom
Sara Schwanke Khilji, Oregon Health & Science University, USA
Seigo Kitano, Oita University, Japan
Seiji Okada, Kumamoto University
Shomei Ryozawa, Saitama Medical University, Japan
Shuji Shimizu, Kyushu University Hospital, Japan
Stanlay James Rogers, University of California, San Francisco, USA
Stephen Dalton, Chinese University of HK & Kyoto University
Tai-Soon Yong, Yonsei University, Republic of Korea
Tomohisa Uchida, Oita University, Japan
Victor Manuel Charoenrook de la Fuente, Centro de Oftalmologia Barraquer, Spain
Wikrom Karnsakul, Johns Hopkins Children's Center, USA
Yasushi Sano, Director of Gastrointestinal Center, Japan
Yik Ying Teo, National University of Singapore, Singapore
Yoshiki Hirooka, Nagoya University Hospital, Japan
Yozo Miyake, Aichi Medical University, Japan
Yuji Murata, Aizenbashi Hospital, Japan

Editorial Board Members

Vitoon Chinswangwatanakul, Mahidol University, Thailand
Jarupim Soongswang, Mahidol University, Thailand
Jaturat Kanpittaya, Khon Kaen University, Thailand
Nopphol Pausawasdi, Mahidol University, Thailand
Nopporn Sittisombut, Chiang Mai University, Thailand
Pa-thai Yenchitsomanus, Mahidol University, Thailand
Pornprom Muangman, Mahidol University, Thailand
Prasit Wattanapa, Mahidol University, Thailand
Prasert Auewarakul, Mahidol University, Thailand
Somboon Kunathikom, Mahidol University, Thailand
Supakorn Rojananin, Mahidol University, Thailand
Suttipong Wacharasindhu, Chulalongkorn University, Thailand
Vasant Sumethkul, Mahidol University, Thailand
Watchara Kasinrerk, Chiang Mai University, Thailand
Wiroon Laupattrakasem, Khon Kaen University, Thailand
Yuen Tanniradorn, Chulalongkorn University, Thailand

Editorial Assistant: Nuchpraweepawn Saleeon, Mahidol University, Thailand
Proofreader: Amornrat Sangkaew, Mahidol University, Thailand, Nuchpraweepawn Saleeon, Mahidol University, Thailand

Office: His Majesty the King's 80th Birthday Anniversary 5th December 2007 Building (SIMR), 2nd Fl., Room No.207
Faculty of Medicine Siriraj Hospital, Mahidol University, Bangkok 10700, Thailand
E-mail: sijournal92@gmail.com

Clinical Outcomes and Predictive Factors in Acute Tandem Occlusion: A Single-Center Experience

Ritthikrai Wichianrat, M.D.[2], Boonrerk Sangpetngam, M.D.[1,2], Thaweesak Aurboonyawat, M.D.[1,3], Ekawut Chankaew, M.D.[1,3], Anchalee Churojana, M.D.[1,2], Pattarawit Withayasuk, M.D.[1,2,*]

[1]Siriraj Center of Interventional Radiology, Siriraj Hospital, Mahidol University, Bangkok, Thailand, [2]Division of Diagnostic Radiology, Department of Radiology, Faculty of Medicine Siriraj Hospital, Mahidol University, Bangkok 10700, Thailand, [3]Division of Neurosurgery, Department of Surgery, Faculty of Medicine Siriraj Hospital, Mahidol University, Bangkok 10700, Thailand.

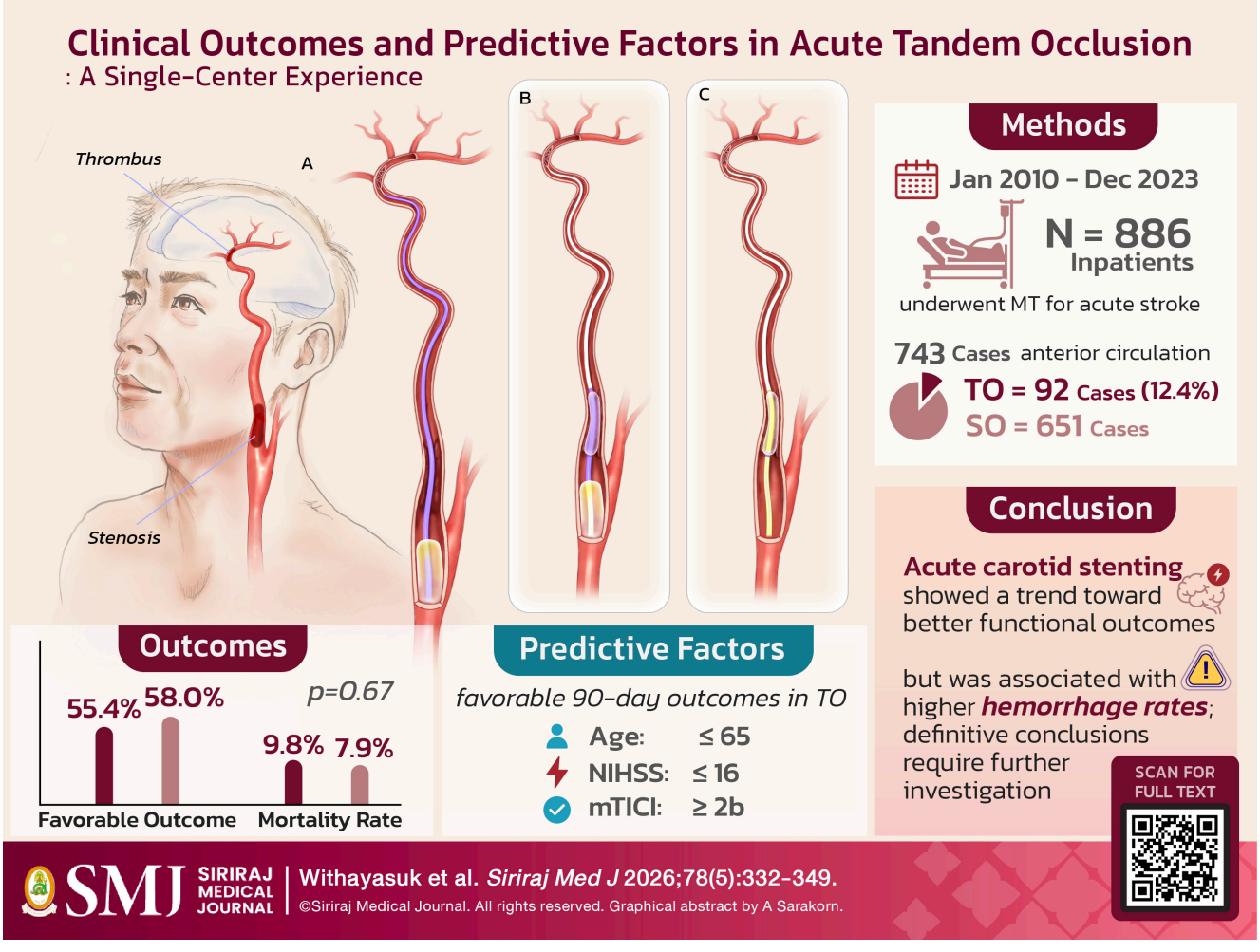

*Corresponding author: Pattarawit Withayasuk
E-mail: Pattarawit.wit@mahidol.ac.th
Received 28 October 2025 Revised 25 February 2026 Accepted 7 March 2026
ORCID ID: http://orcid.org/0000-0001-8662-1315
https://doi.org/10.33192/smj.v78i5.278546

All material is licensed under terms of the Creative Commons Attribution 4.0 International (CC-BY-NC-ND 4.0) license unless otherwise stated.

ABSTRACT

Objective: To evaluate treatment outcomes and analyze predictive factors associated with favorable outcomes in patients with acute tandem occlusion (TO) stroke who underwent mechanical thrombectomy (MT) at a single, high-volume center.

Materials and Methods: This retrospective study analyzed patients with anterior circulation stroke who underwent MT between January 2010 and December 2023. Ninety-two patients with TO, defined as severe stenosis (>70%) or occlusion of the cervical internal carotid artery (c-ICA) with concurrent intracranial occlusion, were identified. The primary endpoint was a favorable functional outcome (modified Rankin Scale [mRS] 0–2) at 90 days. Multivariate logistic regression was performed to identify independent predictors.

Results: Of 743 anterior circulation patients (651 single occlusion [SO], 92 TO [12.4%]), favorable outcomes were achieved in 55.4% of TO patients with a mortality rate of 9.8%, not significantly different from SO (58.0% favorable, 7.9% mortality; p=0.67) in unadjusted comparison. Multivariate analysis identified three independent predictors of favorable outcomes: age ≤65 years (OR 5.2, 95% CI 1.6–16.5, p=0.005), initial NIHSS ≤16 (OR 3.9, 95% CI 1.2–12.5, p=0.022), and successful recanalization (mTICI ≥2b) (OR 6.5, 95% CI 1.1–39.9, p=0.043).

Conclusion: MT for acute TO yields outcomes comparable to SO in unadjusted analysis. Age ≤65 years, lower initial NIHSS, and successful recanalization are key predictors of favorable outcomes. Acute carotid stenting showed a trend toward better functional outcomes but was associated with higher hemorrhage rates; definitive conclusions require further investigation.

Keywords: Tandem occlusion; mechanical thrombectomy; acute ischemic stroke; carotid stenting; clinical outcome; predictive factors (Siriraj Med J 2026;78(5):332-349)

INTRODUCTION

Approximately 10–20%[1–3] of individuals with large vessel occlusion (LVO) undergoing endovascular mechanical thrombectomy (MT) for anterior circulation acute ischemic stroke (AIS) present with tandem occlusion (TO). TO is defined as the simultaneous presence of severe stenosis (>70% based on NASCET criteria) or complete occlusion of the extracranial carotid artery, together with an ipsilateral intracranial vascular territory occlusion.[2]

TO is more prevalent in males than females (approximately 60% versus 40%)[4] and is associated with less favorable functional outcomes compared to single occlusion (SO). Management remains challenging due to limited inclusion of TO cases in randomized controlled MT trials[5] and the absence of definitive, guideline-based recommendations, particularly regarding acute stenting for severe stenosis or occlusion of c-ICA.[6–8] Recanalization strategies vary considerably, influenced by clinical considerations, anatomical factors, and physician preference.[9] Despite undergoing endovascular MT, individuals with tandem occlusion still experience high rates of disability and death.[8]

This study aims to examine the demographics, treatment strategies, and outcomes of TO patients undergoing mechanical thrombectomy at Siriraj Hospital. It further aims to analyze factors associated with favorable results and evaluate the safety, efficacy, and technical strategies employed during the intervention. While the primary clinical findings are consistent with those of major registries such as TITAN, ETIS, and ESCAPE-NA1, this study offers several distinct contributions: (1) a detailed procedural complication profile—including iatrogenic carotid-cavernous fistula and retinal artery occlusion—that has been underreported in prior registries; (2) clot pathology data showing a high prevalence of RBC-rich thrombi; and (3) geographic and practice-pattern diversity as one of the few reports from a high-volume center in Southeast Asia.[6–8,19,20] The ultimate goal is to provide evidence-based insights into the management of tandem occlusion cases to guide optimal management and improve overall patient outcomes.

MATERIALS AND METHODS

This retrospective study utilized data from the Siriraj Center of Interventional Radiology stroke registry, which includes patients who underwent MT at Siriraj Hospital. Data collected included demographic details, premorbid factors, and clinical parameters such as the NIHSS score at admission and discharge. Additionally, the study includes information on pre-interventional radiological studies, procedural variables, complications arising during the intervention, and functional outcomes assessed at 90-day follow-up.

Patients diagnosed with TO who underwent mechanical thrombectomy between January 2010 and December 2023 were included. Out of a total of 866 stroke patients, 92 were identified as having tandem occlusion and subsequently underwent MT. Tandem occlusion was defined as the simultaneous anterior circulation occlusion and ipsilateral severe stenosis (>70% stenosis) or occlusion of the c-ICA. Thorough data regarding baseline characteristics, comorbidities, safety outcomes, and clinical outcomes were collected. The investigation also assessed factors influencing safety and functional outcomes. Ethical approval was duly obtained from the regional ethics committee, and informed consent was secured from patients or their legal representatives.

It is important to acknowledge that the 14-year inclusion period (2010–2023) spans substantial changes in thrombectomy devices, imaging selection criteria, anesthesia practice, and post-procedural management protocols. During the earlier part of the study period, first-generation mechanical thrombectomy devices were predominantly used, whereas later years saw the adoption of newer-generation stent retrievers and large-bore aspiration catheters. Similarly, patient selection evolved with the increasing use of advanced imaging (e.g., CT perfusion) in later years.[19] These temporal changes may introduce confounding that should be considered when interpreting the results.

The Siriraj Protocol for Tandem Occlusion

The choice between antegrade and retrograde approaches was determined by the interventionalist based on the following criteria (Fig 1). The antegrade approach—in which the cervical ICA lesion was treated first before navigating to the intracranial occlusion—was preferred when the cervical ICA stenosis was deemed passable with standard devices (e.g., balloon angioplasty and/or carotid stenting) and when pre-procedural imaging suggested that the cervical lesion could be crossed safely without significant risk of dissection or perforation. The retrograde approach—in which the intracranial occlusion was addressed first by navigating through or bypassing the cervical ICA lesion—was chosen when the cervical ICA was completely occluded or when the operator judged that attempting cervical treatment first would unacceptably delay intracranial reperfusion. In cases where the cervical ICA could not be crossed, alternative access routes (e.g., contralateral ICA via anterior communicating artery) were considered. The primary objective in all cases was to achieve prompt reperfusion of the intracranial occlusion.

The recanalization procedure was carried out under either general anesthesia (GA) or local anesthesia (LA). Overall, GA was used in 91.3% of cases. During the earlier study period (2010–2015), both GA and LA were employed at the clinician's discretion, with LA selected in cases where rapid neurological assessment was prioritized or when anesthesia-related delays were a concern. From 2015 onward, the institutional protocol was standardized to GA for all mechanical thrombectomy procedures to optimize patient immobility and airway control during complex neurointerventional procedures. This transition accounts for the high overall proportion of GA in the cohort. Cerebral angiography and MT were conducted via femoral access. MT for intracranial lesions involved manual aspiration alone, the use of a stent retriever, or a combination of both techniques. Cervical ICA lesions were treated with percutaneous transluminal angioplasty and/or stenting.

For patients undergoing placement of a permanent stent (carotid stenting), Flat-paneled CT was performed beforehand to ensure the absence of intracranial hemorrhage. Regarding the timing of dual antiplatelet therapy (DAPT) relative to stenting: patients were administered either Eptifibatide (a glycoprotein IIb/IIIa inhibitor) intravenously during the procedure immediately prior to stent deployment, or an oral dual antiplatelet regimen (aspirin with clopidogrel or ticagrelor) via nasogastric tube intraoperatively. Stents used included Acculink® (Abbott, USA) and Wallstent® (Boston Scientific, USA). Post-stenting, systolic blood pressure was maintained between 100–140 mmHg for 72 hours, depending on final recanalization status and core infarction size. A follow-up brain CT was performed at 24 hours post-procedure. Once this follow-up imaging confirmed the absence of hemorrhagic complications, patients who had received only the glycoprotein IIb/IIIa inhibitor intraoperatively were transitioned to oral DAPT, which included aspirin (81 mg/day) along with either Clopidogrel (150 mg/day) or Ticagrelor (180 mg/day).

Stroke severity was assessed using the National Institutes of Health Stroke Scale (NIHSS) at both the preprocedural and post-procedural stages. The level of dependence or disability was assessed using the modified Rankin Scale (mRS) 90 days following mechanical thrombectomy.

Early signs of infarction were assessed using the Alberta Stroke Program Early CT Score (ASPECTS). The occlusion site was determined by computed tomography angiography (CTA) or magnetic resonance angiography (MRA). Collateral circulation was evaluated using multiphase CTA, and recanalization success post-MT was evaluated based on the modified Thrombolysis in Cerebral Infarction (mTICI) scale on the final digital subtraction angiography (DSA), with successful reperfusion defined as a mTICI score of 2b, 2c, or 3.

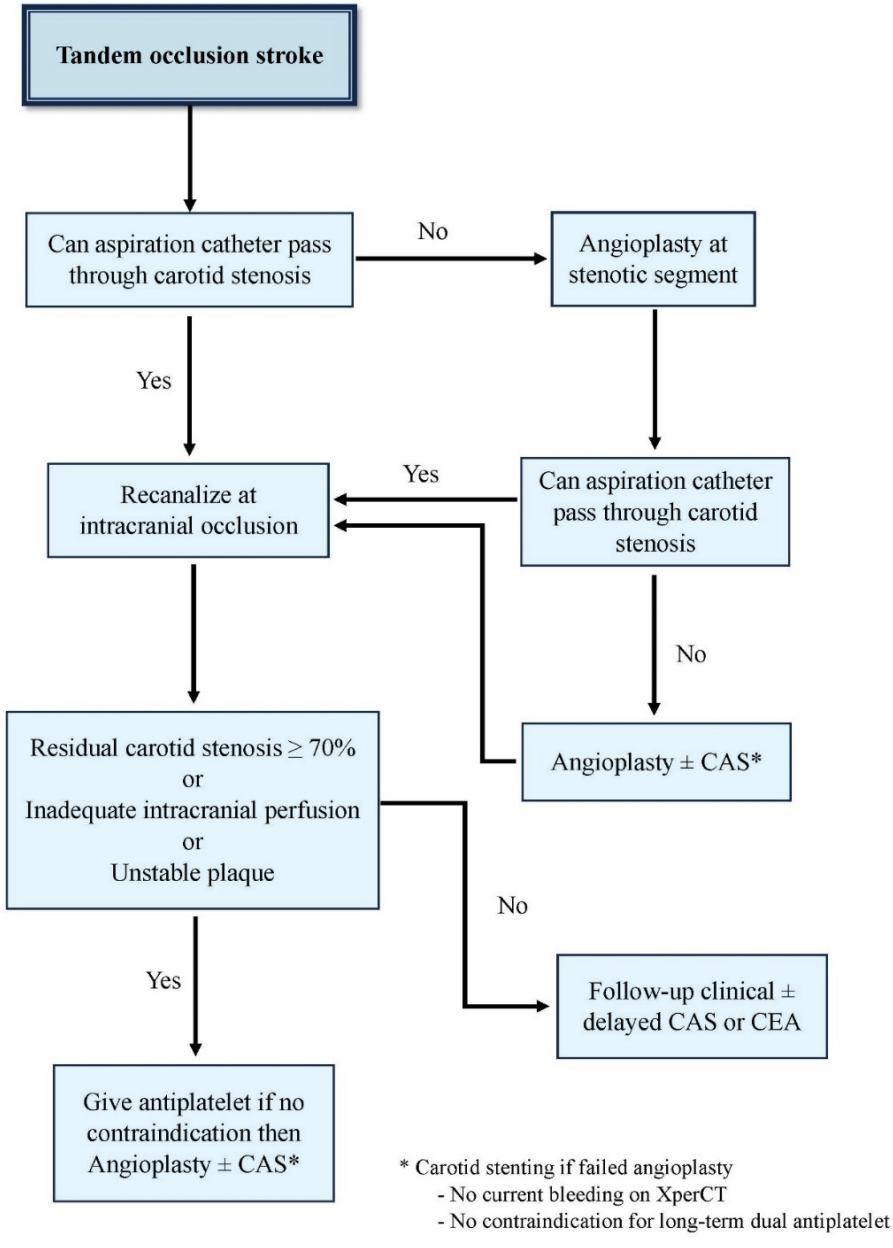

Fig 1. Siriraj treatment protocol for acute tandem occlusion stroke.
Abbreviations: CAS = Carotid artery stenting, CEA = Carotid endarterectomy

Intracranial hemorrhage was classified according to the Heidelberg Bleeding Classification (HBC). Symptomatic intracranial hemorrhage (sICH) was defined as a ≥4-point worsening in NIHSS attributable to hemorrhage.[10]

Statistical analyses

Statistical analyses were performed using SPSS version 26.0. Continuous variables were summarized as mean and standard deviation (SD), and categorical variables as frequency (percentage). Bivariate analyses were conducted using the χ^2 or Fisher's exact test, as appropriate. Binary logistic regression was utilized with favorable functional outcomes as the dependent variable. Variables with a p-value <0.05 in bivariate analyses were entered into a multivariate logistic regression model.

Limitations of statistical comparisons: Given the retrospective, observational design and the relatively small sample size (n=92 for TO), the comparisons between tandem and single occlusion, acute stenting versus no stenting/delayed treatment, and antegrade versus retrograde approaches are descriptive and unadjusted. No propensity-score matching or multivariable adjustment was performed for these subgroup comparisons. Consequently, statements regarding comparability of outcomes between

groups should be interpreted with caution, as residual confounding and limited statistical power may affect the findings.

The study was approved by the Regional Ethics Committee of Siriraj Hospital, Mahidol University. Written informed consent was obtained from each patient or their legally authorized representative.

RESULTS

During the study period, 866 patients underwent MT for acute stroke, of whom 743 had anterior circulation medium or large vessel occlusion (651 with single occlusion and 92 with tandem occlusion). Ninety-two patients met the criteria for TO (Fig 2). The most common lesion locations were left-sided occlusion (52 patients, 56.5%), cervical ICA (52, 56.5%), and M1 segment (71, 77.2%). The mean age of TO patients (Table 1) was 68.88±12.89 years, and 62 patients (67.4%) were male. Comorbidities included diabetes mellitus in 25 patients (27.2%), hypertension in 52 (56.5%), dyslipidemia in 31 (33.7%), atrial fibrillation in 24 (26.1%), coronary disease in 13 (14.1%), previous or current smoking in 30 (32.6%), and prior stroke or TIA in 13 (14.1%). Median NIHSS score on presentation was 17 (IQR 2–28), and 59.8% received rt-PA. Upon imaging examination, median ASPECTS was 8 (IQR 5–10), and the most frequent collateral score was 4 (59.8%).

Mechanical thrombectomy was performed under general anesthesia in 91.3% of cases, using either anterograde or retrograde approaches. Successful recanalization (mTICI ≥ 2b) was achieved in 85.9% of patients. The most common intracranial technique for reperfusion was manual aspiration alone, accounting for 41.3% of cases, followed by a combination of manual aspiration plus stent retriever at 29.3%, stent retriever alone at 18.5%, and the Solumbra technique at 10.9%.

In the management of cervical internal carotid artery, angioplasty was required in 26.1% of cases, angioplasty with primary stenting in 19.6%, and primary stenting alone in 2.2%. Notably, 52.1% of cervical ICA lesions were managed conservatively during the index procedure. In this context, "conservative" management refers to cases where no acute intervention was performed on the cervical ICA during the thrombectomy procedure itself; however, this did not necessarily mean permanent non-intervention. Among these conservatively managed patients, some had spontaneous recanalization of the cervical ICA following intracranial thrombectomy, some had residual stenosis that was deemed hemodynamically non-significant during the acute phase, and others were planned for delayed carotid treatment (CEA or CAS) within 90 days after clinical stabilization. The average time from puncture-to-recanalization was 54.70±51.39 minutes, while the mean onset-to-recanalization time was 337.31±184.61 minutes.

A favorable outcome, defined as a modified Rankin Scale (mRS) score of 0–2 at 90 days post mechanical

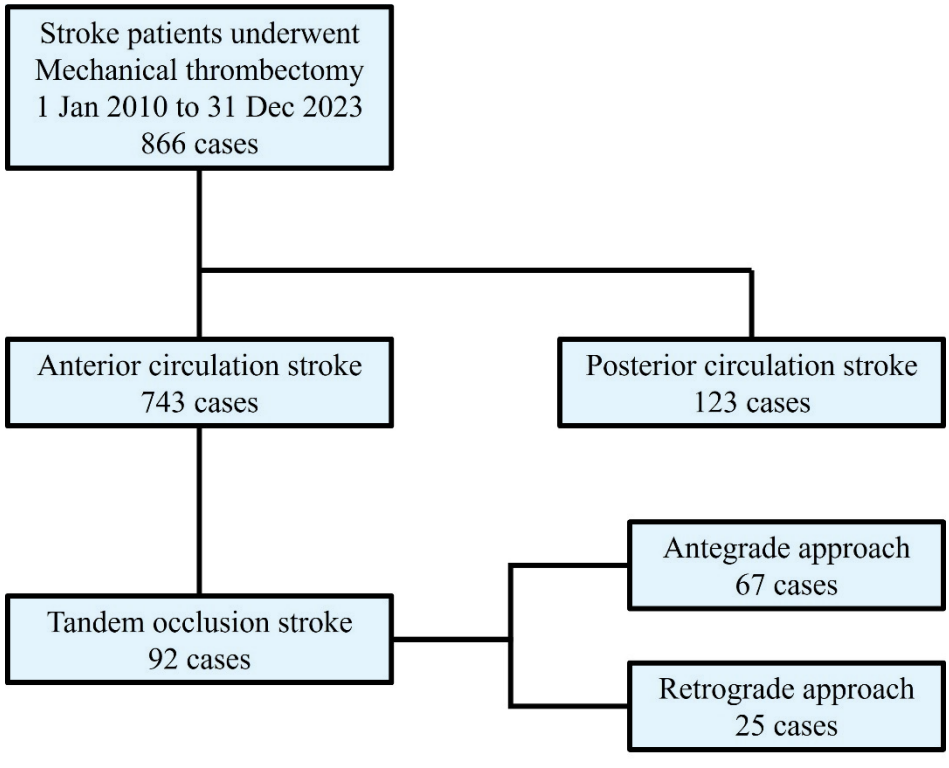

Fig 2. Study flowchart.

TABLE 1. Baseline characteristics of patients with acute tandem occlusion stroke.

Characteristic	Tandem occlusion (N=92)
Age, years	68.88±12.89
Gender	
Male	62 (67.4%)
Female	30 (32.6%)
Comorbidities	
Diabetes mellitus	25 (27.2%)
Hypertension	52 (56.5%)
Dyslipidemia	31 (33.7%)
Atrial fibrillation	24 (26.1%)
Coronary disease	13 (14.1%)
Previous or current smoking	30 (32.6%)
Previous stroke or TIA	13 (14.1%)
Received intravenous rt-PA	55 (59.8%)
NIHSS	
Initial	17 (2-28)
Post mechanical thrombectomy	7 (0-32)
ASPECT	8 (5-10)
Collateral score	
3	11 (12.0%)
4	55 (59.8%)
5	21 (22.8%)
No evaluation	5 (5.4%)
Left side occlusion	52 (56.5%)
Location of occlusions	
C-ICA and M1	71 (77.2%)
C-ICA and M2	6 (6.5%)
C-ICA and intracranial ICA	8 (8.7%)
CCA and M1	5 (5.4%)
CCA and intracranial ICA	2 (2.2%)
Puncture to recanalization, mins	54.70±51.39
Onset to recanalization, mins	337.31±184.61
Successful recanalization (mTICI 2b-3)	79 (85.9%)
Anesthesia	
General anesthesia	84 (91.3%)
Local anesthesia	8 (8.7%)
Cervical ICA pathology	
Atherosclerosis	79 (85.9%)
Dissection	13 (14.1%)

TABLE 1. Baseline characteristics of patients with acute tandem occlusion stroke. (Continue)

Characteristic	Tandem occlusion (N=92)
Approach technique	
Antegrade	67 (72.8%)
Retrograde	25 (27.2%)
Acute cervical ICA treatment	
PTBA	24 (26.1%)
PTBA with CAS	18 (19.6%)
CAS only	2 (2.2%)
Conservative	48 (52.1%)
Intracranial occlusion treatment	
Manual aspiration	38 (41.3%)
Stent retriever	17 (18.5%)
Solumbra technique	10 (10.9%)
Manual aspiration and stent retriever	27 (29.3%)
Favorable outcome at 90 days (mRS 0-2)	51 (55.4%)
Symptomatic ICH	4 (4.3%)
Mortality rate	9 (9.8%)
Delayed cervical ICA treatment within 90 days	
Carotid endarterectomy	4 (4.3%)
Carotid stenting	9 (9.8%)
Antiplatelet/Anticoagulant	
Aspirin	65 (70.7%)
Ticagrelor	15 (16.3%)
Clopidogrel	28 (30.4%)
Warfarin	11 (11.9%)
Dual antiplatelet/anticoagulant	44 (47.8%)

Abbreviations: TIA = Transient ischemic attack, rt-PA = Recombinant Tissue Plasminogen Activator, NIHSS = National Institutes of Health Stroke Scale, ASPECT = Alberta Stroke Program Early CT Score, C-ICA = cervical segment of internal carotid artery, ICA = internal carotid artery, CCA = common carotid artery, mTICI = Modified Treatment in Cerebral Ischemia score, PTBA = percutaneous transluminal balloon angioplasty, CAS = Carotid artery stenting, mRS = modified Rankin Scale, ICH = intracranial hemorrhage

thrombectomy, was achieved in 55.4% of patients. The mortality rate was 9.8%, and symptomatic intracranial hemorrhage (ICH) occurred in 4.3% of cases. Importantly, outcomes following mechanical thrombectomy for tandem occlusion did not differ significantly from those for single occlusion cases (p=0.67), Fig 3; however, this comparison is unadjusted and should be interpreted with caution given potential confounders and limited power. A formal comparison of baseline characteristics between the TO and SO groups was not performed in the current study; this limitation is acknowledged in the Limitations section, and we recognize that baseline imbalances may have influenced the observed similarity in outcomes.

Most collected clot pathologies were characterized as RBC-rich (red clots), constituting 89% of cases. This high proportion of RBC-rich clots is noteworthy, as RBC-rich thrombi are classically associated with cardioembolic or stasis-related mechanisms—such as thrombi formed in the cardiac chambers in the setting of atrial fibrillation—rather than platelet-rich (white) thrombi typically seen in local arterial atherothrombosis. In our cohort, 26.1%

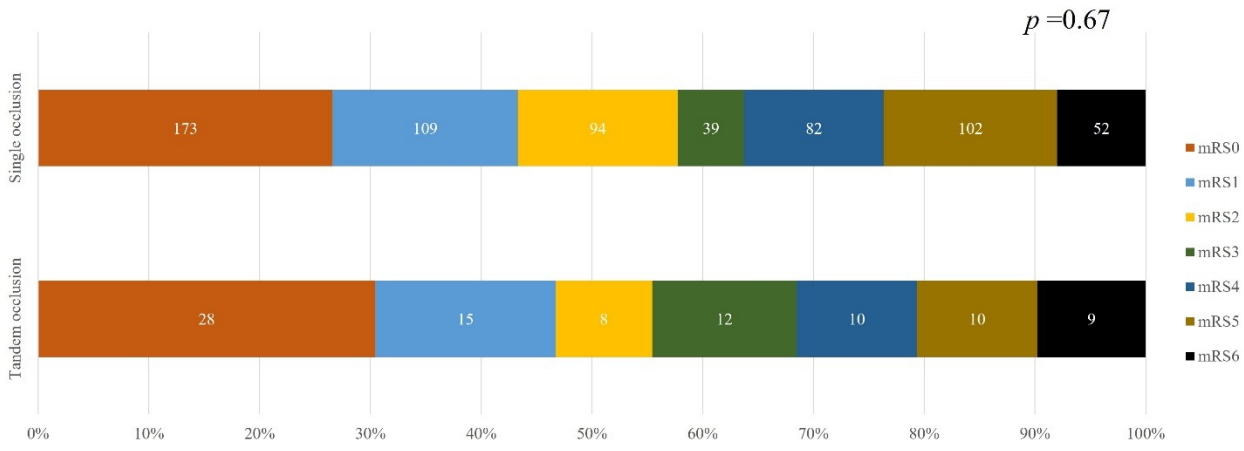

Fig 3. Functional outcomes at 90 days after mechanical thrombectomy: comparison between tandem occlusion and single occlusion.
Abbreviation: mRS = modified Rankin Scale

of patients had atrial fibrillation, which aligns with this finding and suggests that a substantial proportion of intracranial occlusions in TO may represent cardioembolism superimposed on pre-existing carotid atherosclerosis, rather than local propagation of carotid thrombus. This dual pathological mechanism has implications for both acute management (anticoagulation strategy) and long-term secondary prevention.[20]

Thirteen patients (14.1%) scheduled appointments for delayed cervical ICA treatment within 90 days post mechanical thrombectomy, with carotid endarterectomy (CEA) performed in 4.3% of cases and carotid artery stenting (CAS) in 9.8% of cases. The average length of hospital stay was approximately 10.9±10.4 days.

Among the nine deaths recorded, the causes varied and encompassed a range of complications and medical conditions, including two cases of periprocedural complications occurring after the completion of thrombectomy (within 24 hours) that led to intracerebral hemorrhage. Additionally, sequelae from poor recanalization in two cases resulted in the subsequent development of malignant brain infarction. Cardiac complications were also identified as the cause of death in two cases (one patient experienced immediate postoperative cardiac arrest of unknown cause, while another suffered acute myocardial infarction 72 hours post MT). In-hospital infections also played a role in mortality in two cases (acute pyelonephritis and COVID-19 pneumonia). One case presented with hemorrhagic shock, and the precise point of bleeding could not be defined, ultimately exacerbating progressive brain swelling.

Procedural complications were classified as intraprocedural or post-procedural. During MT, six patients sustained puncture site injuries, and three developed iatrogenic CCF, which fortunately resolved spontaneously. Ischemic events were observed, including six cases of distal emboli, one central retinal artery occlusion, and one branch retinal artery occlusion. Additionally, three patients suffered from malignant MCA infarction post-MT.

When comparing outcomes between TO and SO following mechanical thrombectomy (Fig 3), no statistically significant differences were observed (p=0.67). In the SO group, favorable outcomes occurred in 58% of cases with a mortality rate of 7.9%, while in the TO group, favorable outcomes were noted in 55% of cases with a mortality rate of 9.8%. These unadjusted comparisons should be interpreted cautiously, as baseline differences between groups may have influenced the observed outcomes. Detailed baseline characteristics of the SO group were not available for direct comparison in the current study design; this is acknowledged as a limitation.

Regarding procedural approach (Table 2), 67 patients underwent the antegrade method and 25 the retrograde method. No significant difference in age was observed between the antegrade and retrograde groups (69.06±12.95 vs. 67.68±13.05 years, p=0.65). No significant differences were observed in successful recanalization rates (86.6% vs. 84.0%, p=0.75), puncture-to-recanalization time (55.02±49.42 vs. 50.94±48.59 min, p=0.76), or symptomatic intracranial hemorrhage (4.5% vs. 4.0%, p=0.92). Occlusion sites were mainly the cervical ICA and M1 segment in both groups. No significant differences were found between groups regarding comorbidities, pre-stroke mRS (p=0.49), initial NIHSS (p=0.65), left occlusion side (p=0.59), ASPECTS (p=0.73), and good collateral

TABLE 2. Comparison of treatment strategies for acute tandem occlusion stroke.

Characteristic (N=92)	Strategies		*p* value
	Antegrade (N=67)	Retrograde (N=25)	
Gender			
Male	44 (65.7%)	18 (72.0%)	0.57
Female	23 (34.3%)	7 (28.0%)	
Age, years	69.06±12.95	67.68±13.05	0.65
Comorbidities			
Diabetes mellitus	20 (29.9%)	5 (20.0%)	0.35
Hypertension	40 (59.7%)	12 (48.0%)	0.31
Dyslipidemia	21 (31.3%)	10 (40.0%)	0.44
Atrial fibrillation	18 (26.9%)	6 (24.0%)	0.78
Coronary disease	11 (16.4%)	2 (8.0%)	0.30
Previous or current smoking	20 (29.9%)	10 (40.0%)	0.36
Previous stroke or TIA	11 (16.4%)	2 (8.0%)	0.30
Pre-stroke mRS at 90 days			
0	57 (85.1%)	24 (96.0%)	
1	5 (7.5%)	1 (4.0%)	0.49
2	1 (1.5%)	0	
3	4 (5.9%)	0	
Initial NIHSS	17 (2-28)	18 (6-26)	0.65
ASPECTS	8 (5-10)	8 (5-10)	0.73
IV rt-PA	40 (59.7%)	15 (60.0%)	0.98
Good collateral score	56 (83.6%)	20 (80.0%)	0.95
Location			
C-ICA, M1	51 (76.1%)	20 (80.0%)	
C-ICA, M2	5 (7.5%)	1 (4.0%)	
C-ICA, intracranial ICA	4 (5.9%)	4 (16.0%)	0.46
CCA, M1	5 (7.5%)	0	
CCA, intracranial ICA	2 (3.0%)	0	
Left side occlusion	39 (58.2%)	13 (52.0%)	0.59
Cervical ICA pathology			
Dissection	8 (11.9%)	5 (20.0%)	0.32
Atherosclerosis	59 (88.1%)	20 (80.0%)	
Cervical ICA stenosis/occlusion			
100%	30 (44.8%)	10 (40.0%)	0.68
70-99%	37 (55.2%)	15 (60.0%)	

TABLE 2. Comparison of treatment strategies for acute tandem occlusion stroke. (Continue)

Characteristic (N=92)	Strategies		*p* value
	Antegrade (N=67)	Retrograde (N=25)	
Successful recanalization (mTICI ≥ 2b)	58 (86.6%)	21 (84.0%)	0.75
Puncture to recanalization, minutes	55.02±49.42	50.94±48.59	0.76
Onset to recanalization, minutes	349.40±184.47	316.77±172.90	0.55
Anesthesia			
GA	63 (94.0%)	21 (84.0%)	0.13
LA	4 (6.0%)	4 (16.0%)	
Antiplatelet/Anticoagulant			
Aspirin	46 (68.7%)	19 (76.0%)	0.49
Ticagrelor	10 (14.9%)	5 (20.0%)	0.56
Clopidogrel	20 (29.9%)	8 (32.0%)	0.84
Warfarin	9 (13.4%)	2 (8.0%)	0.48
Cervical ICA treatment within 90 days			
Stenting or CEA	24 (35.8%)	9 (36.0%)	0.99
Non-Stenting	43 (64.2%)	16 (64.0%)	
Symptomatic ICH	3 (4.5%)	1 (4.0%)	0.92
Length of hospital stay, days	7 (3-47)	7 (5-55)	0.14
Clot pathology			
RBC-rich	60 (89.6%)	22 (88.0%)	0.83
Fibrin-rich	7 (10.4%)	3 (12.0%)	

Abbreviations: TIA = Transient ischemic attack, mRS = modified Rankin Scale, NIHSS = National Institutes of Health Stroke Scale, ASPECT = Alberta Stroke Program Early CT Score, IV rt-PA = Intravenous Recombinant Tissue Plasminogen Activator, C-ICA = cervical segment of internal carotid artery, ICA = internal carotid artery, CCA = common carotid artery, mTICI = Modified Treatment in Cerebral Ischemia score, GA = General anesthesia, LA = Local anesthesia, CEA = Carotid endarterectomy, ICH = intracranial hemorrhage

score (p=0.95). Furthermore, post-MT treatment with antiplatelet or anticoagulant therapy did not significantly differ between the groups.

For patients with tandem occlusion stroke, 13 underwent extracranial carotid treatment within 90 days. Among the 79 patients analyzed, acute carotid stenting was performed in 20 cases, while 59 were managed without stenting. Favorable functional outcomes at 90 days (Fig 4) were numerically more frequent in the stenting group (65% vs 46%), although the difference was not statistically significant (p=0.15). The mortality rate associated with acute carotid stenting was 15%, with causes including malignant brain edema resulting from infarction (n=1), intracerebral hemorrhage (n=1), and cardiac arrest due to unknown arrhythmia (n=1). Intracranial hemorrhage occurred significantly more often in the stenting group (p=0.01), although the incidence of symptomatic ICH did not differ significantly (p=0.99). These findings should be interpreted with caution given the small subgroup sizes and absence of adjusted analyses.

Comparing acute carotid stenting with delayed carotid treatment within 90 days after mechanical thrombectomy, no significant differences were observed in successful recanalization (p=0.75), favorable outcomes (p=0.22), or symptomatic ICH (p=0.41).

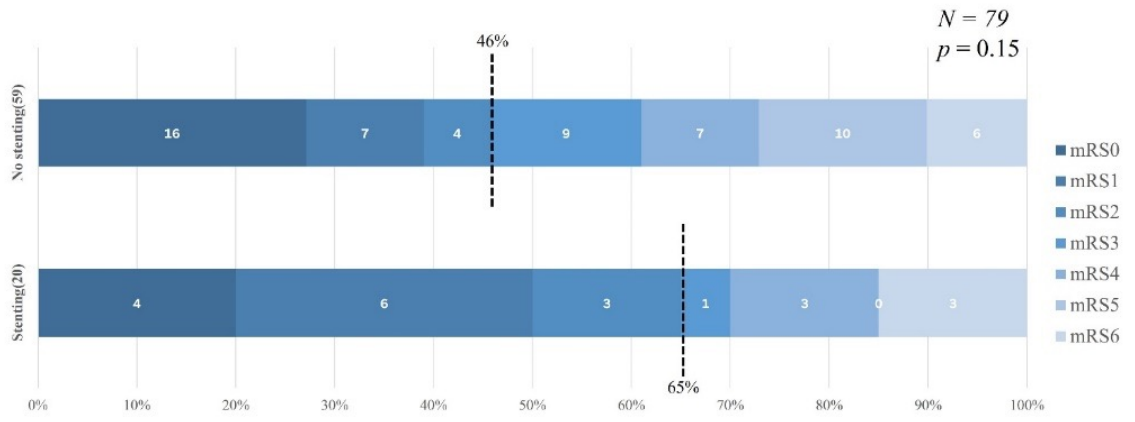

Fig 4. Functional outcomes at 90 days after mechanical thrombectomy: comparison between acute carotid stenting and non-carotid stenting.
Abbreviation: mRS = modified Rankin Scale

TABLE 3. Procedure-related complications.

Intraprocedural complications	Post procedural complications
Access site	Neurological complication
4 Groin hematoma	3 Malignant MCA territory infarction
2 Groin pseudoaneurysm	3 Symptomatic ICH
Vascular injury	17 Asymptomatic ICH/SAH
3 Carotid-cavernous fistula	
Hemorrhagic	
1 Asymptomatic SAH	
1 Symptomatic ICH	
Ischemic	
6 Distal territory emboli	
3 Femoral artery emboli	
1 CRAO	
1 BRAO	

Abbreviations: SAH = Subarachnoid hemorrhage, ICH = Intracranial hemorrhage, CRAO = Central retinal artery occlusion, BRAO = Branch retinal artery occlusion, MCA = Middle cerebral artery

The primary outcome of the study was the 90-day mRS score, with favorable outcomes achieved in 51 cases (Table 4). There were notable differences between this group and the remaining 41 cases regarding gender (p=0.004), age (p<0.001), atrial fibrillation (p=0.04), left side occlusion (p=0.04), and initial NIHSS scores (p<0.001). Furthermore, treatment-related parameters such as cervical ICA treatment within 90 days (p=0.01), successful recanalization (p=0.004), and the administration of dual antiplatelet therapy post MT (p=0.02) varied significantly between the groups. The incidence of symptomatic ICH was higher in the poor outcome group (p=0.04), along with a significantly longer length of hospital stay (p<0.001).

Subgroup analysis with univariate logistic regression identified potential predictors of favorable outcomes at 90 days: male gender, age ≤ 65 years, absence of atrial fibrillation, initial NIHSS score ≤ 16, right-side occlusion, successful recanalization, cervical carotid treatment within 90 days, and dual antiplatelet therapy post MT. Multivariate logistic regression confirmed three independent predictors of favorable outcomes: age ≤ 65 years (p=0.005, OR 5.2, 95% CI 1.6–16.5), initial NIHSS score ≤ 16 (p=0.022, OR 3.9, 95% CI 1.2–12.5),

TABLE 4. Ninety-day functional outcomes after mechanical thrombectomy in acute tandem occlusion stroke.

Characteristic (N=92)	Outcome		*p* value
	Favorable outcome (N=51)	Poor outcome (N=41)	
Gender			
Male	41 (80.4%)	21 (51.2%)	0.004*
Female	10 (19.6%)	20 (48.8%)	
Age, years	63.75±13.03	75.27±12.95	<0.001*
Comorbidities			
Diabetes mellitus	10 (19.6%)	15 (36.6%)	0.77
Hypertension	27 (52.9%)	25 (60.9%)	0.45
Dyslipidemia	20 (39.2%)	11 (26.8%)	0.21
Atrial fibrillation	9 (17.6%)	15 (36.6%)	0.04*
Coronary disease	7 (13.7%)	6 (14.6%)	0.90
Previous or current smoking	20 (39.2%)	10 (24.4%)	0.13
Previous stroke or TIA	7 (13.7%)	6 (14.6%)	0.90
Pre-stroke mRS			
0	48 (94.0%)	33 (80.5%)	
1	1 (2.0%)	5 (12.2%)	0.14
2	1 (2.0%)	0	
3	1 (2.0%)	3 (7.3%)	
Initial NIHSS	16 (2-26)	17 (9-28)	<0.001*
ASPECT	8 (5-10)	8 (5-10)	0.58
IV rt-PA	32 (62.7%)	23 (56.1%)	0.52
Good collateral score	46 (90.2%)	30 (73.2%)	0.13
Location			
C-ICA, M1	41 (80.4%)	30 (73.2%)	
C-ICA, M2	5 (9.8%)	1 (2.4%)	
C-ICA, intracranial ICA	3 (5.9%)	5 (12.2%)	0.12
CCA, M1	2 (3.9%)	3 (7.3%)	
CCA, intracranial ICA	0	2 (4.9%)	
Left side occlusion	24 (47.1%)	28 (68.3%)	0.04*
Cervical ICA pathology			
Dissection	7 (13.7%)	6 (14.6%)	0.90
Atherosclerosis	44 (86.3%)	35 (85.4%)	
Cervical ICA stenosis/occlusion			0.30
100%	17 (33.3%)	23 (56.1%)	
70-99%	34 (66.7%)	18 (43.9%)	
Successful recanalization (mTICI ≥ 2b)	49 (96.1%)	30 (73.2%)	0.004*
Puncture to recanalization, minutes	46.26±51.09	65.65±51.03	0.10
Onset to recanalization, minutes	348.49±186.31	332.24±185.62	0.51

TABLE 4. Ninety-day functional outcomes after mechanical thrombectomy in acute tandem occlusion stroke. (Continue)

Characteristic (N=92)	Outcome		*p* value
	Favorable outcome (N=51)	Poor outcome (N=41)	
Anesthesia			
GA	46 (90.2%)	38 (92.7%)	0.68
LA	5 (9.8%)	3 (7.3%)	
Technique			
Antegrade	37 (72.5%)	30 (73.2%)	0.95
Retrograde	14 (27.5%)	11 (26.8%)	
Cervical ICA treatment within 90 days			
Stenting or CEA	24 (47.1%)	9 (21.9%)	0.01*
Non-Stenting	27 (52.9%)	32 (78.1%)	
Dual antiplatelet post MT	30 (58.8%)	14 (34.1%)	0.02*
Symptomatic ICH	0	4 (9.7%)	0.04*
Length of hospital stay, day	7 (3-18)	7 (1-55)	<0.001*
Clot pathology			
RBC-rich	46 (90.2%)	36 (87.8%)	0.72
Fibrin-rich	5 (9.8%)	5 (12.2%)	

Abbreviations: TIA = Transient ischemic attack, mRS = modified Rankin Scale, NIHSS = National Institutes of Health Stroke Scale, ASPECT = Alberta Stroke Program Early CT Score, IV rt-PA = Intravenous Recombinant Tissue Plasminogen Activator, C-ICA = cervical segment of internal carotid artery, ICA = internal carotid artery, CCA = common carotid artery, mTICI = Modified Treatment in Cerebral Ischemia score, GA = General anesthesia, LA = Local anesthesia, CEA = Carotid endarterectomy, MT = mechanical thrombectomy, ICH = intracranial hemorrhage

TABLE 5. Univariate and multivariate analyses of predictors of favorable outcomes.

Characteristic	Univariate		Multivariate	
	p value	Odds ratio (95%CI)	*p* value	Odds ratio (95%CI)
Gender, male	0.004*	3.9 (1.55-9.83)	0.284	2.0 (0.57-6.91)
Age ≤ 65 years	<0.001*	5.5 (2.21-13.46)	0.005*	5.2 (1.67-16.53)
Atrial fibrillation	0.043*	0.4 (0.14-0.97)	0.728	0.8 (0.2-3.03)
Initial NIHSS ≤ 16	0.004*	3.6 (1.52-8.65)	0.022*	3.9 (1.22-12.81)
Left side occlusion	0.043*	0.4 (0.18-0.97)	0.357	0.6 (0.18-1.85)
Successful recanalization (mTICI ≥ 2b)	0.006*	9.0 (1.86-43.34)	0.043*	6.5 (1.06-39.41)
Cervical carotid treatment within 90 days	0.014*	3.2 (1.26-7.94)	0.373	1.7 (0.53-5.49)
Dual antiplatelet post MT	0.020*	2.8 (1.17-6.47)	0.824	1.1 (0.36-3.66)

Abbreviations: CI = confidence interval, NIHSS = National Institutes of Health Stroke Scale, mTICI = Modified Treatment in Cerebral Ischemia score, MT = mechanical thrombectomy bral Ischemia score, MT = mechanical thrombectomy

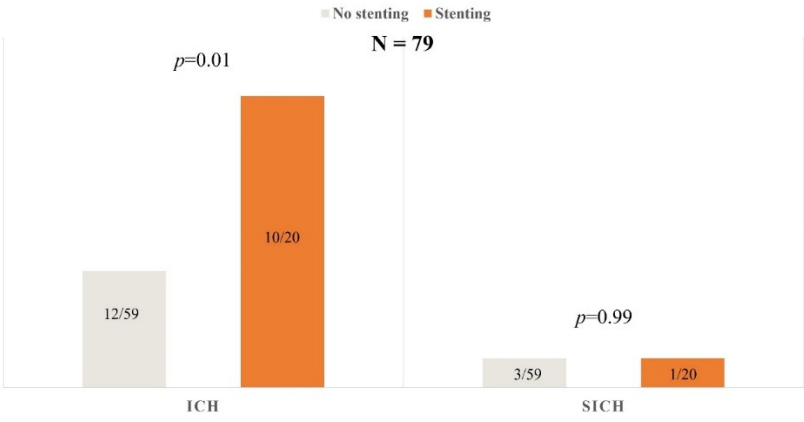

Fig 5. Procedural-related hemorrhage between acute carotid stenting and non-stenting.
Abbreviations: ICH = intracranial hemorrhage, SICH = symptomatic hemorrhage

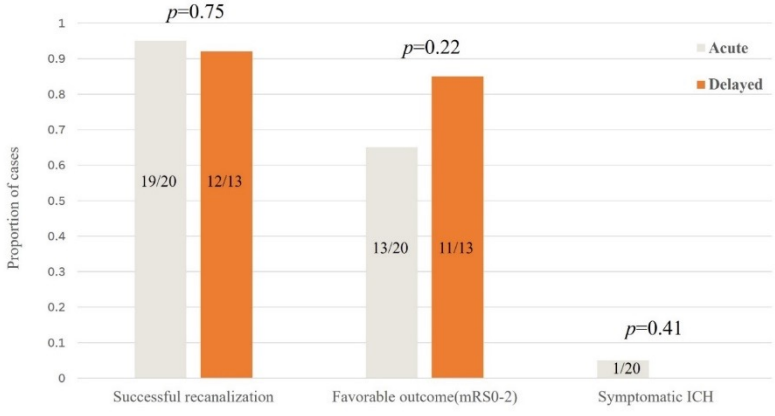

Fig 6. Comparison of acute carotid stenting and delayed cervical ICA treatment in successful recanalization, favorable outcomes and symptomatic ICH.
Abbreviations: ICA = Internal carotid artery, mRS = modified Rankin Scale, ICH = Intracranial hemorrhage

and successful recanalization (p=0.043, OR 6.5, 95% CI 1.1–39.9) (Table 5). The complete multivariate results for all variables, including those that did not reach statistical significance, are presented in Table 5.

DISCUSSION

Tandem occlusion in acute stroke did not significantly decrease the likelihood of a favorable outcome compared with single occlusion cases in unadjusted analysis. Predictive factors for favorable outcomes 90 days after treatment included age ≤ 65 years old, initial NIHSS ≤ 16, and successful recanalization (mTICI ≥ 2b). These predictors are consistent with those reported in multiple prior tandem occlusion cohorts and registries[1,4,7,8], providing confirmatory evidence from a high-volume Southeast Asian center. The Siriraj protocol for mechanical thrombectomy in tandem occlusion emphasizes rapid intracranial reperfusion to minimize infarction progression, although extracranial carotid artery access was often technically challenging. Notably, the study found no significant difference in time from puncture to recanalization between antegrade and retrograde approaches, with both methods yielding comparable outcomes and rates of symptomatic ICH.

Novelty and added value of this study: While the primary outcome findings align with those of major registries (TITAN, ETIS, ESCAPE-NA1), this study offers several distinct contributions. First, it provides a detailed procedural complication profile, including three cases of iatrogenic carotid-cavernous fistula (CCF) associated with cavernous ICA tortuosity type III, a complication that has been underreported in the tandem occlusion literature. Second, the high prevalence of RBC-rich clot pathology (89%) is noteworthy and adds to the limited data available on clot composition in tandem occlusion, supporting a cardioembolic mechanism in a substantial proportion of cases. Third, this is one of the few single-center reports from Southeast Asia with a substantial sample size, contributing geographic and practice-pattern diversity to a field dominated by Western and European registries.[6–8,19–22]

The ESCAPE-NA1 trial[7] reported a notable contrast in 90-day favorable outcomes between tandem occlusion and non-tandem occlusion cases, with rates of 71.3% and 59.5%, respectively. However, our study observed similar favorable outcomes across both groups. In the context of carotid stenosis during mechanical thrombectomy, many cases involved acute carotid stenting. Previous research[6,7,11] has highlighted the favorable impact of this approach, reporting superior 90-day outcomes ranging from 56.6% to 75.8%, alongside reduced mortality rates

Subgroup	OR	95% CI		P value
Gender				
Male	3.9	1.55	9.83	0.004
Female	0.3	0.10	0.65	
Age				
≤ 65 yr	5.5	2.21	13.46	<0.001
> 65 yr	0.2	0.07	0.45	
Atrial fibrillation				
Yes	0.4	0.14	0.97	0.04
No	2.7	1.03	7.03	
Initial NIHSS				
≤ 16	3.6	1.52	8.65	0.004
> 16	0.3	0.12	0.66	
Occlusion side				
Right	2.4	1.03	5.71	0.04
Left	0.4	0.18	0.97	
Collateral score				
Good	1.8	0.52	6.57	0.35
Intermediate	0.6	0.18	2.25	0.48
ASPECT				
8-10	1.0	0.45	2.41	0.92
5-7	1.0	0.42	2.21	
Technique				
Antegrade approach	0.9	0.38	2.44	0.95
Retrograde approach	1.0	0.41	2.60	
Recanalization				
mTICI 2b to 3	9.0	1.86	43.34	0.006
mTICI 0 to 2a	0.1	0.02	0.54	
C-ICA treatment within 90 days				
Stenting or CEA	3.2	1.26	7.94	0.01
No treatment	0.3	0.13	0.79	
Dual antiplatelet post MT				
Yes	2.8	1.17	6.47	0.02
No	0.4	0.16	0.85	

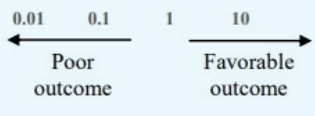

Fig 7. Univariate logistic regression for subgroup analysis of factors associated with 90-day favorable outcomes.
Abbreviations: OR = Odds ratio, 95%CI = 95% confidence interval, NIHSS = National Institutes of Health Stroke Scale, ASPECT = Alberta Stroke Program Early CT Score, mTICI = Modified Treatment in Cerebral Ischemia score, C-ICA = cervical segment of internal carotid artery, CEA = Carotid endarterectomy, MT = Mechanical thrombectomy

ranging from 6.5% to 11.6%. In our study, a numerically higher rate of favorable outcomes was observed in the acute stenting group compared to those without stenting (65% vs. 46%); however, this difference did not reach statistical significance (p=0.15). Importantly, the acute stenting group also exhibited a higher mortality rate (15%) and a significantly higher rate of any intracranial hemorrhage (p=0.01), although symptomatic ICH rates were similar (p=0.99). These findings do not allow us to conclude that acute stenting is definitively safe or beneficial, and the observed trends should be validated in larger, adequately powered studies with appropriate adjustment for confounders.

Stenting and mortality: The higher mortality rate in the acute stenting group (15% vs. 10.2% in the non-stenting group) warrants further discussion. Among the three deaths in the stenting group, one was attributed to intracerebral hemorrhage. The significantly higher rate of any intracranial hemorrhage in the stenting group (p=0.01) likely reflects the need for periprocedural antiplatelet therapy (glycoprotein IIb/IIIa inhibitors or oral DAPT) administered during the acute phase of infarction, which may increase hemorrhagic risk. This relationship between acute stenting, early antiplatelet administration, and hemorrhagic complications has been noted in previous studies.[11,12] However, the other two deaths in the stenting group (malignant brain edema and cardiac arrest from unknown arrhythmia) were

not directly related to hemorrhage, suggesting that the higher mortality may be multifactorial rather than solely attributable to stenting-related hemorrhage. These observations underscore the importance of careful patient selection for acute stenting and close monitoring in the post-procedural period.

Clot pathology considerations: The striking finding that 89% of retrieved clots were RBC-rich (red clots) merits further discussion. RBC-rich thrombi are classically associated with cardioembolic or stasis-related mechanisms, where thrombi formed under low-flow conditions—such as in the left atrial appendage during atrial fibrillation—tend to trap a high proportion of red blood cells within a fibrin meshwork. This is in contrast to platelet-rich (white) thrombi typically seen in local arterial atherothrombosis at sites of high shear stress. In our cohort, 85.9% of cervical ICA pathology was attributed to atherosclerosis, yet the predominance of RBC-rich intracranial clots (89%) suggests that many of these intracranial occlusions may not have arisen from local propagation of the carotid plaque. Instead, they may represent concurrent cardioembolic events—consistent with the 26.1% rate of diagnosed atrial fibrillation in our cohort—or embolism of stasis-formed thrombus from the post-stenotic segment of a severely stenosed ICA where flow is markedly reduced. Some patients may also have had undiagnosed paroxysmal atrial fibrillation as a concurrent cardioembolic source. This dual pathological mechanism has important implications: for acute management, it supports consideration of anticoagulation alongside antiplatelet therapy; for long-term secondary prevention, screening for occult atrial fibrillation may be warranted in tandem occlusion patients.[20]

Temporal considerations: The 14-year study period (2010–2023) encompasses substantial evolution in thrombectomy technology, imaging-based patient selection, and periprocedural care. While we were unable to perform formal stratified or sensitivity analyses by era (e.g., pre- vs. post-2015) due to the limited sample size, we acknowledge that secular trends in device technology (first-generation devices vs. modern stent retrievers and large-bore aspiration catheters), imaging selection (expansion of treatment windows with perfusion imaging), and anesthetic management may confound the observed outcomes. A pre- vs. post-2015 subgroup analysis would be valuable to determine whether the Siriraj protocol remained equally effective as technology advanced; however, this was not feasible with the current sample size and will be addressed in future studies with larger cohorts.

The treatment strategy for acute tandem stroke requires balancing the speed of intracranial recanalization and weighing the merits of antegrade and retrograde approaches in expediting penumbral salvage. While the retrograde approach[13,14] often achieves faster reperfusion, outcomes remain comparable to the antegrade method in terms of successful reperfusion and clinical efficacy. The antegrade approach[15,16] provides enhanced accessibility to intracranial lesions for MT, reducing the risk of vessel dissection or perforation attributed to non-blind navigation of the ICA. However, this approach may prolong reperfusion time and increase infarct development. Moreover, stenting during antegrade MT carries the risk of device entrapment within the stent. Our findings are consistent with prior reports, demonstrating similar outcomes and complication rates across both approaches.

Procedural-related complications were observed, with three patients developing vascular injury in the form of carotid-cavernous fistula (CCF) during MT. Importantly, all three cases exhibited cavernous ICA tortuosity type III[17,18], a known predisposing factor for such complications. In these cases, the CCF likely resulted from microwire or microcatheter perforation of the thin-walled cavernous ICA during navigation through severely tortuous segments. The use of stiffer guidewires to maintain access through the tortuous cavernous segment, combined with repeated device passes (stent retriever deployment and aspiration catheter advancement), may have contributed to cumulative vessel wall trauma. Although CCFs can resolve spontaneously, two of these cases resulted in poor outcomes. These findings highlight the importance of pre-procedural assessment of cavernous ICA tortuosity and consideration of alternative strategies (e.g., softer microwires, reduced number of passes) when severe tortuosity is identified. Additionally, ischemic events occurred in the form of central retinal artery occlusion and branch retinal artery occlusion, with no subsequent improvement noted in either case.

We observed hemorrhagic complications in 22 cases, with four cases manifesting as symptomatic ICH (4.3%), which is a lower incidence compared to previous studies.[1,4,7,8] Notably, patients undergoing acute stenting displayed a higher risk of any hemorrhage compared to the non-stenting group, although this did not significantly differ in terms of symptomatic ICH.[11] This finding suggests a potential association between the need for early antiplatelet therapy during acute infarction and the occurrence of hemorrhage. One patient in the acute stenting group died from massive intracerebral hemorrhage.

Limitations

This study has several important limitations. First, this retrospective analysis was based on medical records and radiographic data retrieved from the hospital's PACS system. Data inconsistencies were present, and there was no established protocol for determining the optimal timing of delayed carotid stenosis treatment following mechanical thrombectomy. Second, the study's relatively small sample size (n=92) limits the generalizability of the findings and the statistical power for subgroup comparisons. Third, the comparisons between tandem and single occlusion, acute stenting versus non-stenting/delayed treatment, and antegrade versus retrograde approaches are largely descriptive and unadjusted; no propensity-score matching or multivariable adjustment was performed for these subgroup analyses. Therefore, statements regarding the comparability or equivalence of outcomes between these groups should be interpreted as hypothesis-generating rather than definitive. Fourth, detailed baseline characteristics of the single occlusion group (age, NIHSS, ASPECTS) were not available for formal comparison with the tandem occlusion group; therefore, the observed similarity in outcomes between TO and SO may be influenced by unmeasured baseline imbalances. Fifth, the 14-year inclusion period spans substantial changes in thrombectomy devices, imaging selection, anesthesia practice, and post-procedural management, which may introduce confounding by secular trends. Formal era-stratified or sensitivity analyses (e.g., pre- vs. post-2015 or by device generation) were not feasible due to the limited sample size. Sixth, only dichotomized mRS outcomes (0–2 vs. 3–6) are reported; full mRS distributions and ordinal shift analysis were not performed. Finally, as a single-center study from a high-volume, experienced center[19,20], the results may reflect the institutional expertise and may not be easily replicable in lower-volume settings. Nonetheless, prior analyses from the TITAN, ETIS, and ESCAPE-NA1 trials[6–8] reported similar functional outcomes, consistent with those observed under the treatment protocol employed in this study.

CONCLUSIONS

The Siriraj protocol for mechanical thrombectomy in acute tandem occlusion stroke demonstrates outcomes and mortality rates comparable to those seen in single occlusion cases in unadjusted analysis. Independent predictors of favorable 90-day outcomes included age ≤ 65 years old, initial NIHSS score ≤ 16, and successful recanalization (mTICI ≥2b). Acute carotid stenting showed a trend toward higher rates of favorable functional outcomes (65% vs. 46%, p=0.15) but was also associated with a higher rate of overall intracranial hemorrhage (p=0.01) and a numerically higher mortality rate (15%). These observational findings do not allow definitive conclusions about the safety and efficacy of acute stenting and should be interpreted with caution. Larger, preferably prospective, multicenter studies with adjusted analyses are needed to clarify the role of acute carotid stenting in tandem occlusion management.

Data Availability Statement

The data that support the findings of this study are available from the Siriraj Center of Interventional Radiology stroke registry, Siriraj Hospital, Mahidol University. However, restrictions apply to the availability of these data due to patient privacy and ethical considerations, and the data are not publicly available. Data may be available from the corresponding author upon reasonable request and with the approval of the Siriraj Institutional Review Board.

ACKNOWLEDGEMENTS

The authors would like to express their sincere gratitude to the dedicated staff of the Siriraj Center of Interventional Radiology, the Division of Neurosurgery, and the nursing team at Siriraj Hospital for their invaluable assistance in data collection and patient care throughout this study. We also thank the patients and their families for their trust and participation.

DECLARATIONS

Grants and Funding Information

This research received no specific grant from any funding agency in the public, commercial, or not-for-profit sectors. The study was conducted using the institutional resources of the Faculty of Medicine, Siriraj Hospital, Mahidol University.

Conflict of Interest

The authors declare that they have no conflict of interest.

Registration Number of Clinical Trial

Not applicable. This study is a retrospective analysis of existing clinical data and was not registered as a prospective clinical trial.

Author Contributions

Conceptualization and Methodology: R.W., P.W. ; Investigation and Data Curation: R.W., B.S., T.A., E.C., A.C. ; Formal Analysis: R.W., P.W. ; Writing – Original

Draft: R.W. ; Writing – Review & Editing: R.W., B.S., T.A., E.C., A.C., P.W. ; Supervision: P.W., A.C. ; All authors have read and agreed to the published version of the manuscript.

Use of Artificial Intelligence

During the preparation of this manuscript, artificial intelligence (AI) was not used for the analysis of clinical data or the generation of scientific conclusions. AI language models were utilized solely for proofreading, grammar correction, and formatting of the final text to improve clarity and conform to publication standards.

REFERENCES

1. Feil K, Herzberg M, Dorn F, Tiedt S, Küpper C, Thunstedt DC, et al. Tandem Lesions in Anterior Circulation Stroke: Analysis of the German Stroke Registry-Endovascular Treatment. Stroke. 2021;52(4):1265–75.
2. Bracco S, Zanoni M, Casseri T, Castellano D, Cioni S, Vallone IM, et al. Endovascular treatment of acute ischemic stroke due to tandem lesions of the anterior cerebral circulation: a multicentric Italian observational study. Radiol Med (Torino). 2021;126(6):804–17.
3. Jadhav AP, Zaidat OO, Liebeskind DS, Yavagal DR, Haussen DC, Hellinger FRJ, et al. Emergent Management of Tandem Lesions in Acute Ischemic Stroke. Stroke. 2019;50(2):428–33.
4. Enriquez BAB, Nome T, Nome CG, Tennøe B, Lund CG, Beyer MK, et al. Predictors of outcome after endovascular treatment for tandem occlusions: a single center retrospective analysis. BMC Neurol. 2023;23(1):82.
5. Zevallos CB, Farooqui M, Quispe-Orozco D, Mendez-Ruiz A, Patterson M, Below K, et al. Proximal Internal Carotid artery Acute Stroke Secondary to tandem Occlusions (PICASSO) international survey. J Neurointerventional Surg. 2021;13(12):1106–10.
6. Zhu F, Bracard S, Anxionnat R, Derelle AL, Tonnelet R, Liao L, et al. Impact of Emergent Cervical Carotid Stenting in Tandem Occlusion Strokes Treated by Thrombectomy: A Review of the TITAN Collaboration. Front Neurol. 2019;10:206.
7. Marko M, Cimflova P, Poppe AY, Kashani N, Singh N, Ospel J, et al. Management and outcome of patients with acute ischemic stroke and tandem carotid occlusion in the ESCAPE-NA1 trial. J Neurointerventional Surg. 2022;14(5):neurintsurg-2021-017474.
8. Anadani M, Marnat G, Consoli A, Papanagiotou P, Nogueira RG, Siddiqui A, et al. Endovascular Therapy of Anterior Circulation Tandem Occlusions: Pooled Analysis From the TITAN and ETIS Registries. Stroke. 2021;52(10):3097–105.
9. Wilson MP, Murad MH, Krings T, Pereira VM, O'Kelly C, Rempel J, et al. Management of tandem occlusions in acute ischemic stroke - intracranial versus extracranial first and extracranial stenting versus angioplasty alone: a systematic review and meta-analysis. J Neurointerventional Surg. 2018;10(8):721–8.
10. von Kummer R, Broderick JP, Campbell BCV, Demchuk A, Goyal M, Hill MD, et al. The Heidelberg Bleeding Classification: Classification of Bleeding Events After Ischemic Stroke and Reperfusion Therapy. Stroke. 2015;46(10):2981–6.
11. Farooqui M, Zaidat OO, Hassan AE, Quispe-Orozco D, Petersen N, Divani AA, et al. Functional and Safety Outcomes of Carotid Artery Stenting and Mechanical Thrombectomy for Large Vessel Occlusion Ischemic Stroke With Tandem Lesions. JAMA Netw Open. 2023;6(3):e230736.
12. Diana F, Romoli M, Toccaceli G, Rouchaud A, Mounayer C, Romano DG, et al. Emergent carotid stenting versus no stenting for acute ischemic stroke due to tandem occlusion: a meta-analysis. J Neurointerventional Surg. 2023;15(5):428–32.
13. Min X, Du J, Bai X, Wei T, Dmytriw AA, Patel AB, et al. Antegrade or Retrograde Approach for the Management of Tandem Occlusions in Acute Ischemic Stroke: A Systematic Review and Meta-Analysis. Front Neurol. 2021;12:757665.
14. Yang D, Shi Z, Lin M, Zhou Z, Zi W, Wang H, et al. Endovascular retrograde approach may be a better option for acute tandem occlusions stroke. Interv Neuroradiol J Peritherapeutic Neuroradiol Surg Proced Relat Neurosci. 2019;25(2):194–201.
15. Grigoryan M, Haussen DC, Hassan AE, Lima A, Grossberg J, Rebello LC, et al. Endovascular Treatment of Acute Ischemic Stroke Due to Tandem Occlusions: Large Multicenter Series and Systematic Review. Cerebrovasc Dis Basel Switz. 2016;41(5–6):306–12.
16. Lockau H, Liebig T, Henning T, Neuschmelting V, Stetefeld H, Kabbasch C, et al. Mechanical thrombectomy in tandem occlusion: procedural considerations and clinical results. Neuroradiology. 2015;57(6):589–98.
17. Koge J, Tanaka K, Yoshimoto T, Shiozawa M, Kushi Y, Ohta T, et al. Internal Carotid Artery Tortuosity: Impact on Mechanical Thrombectomy. Stroke. 2022;53(8):2458–67.
18. Qu LZ, Dong GH, Zhu EB, Lin MQ, Liu GL, Guan HJ. Carotid-cavernous fistula following mechanical thrombectomy of the tortuous internal carotid artery: A case report. World J Clin Cases. 2023;11(25):6005–11.
19. Chudapongse R, Sangpetngam B, Chankaew E, Aurboonyawat T, Churojana A, Withayasuk P. Comparative Evaluation of Imaging Modalities for Eligibility in Endovascular Treatment of Delayed Onset Acute Anterior Circulation Ischemic Stroke in Siriraj Hospital: A Retrospective Analysis. Siriraj Med J. 2024;76(9):573–80.
20. Churojana A, Mongkolratnan A, Sangpetngam B, Aurboonyawat T, Chankaew E, Withayasuk P, et al. A Comparison of Mechanical Thrombectomy for Large Vessel Occlusion in Acute Ischemic Stroke between Patients with and without Atrial Fibrillation. Siriraj Med J. 2018;70(4):278–83.
21. Chaivanit T, Chaivanit P, Bumrungrachapukdee P, Unprasert P, Wattanavaekin K, Benyakorn T. Comparison of Primary Patency Rate between Drug-Coated Balloon and Plain Balloon Angioplasty in Hemodialysis Access. Siriraj Med J. 2022;74(6):388–94.
22. Puangpunngam N, Supokaivanich N, Ruangsetakit C, Wongwanit C, Sermsathanasawadi N, Chinsakchai K, et al. Endovascular thrombectomy versus open surgical thrombectomy for thrombosed arteriovenous hemodialysis graft. Siriraj Med J. 2019;71(6):491–8.

Intraoperative Cerebral Angiography in the Surgical Resection of Brain Arteriovenous Malformations

Kan Tapunya, M.D., Thaweesak Aurboonyawat, M.D.*

Division of Neurosurgery, Department of Surgery, Faculty of Medicine Siriraj Hospital, Mahidol University, Bangkok, Thailand.

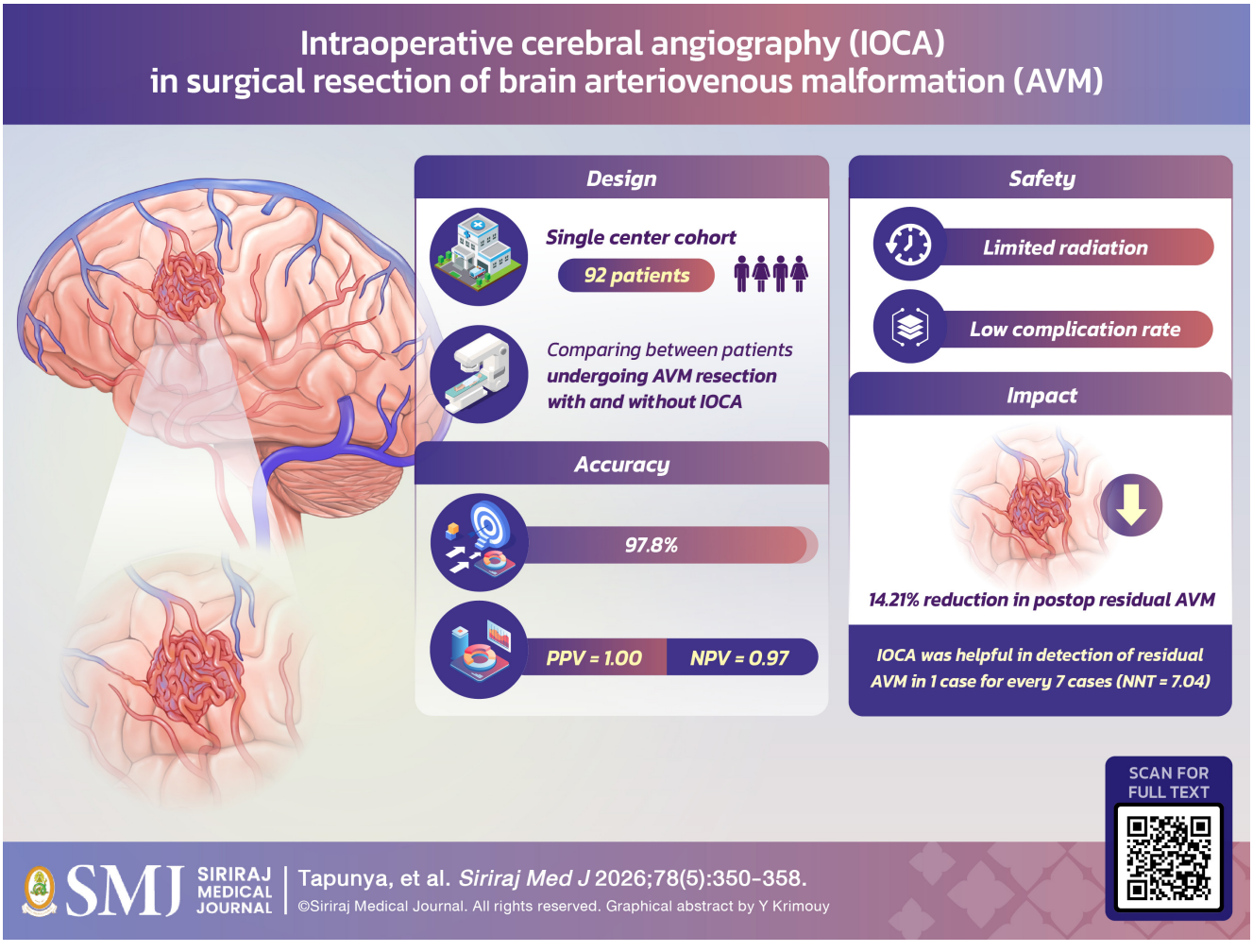

*Corresponding author: Thaweesak Aurboonyawat
E-mail: aurboonyawat@gmail.com
Received 1 September 2025 Revised 19 February 2026 Accepted 23 February 2026
ORCID ID: http://orcid.org/0009-0008-7715-0660
https://doi.org/10.33192/smj.v78i5.277427

All material is licensed under terms of the Creative Commons Attribution 4.0 International (CC-BY-NC-ND 4.0) license unless otherwise stated.

ABSTRACT

Objective: This study aimed to determine the effectiveness of IOCA in reducing residual AVMs after surgery.

Materials and Methods: We retrospectively reviewed all AVM resection surgeries performed at Siriraj Hospital between January 2008 and December 2022. The use of intraoperative cerebral angiography was recorded. The primary outcome was the presence of residual AVM on postoperative imaging.

Results: The study included 92 patients, who were divided into two groups: those undergoing IOCA (44) and those undergoing surgery without IOCA (48). The initial incidence of residual AVMs prior to IOCA did not differ between the two groups (15.90% vs. 18.75%, p=0.720). However, postoperative imaging revealed significantly fewer missed residual AVMs in the IOCA group compared to the non-IOCA group (4.54% vs. 18.75%, p=0.036; absolute risk reduction (ARR) = 14.21% and a number needed to treat (NNT) = 7.04). The overall rate of acute complications did not differ significantly between the two groups (p = 0.108), but the mean length of hospital stay was higher in the non-IOCA group (19.31 vs. 8.57, p=0.001).

Conclusion: Intraoperative cerebral angiography may help reduce the incidence of residual AVMs after surgery and decrease the length of hospital stays.

Keywords: AVM; cerebral arteriovenous malformation; intraoperative cerebral angiography; residual; surgical resection (Siriraj Med J 2026;78(5):350-358)

INTRODUCTION

Cerebral arteriovenous malformation (AVM) remains a significant condition within the field of neurovascular surgery, despite its relatively low incidence.[1-3] The inherent risks and complications associated with AVMs have prompted extensive research and efforts aimed at improving treatment strategies and patient outcomes.[4,5]

Historically, surgical resection has been a primary treatment approach for cerebral AVMs. However, literature reports show that even at experienced centers, residual AVMs may persist in up to 33% of cases post-surgery, with patients in this category generally experiencing worse outcomes.[6,7] Moreover, the risk of rebleeding may be higher in these cases than in untreated patients, with some rebleeding events occurring as early as during transport from the operating room. These findings underscore the need for effective intraoperative measures to minimize the risk of such undesirable events.[8]

Intraoperative cerebral angiography (IOCA), introduced in the 1970s, has proven to be a valuable adjunct in neurovascular surgery.[9] Its use extends to lesion localization and detection of residual AVMs, thereby supporting a more comprehensive surgical approach.[10,11] However, the adoption of IOCA has varied across medical centers, leading to diverse treatment guidelines.[12,13]

Although several case series and institutional reports have evaluated the role of IOCA in cerebral AVM resection, most studies are limited by small sample sizes and the absence of direct comparisons with surgeries performed without IOCA.[19-21] Consequently, the true effectiveness of IOCA in improving surgical completeness and patient outcomes remains incompletely defined.

In this context, our study aims to present our institution's experience with cerebral AVM resection performed with and without IOCA. Although this is a single-center retrospective study, it represents one of the largest series to date and one of the few to directly compare outcomes between IOCA and non-IOCA groups. This analysis seeks to provide further evidence regarding the clinical value of IOCA and its impact on residual AVM rates, perioperative outcomes, and overall patient care.

MATERIALS AND METHODS

Study design

This was a single-center, retrospective review of patients with intracranial AVMs who underwent surgical resection at Siriraj Hospital between January 2008 and December 2022. Patient demographic data, as well as all previous treatments, were reviewed. Clinical and functional status were documented using the Glasgow Coma Scale and the Modified Rankin Scale for both preoperative and postoperative evaluations. Additionally, AVMs were graded using the two most widely accepted classification systems — Spetzler-Martin grading and supplementary grading.[14-16]

Most patients underwent postoperative imaging (CTA, MRA, or DSA). Residual AVM was defined as a residual nidus identified on postoperative imaging. Initially, 116 eligible patients were identified. Among them, 14 patients lacked postoperative images, and 10 had received other

intraoperative interventions such as indocyanine green injection (ICG). After excluding these cases, 92 patients remained, who were categorized into two groups based on whether intraoperative cerebral angiography (IOCA) was performed. The decision to use IOCA was made at the discretion of the attending neurosurgeon, based on factors such as anatomical complexity or personal preference. The IOCA group included 44 patients (47.8%) who underwent the procedure, while the conventional group included 48 patients who did not (Fig 1).

Intraoperative cerebral angiography

As described above, the use of IOCA was based on surgeon discretion and was planned preoperatively in all cases. All procedures were performed in a hybrid operating room equipped with a radiolucent carbon head holder frame, angiography table, and C-arm imaging system. Vascular access for intraoperative angiography was typically established prior to surgical resection. Angiography was then performed after the surgeon deemed the resection complete, allowing for intraoperative confirmation of complete nidus obliteration and immediate detection of residual AVMs, which could prompt further resection during the same procedure.

Outcomes

The primary objective was to assess the incidence of residual AVM on postoperative imaging, used to assess the effectiveness of IOCA in AVM resection. Our secondary objective was to compare additional perioperative parameters such as hospital stay, operative time, and complications.

Statistical analysis

Statistical analysis was conducted using SPSS version 18. Data are presented as mean ± SD or as frequency (percent). For ordinal and scale parameters, patient age was analyzed using the independent t-test. The number of feeders, drainage pattern, presence of aneurysm, Spetzler-Martin scale, supplementary scale, operative time, blood loss, length of hospital stays, duration of follow-up, pre- and post-operative Glasgow Coma Scale, and pre- and post-operative Modified Rankin Scale were compared using the Mann-Whitney U test. For nominal parameters such as age group, lesion side and location, gender, presenting symptoms, history of prior bleeding or treatment, emergency setting, complications, re-operation rate, and residual AVM, the Chi-square test was used.

RESULTS

Patient demographics

Patient demographic data are presented in Table 1. Most demographic factors were not significantly different between the groups, except for the emergency setting, which included 12 cases (25%) in the conventional group compared to one case (2.3%) in the IOCA group (p-value = 0.002). Additionally, the pre-operative Glasgow Coma Scale was significantly lower in the conventional group (14.11 ± 2.53 vs. 13.52 ± 3.16, p-value = 0.028). The Spetzler-Martin and supplementary grading scores were comparable between the groups (p-value = 0.481 and 0.224, respectively) (Table 2).

Residual AVM

In the conventional group, residual AVMs were identified in post-operative imaging in nine cases (18.75%). Notably, all these cases were documented in the operative notes as having undergone complete resection.

In the IOCA group, all patients underwent at least

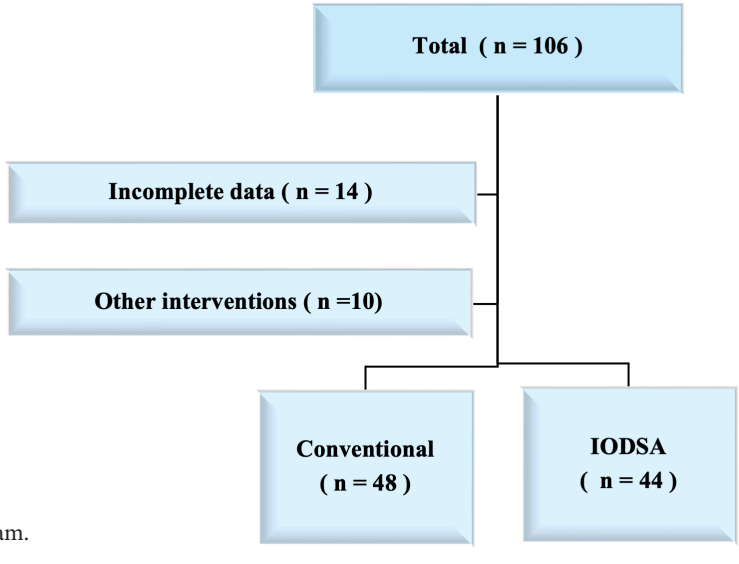

Fig 1. Patient flow diagram.

TABLE 1. Patient demographic data.

Characteristic	Total (N=92)	Conventional (N=48)	IOCA (N=44)	p-value
Mean age (years)	31.7 ± 16	31 ± 15.1	32.6 ± 16	0.631
Sex				0.714
Female	52 (56.5%)	28 (58.3%)	24 (54.5%)	
Male	40 (43.5%)	20 (41.7%)	20 (45.5%)	
Underlying diseases	27 (29.3%)	14 (29.1%)	13 (29.5%)	0.968
Previous resection	11 (12.0%)	6 (12.5%)	5 (11.4%)	0.867
Previous embolization	43 (46.7%)	22 (45.8%)	21 (47.7%)	0.856
Side				0.856
Right	49 (53.3%)	26 (54.2%)	23 (52.3%)	
Left	43 (46.7%)	22 (45.8%)	21 (47.7%)	
Location				0.324
Frontal	35 (38%)	21 (43.8%)	14 (31.8%)	
Temporal	18 (19.6%)	10 (20.8%)	8 (18.2%)	
Parietal	24 (26.1%)	10 (20.8%)	14 (31.8%)	
Occipital	8 (8.7%)	5 (10.4%)	3 (6.8%)	
Insular	2 (2.2%)	0 (0%)	2 (4.5%)	
Cerebellum	3 (3.3%)	2 (4.2%)	0 (0%)	
Corpus callosum	2 (2.2%)	0 (0%)	2 (4.5%)	
Presenting symptoms				0.532
None	1 (1.1%)	1 (2.1%)	0 (0%)	
Headache	8 (8.7%)	3 (6.3%)	5 (11.4%)	
Hemorrhage	52 (56.5%)	31 (64.6%)	21 (47.7%)	
Seizure	24 (26.1%)	10 (20.8%)	14 (31.8%)	
Neurological deficit	2 (2.2%)	1 (2.1%)	1 (2.3%)	
Other	5 (5.4%)	2 (4.2%)	3 (6.8%)	
Emergency case	13 (14.1%)	12 (25%)	1 (2.3%)	0.002*
Preoperative GCS	15 ± 2.53	15 ± 3.16	15 ± 1.39	0.028*
Preoperative MRS	1 ± 1.47	1 ± 1.65	1 ± 1.24	0.505

* indicates statistically significant difference ($p < 0.05$)

TABLE 2. Spetzler-Martin grade and supplementary score.

Characteristic	Total (N=92)	Conventional (N=48)	IOCA (N=44)	p-value
Size of AVM				0.946
< 3 cm	56 (60.9%)	30 (62.5%)	26 (59.1%)	
3-6 cm	34 (36.9%)	17 (35.4%)	17 (38.6%)	
> 6 cm	2 (2.2%)	1 (2.1%)	1 (2.3%)	
Eloquent area	15 (16.3%)	8 (16.7%)	7 (15.9%)	0.922
Deep venous drainage	18 (19.5%)	7 (14.6%)	11 (25%)	0.208
Spetzler-Martin grading				0.481
1	39 (42.4%)	20 (41.7%)	19 (43.2%)	
2	36 (39.1%)	23 (47.9%)	13 (29.5%)	
3	16 (17.4%)	4 (8.3%)	12 (27.5%)	
4	1 (1.1%)	1 (2.1%)	0 (0%)	
Age group				0.360
< 20 years	28 (30.4%)	16 (33.3%)	12 (27.3%)	
20-40 years	39 (42.4%)	17 (35.4%)	22 (50%)	
> 40 years	25 (27.2%)	15 (31.3%)	10 (22.7%)	
Prior bleeding	61 (66.3%)	35 (72.9%)	26 (59.1%)	0.161
Compact nidus	91 (98.9%)	47 (97.9%)	44 (100%)	0.336
Total score				0.224
2	7 (7.6%)	3 (6.3%)	4 (9.1%)	
3	28 (30.4%)	19 (39.6%)	9 (20.5%)	
4	24 (26.1%)	11 (22.9%)	13 (29.5%)	
5	19 (20.7%)	9 (18.8%)	10 (22.7%)	
6	13 (14.1%)	5 (10.4%)	8 (18.2%)	
9	1 (1.1%)	1 (2.1%)	0 (0%)	

one session of intraoperative cerebral angiography after the surgeon initially deemed the resection complete. Residual AVMs were identified intraoperatively in seven patients (15.90%), a rate comparable to that of the conventional group. In most of these cases, additional resection was performed, reducing the number of residual AVMs confirmed on postoperative imaging to three cases (6.81%). When further resection was undertaken, repeat intraoperative angiography was performed selectively rather than routinely.

In the first case, intraoperative imaging revealed a residual AVM, but it was considered unresectable. So, the operation was terminated and residual AVM was expected in postoperative images. This patient was later treated by stereotactic radiosurgery. In the second case, a small nidus was initially overlooked during IOCA, which was falsely interpreted as complete resection (a false-negative result). The residual AVM was later identified on postoperative imaging. In the last case, a residual AVM was observed, and additional resection

was performed. However, repeat angiography was not performed after the additional resection, and postoperative imaging later revealed residual AVM. This case was also classified as a false negative due to the lack of post-resection confirmation during surgery.

Secondary outcomes

There was no significant difference in acute complications or long-term deficits between the two groups (45.8% vs 29.5%, p-value = 0.108 and 70.8% vs 59.1%, p-value = 0.237, respectively). No angiography-related complications were reported. Operative time was significantly longer in the IOCA group (6.36 ± 2.33 vs 4.83 ± 1.98, p-value 0.001). Postoperative Glasgow Coma Scale scores and length of hospital stay were worse in the conventional group (14.29 ± 1.91 vs 15 ± 0, p-value = 0.009 and 19.31 ± 22.80 vs 8.57 ± 3.73, p-value = 0.001) (Table 3).

Radiation exposure

In the IOCA group, the mean DAP was 35.02 ± 17.07 Gy-cm^2, with a mean effective dose of 1.4 ± 0.68 mSv.

Rebleeding rate and other complication

Among the 12 cases with residual AVMs across both groups, there were three instances of rebleeding (25%), whereas no rebleeding occurred in the complete resection group (p-value < 0.001). Additionally, postoperative seizures during the same admission were more frequent in the incomplete resection group (two cases, 16.6%) compared to the complete resection group (five cases, 6.3%) (p-value 0.204).

DISCUSSION

Our findings demonstrate several advantages of intraoperative cerebral angiography (IOCA) in the surgical resection of arteriovenous malformations (AVMs). First, IOCA served as a reliable tool for confirming complete AVM resection. In our study, IOCA demonstrated a positive predictive value of 1.0, a negative predictive value of 0.97, and an overall diagnostic accuracy of 97.8%, respectively. These findings are consistent with a previous study and comparable to standard postoperative imaging.[6] These results highlight the utility of IOCA, particularly in cases where complete resection is difficult to assess visually, such as in anatomically complex or ambiguous lesions. IOCA may also offer significant advantages for less experienced surgeons and in cases involving patients referred from remote areas where follow-up is challenging or access to advanced imaging facilities is limited.

Second, IOCA significantly impacted intraoperative decision-making by identifying residual AVMs and

TABLE 3. Secondary outcomes.

Characteristic	Conventional (N=48)	IOCA (N=44)	p-value
Acute complication	22 (45.8%)	13 (29.5%)	0.108
Long-term deficit	34 (70.8%)	26 (56.9%)	0.237
Missed residual AVM	9 (18.7%)	2 (4.5%)	0.036
Operative time (hours), mean ± S.D.	4.83 ± 1.98	6.36 ± 2.33	0.001*
Blood loss (mL), mean ± S.D.	962 .71 ± 1406.36	843.64 ± 1126.42	0.526
Hospital stay (days), mean ± S.D.	19.31 ± 22.80	8.57 ± 3.73	0.001*
Postoperative GCS, mean ± S.D.	14.29 ± 1.91	15 ± 0	0.009*
Postoperative MRS, mean ± S.D.	1.46 ± 1.58	0.95 ± 1.03	0.198
Time to postoperative image (months), mean ± S.D.	11.58 ± 18.64	13.86 ± 14.59	0.035*
Modality of follow-up			
Cerebral angiography	28 (58.3%)	32 (72.7%)	0.328

* indicates statistically significant difference (p < 0.05)

prompting further resection. In six out of the seven cases with intraoperatively detected residual lesions (13.64%), the surgical procedure was modified to pursue additional resection. Notably, intraoperative imaging also aided the surgeon in precise localization and navigation to the residual nidus. As a result, only two residual AVMs were observed on postoperative imaging in the IOCA group compared to nine in the conventional group. This corresponds to an absolute risk reduction of 14.21% in residual AVMs and a number needed to treat (NNT) of 7.04 ($p = 0.036$).

Lastly, although the overall rate of acute complications did not differ significantly between the two groups ($p = 0.108$), the nature of the complications varied. Among the three patients who experienced rebleeding, two were in the conventional group; both events occurred during the same hospital admission and resulted in severe outcomes. In contrast, the single rebleeding case in the IOCA group presented only with a headache and no neurological deficits. These findings further underscore the importance of achieving complete AVM resection — an outcome that IOCA can help facilitate during the initial surgery — potentially reducing the risk of severe postoperative complications.

Despite the demonstrated benefits of IOCA, false-negative results remain a recognized limitation. In our cohort, IOCA failed to detect residual AVMs in two cases (4.5%), a finding consistent with previously reported in the literature. Both cases highlight important technical and procedural factors that may contribute to missed residual lesions during intraoperative angiography.

Several mechanisms may underlie false-negative IOCA findings. Small residual nidus size, low-flow shunts, transient vasospasm, or temporary thrombosis following resection may obscure residual arteriovenous shunting at the time of angiography. In addition, complex angioarchitecture, deep-seated lesions, or overlapping vascular territories may limit visualization. In one case in our series, a small nidus was initially overlooked and misinterpreted as complete resection, while in another case, residual AVM was identified and further resection was performed but not followed by repeat angiography, ultimately resulting in persistent residual disease on postoperative imaging.

Several strategies may help mitigate the risk of false-negative IOCA results. First, routinely repeat angiography after additional resection may improve diagnostic confidence. Second, obtaining multiple angiographic projections and selectively injecting feeding arteries may enhance detection of small or anatomically complex residual lesions. Third, close collaboration between the operating surgeon and an experienced neurointerventionalist during image acquisition and interpretation may reduce the likelihood of misinterpretation. Finally, adjunctive intraoperative tools such as indocyanine green (ICG) videoangiography or intraoperative Doppler ultrasonography may provide complementary information.

Additionally, concerns regarding radiation exposure during intraoperative angiography are valid. However, the radiation dose associated with IOCA in our cohort was relatively low (mean: 1.4 ± 0.68 mSv), which is significantly lower than in standard postoperative imaging (3.79 ± 1.77 mSv). This level of exposure is roughly equivalent to 6–7 months of background natural radiation or a single-phase CT scan, according to established reference data. Thus, the potential risk from radiation appears minimal when weighed against the diagnostic and therapeutic advantages offered by IOCA (Table 4).[17-19]

We also examined outcomes in patients who underwent emergency surgery, recognizing that the urgent nature of these cases often limits the feasibility of comprehensive intraoperative evaluation such as IOCA. Of the 13 emergency cases, only one received IOCA. Although these patients demonstrated significantly different initial and final Glasgow Coma Scale (GCS) scores compared to elective cases, the rate of complete AVM resection did not differ significantly (23.1% vs. 10.1%, $p = 0.182$). This suggests that while emergency status may influence clinical presentation and outcomes, it does not generally impact resection completeness (Table 5).

Limitations and future directions

This study has several limitations that warrant consideration. First, its retrospective design is inherently associated with limitations such as reliance on existing medical records, potential missing data, and limited control over confounding variables. In addition, as a single-center study, the results may reflect institutional practice patterns, surgeon experience, and available resources, which could limit the generalizability of the findings to other centers with different patient populations or treatment approaches.

Second, selection bias cannot be entirely excluded. The decision to perform IOCA was not standardized and may have been influenced by surgeon preference, lesion characteristics, or intraoperative findings. Furthermore, some patients were excluded due to the absence of postoperative imaging or the use of other intraoperative adjuncts, which may have affected group comparability and introduced additional bias.

Third, certain data elements were incomplete. In

TABLE 4. Radiation exposure.

Procedure	Study	Mean DAP (Gy-cm²)	Energy (mSv)
Intraoperative cerebral angiography	Our study	35.02 ± 17.07	1.4 ± 0.68
Diagnostic cerebral angiography	Our study	94.93 ± 44.30	3.79 ±1.77
Diagnostic cerebral angiography	Ihn YK. et al, 2016[17]	106.2 ± 66.4	
CT brain single phase	Wonglao et al, 2022[18]		1.6-2.08
CTA brain multiphase	Wonglao et al, 2022[18]		2.89-5.46

TABLE 5. Subgroup analysis of emergency cases.

Characteristic	Emergency (N=13)	Elective (N=79)	p-value
Preoperative Glasgow coma scale (median)	8 (3,15)	15 (13,15)	< 0.001*
Postoperative Glasgow coma scale (median)	15 (7,15)	15 (9,15)	< 0.001*
Residual AVMs	3 (23.1%)	8 (10.1%)	0.182

* indicates statistically significant difference ($p < 0.05$)

particular, detailed information regarding hospital costs and cumulative radiation exposure was unavailable for some patients, limiting a comprehensive evaluation of the economic implications and radiation-related risks associated with IOCA.

Finally, postoperative imaging modalities were not uniform across all patients. Although digital subtraction angiography (DSA) is considered the reference standard for detecting residual AVMs, approximately one-third of patients in this study were evaluated using CTA or MRA alone. Previous studies have reported that MRI has a sensitivity of approximately 75–90% and a specificity of 90–100% for detecting AVMs, while CTA demonstrates higher sensitivity, around 90%, with specificity ranging from 95–100%.[22,23] Despite these favorable diagnostic performances, both modalities may be less sensitive than DSA in identifying small residual nidus, particularly in small or complex AVM lesions. As a result, the use of CTA or MRA alone may have led to an underestimation of residual AVM rates in a subset of patients.

Future studies with prospective designs, standardized criteria for IOCA utilization, and uniform postoperative imaging protocols would help address these limitations. Multicenter collaborations may further improve generalizability and allow for larger sample sizes, facilitating subgroup analyses and adjustment for confounding factors. In addition, randomized controlled trials comparing IOCA with other intraoperative adjuncts could provide valuable alternatives for centers without access to IOCA.

CONCLUSIONS

Although not infallible, intraoperative cerebral angiography appears to be a safe and potentially effective adjunct during AVM resection, with a low observed complication rate and limited additional radiation exposure. Its use facilitates the detection of residual disease and enables immediate corrective action, which was associated with a lower incidence of residual AVMs, as well as reduced postoperative rebleeding and shorter hospital stays.

Data Availability Statement

None.

ACKNOWLEDGEMENTS

None.

DECLARATIONS

Grants and Funding Information

No grants or funding.

Conflict of Interest

No conflicts of interest.

Registration Number of Clinical Trial

Not applicable.

Author Contributions

Conceptualization and methodology, K.T., T.A. ; Formal analysis, Visualization and writing – original draft, K.T. ; Writing – review and editing, T.A. ; All authors have read and agreed to the final version of the manuscript.

Use of Artificial Intelligence

Use of artificial intelligence (ChatGPT version 5.0-5.2) for checking the manuscript for grammatical errors.

REFERENCES

1. Al-Shahi R, Bhattacharya JJ, Currie DG, Papanastassiou V, Ritchie V, Roberts RC, et al. Prospective, population-based detection of intracranial vascular malformations in adults: the Scottish Intracranial Vascular Malformation Study (SIVMS). Stroke. 2003;34(5):1163-9.
2. Al-Shahi R, Fang JS, Lewis SC, Warlow CP. Prevalence of adults with brain arteriovenous malformations: a community based study in Scotland using capture-recapture analysis. J Neurol Neurosurg Psychiatry. 2002;73(5):547-51.
3. ApSimon HT, Reef H, Phadke RV, Popovic EA. A population-based study of brain arteriovenous malformation: long-term treatment outcomes. Stroke. 2002;33(12):2794-800.
4. Fults D, Kelly DL, Jr. Natural history of arteriovenous malformations of the brain: a clinical study. Neurosurgery. 1984;15(5):658-62.
5. Madzar D, Kuramatsu JB, Gollwitzer S, Lucking H, Kloska SP, Hamer HM, et al. Seizures among long-term survivors of conservatively treated ICH patients: incidence, risk factors, and impact on functional outcome. Neurocrit Care. 2014;21(2):211-9.
6. Bilbao CJ, Bhalla T, Dalal S, Patel H, Dehdashti AR. Comparison of indocyanine green fluorescent angiography to digital subtraction angiography in brain arteriovenous malformation surgery. Acta Neurochir (Wien). 2015;157(3):351-9.
7. Bauer BL. Intraoperative angiography in cerebral aneurysm and AV-malformation. Neurosurg Rev. 1984;7(2-3):209-17.
8. Anegawa S, Hayashi T, Torigoe R, Harada K, Kihara S. Intraoperative angiography in the resection of arteriovenous malformations. J Neurosurg. 1994;80(1):73-8.
9. Chalouhi N, Theofanis T, Jabbour P, Dumont AS, Fernando Gonzalez L, Starke RM, et al. Safety and efficacy of intraoperative angiography in craniotomies for cerebral aneurysms and arteriovenous malformations: a review of 1,093 consecutive cases. Neurosurgery. 2012;71(6):1162-9.
10. Komatsu K, Takagi Y, Ishii A, Kikuchi T, Yamao Y, Yoshida K, et al. Changes in treatment strategy over time for arteriovenous malformation in a Japanese high-volume center. BMC Neurol. 2020;20(1):404.
11. Vitaz TW, Gaskill-Shipley M, Tomsick T, Tew JM, Jr. Utility, safety, and accuracy of intraoperative angiography in the surgical treatment of aneurysms and arteriovenous malformations. AJNR Am J Neuroradiol. 1999;20(8):1457-61.
12. Al-Shahi Salman R, White PM, Counsell CE, du Plessis J, van Beijnum J, Josephson CB, et al. Outcome after conservative management or intervention for unruptured brain arteriovenous malformations. JAMA. 2014;311(16):1661-9.
13. Spetzler RF, Martin NA. A proposed grading system for arteriovenous malformations. J Neurosurg. 1986;65(4):476-83.
14. Lawton MT, Kim H, McCulloch CE, Mikhak B, Young WL. A supplementary grading scale for selecting patients with brain arteriovenous malformations for surgery. Neurosurgery. 2010;66(4):702-13; discussion 13.
15. Hafez A, Koroknay-Pal P, Oulasvirta E, Elseoud AA, Lawton MT, Niemela M, et al. The Application of the Novel Grading Scale (Lawton-Young Grading System) to Predict the Outcome of Brain Arteriovenous Malformation. Neurosurgery. 2019;84(2):529-36.
16. Ihn YK, Kim BS, Byun JS, Suh SH, Won YD, Lee DH, et al. Patient Radiation Exposure During Diagnostic and Therapeutic Procedures for Intracranial Aneurysms: A Multicenter Study. Neurointervention. 2016;11(2):78-85.
17. Wonglao S. Evaluation of the Patient Radiation Doses from Computed Tomography (CT) in Neurological Institute of Thailand. Journal of the Department of Medical Services. 2022;47(3):51-9.
18. Lin EC. Radiation risk from medical imaging. Mayo Clin Proc. 2010;85(12):1142-6; quiz 6.
19. Gaballah M, Storm PB, Rabinowitz D, Ichord RN, Hurst RW, Krishnamurthy G, et al. Intraoperative cerebral angiography in arteriovenous malformation resection in children: a single institutional experience. J Neurosurg Pediatr. 2014;13(2):222-8.
20. Yoon W, Kim H, Kim YW, Kim SR, Park IS. Usefulness and Stability of Intraoperative Digital Subtraction Angiography Using the Transradial Route in Arteriovenous Malformation Surgery. World Neurosurg. 2018;111:e799-e805.
21. Ellis MJ, Kulkarni AV, Drake JM, Rutka JT, Armstrong D, Dirks PB. Intraoperative angiography during microsurgical removal of arteriovenous malformations in children. J Neurosurg Pediatr. 2010;6(5):435-43.
22. Gross BA, Frerichs KU, Du R. Sensitivity of CT angiography, T2-weighted MRI, and magnetic resonance angiography in detecting cerebral arteriovenous malformations and associated aneurysms. J Clin Neurosci. 2012;19(8):1093-5.
23. Lim HK, Choi CG, Kim SM, Kim JL, Lee DH, Kim SJ, et al. Detection of residual brain arteriovenous malformations after radiosurgery: diagnostic accuracy of contrast-enhanced four-dimensional MR angiography at 3.0 T. Br J Radiol. 2012;85(1016):1064-9.

Long-Term Refractive Outcomes Following Pediatric Cataract Surgery with Primary IOL Implantation

Arnan Limmahachai, M.D., Thammanoon Surachatkumtonekul, M.D.*

Department of Ophthalmology, Faculty of Medicine Siriraj Hospital, Mahidol University, Bangkok, 10700, Thailand.

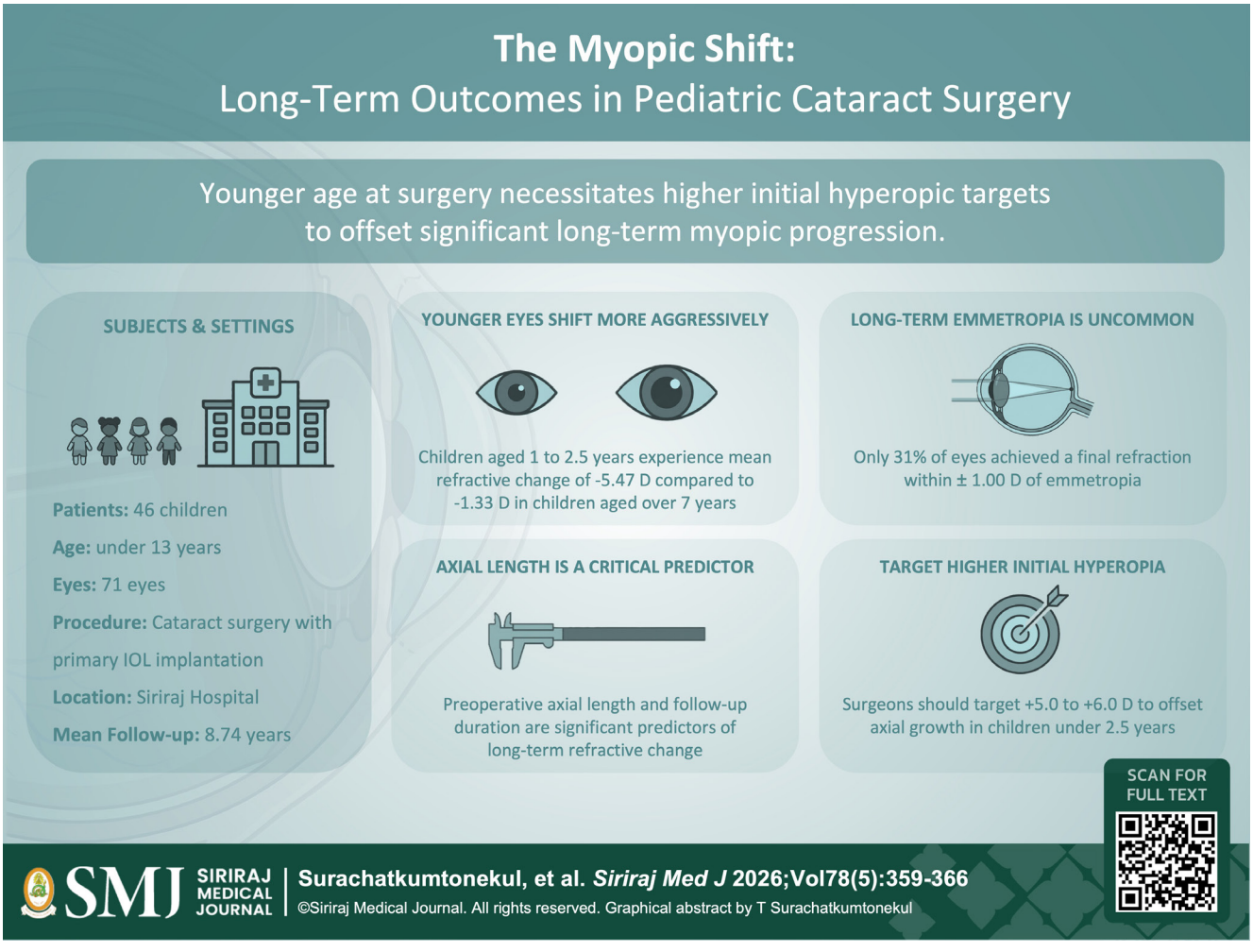

*Corresponding author: Thammanoon Surachatkumtonekul
E-mail: Si95thim@gmail.com
Received 16 February 2026 Revised 30 March 2026 Accepted 30 March 2026
ORCID ID: http://orcid.org/0000-0002-0037-6863
https://doi.org/10.33192/smj.v78i5.280456

All material is licensed under terms of the Creative Commons Attribution 4.0 International (CC-BY-NC-ND 4.0) license unless otherwise stated.

ABSTRACT

Objective: To evaluate long-term refractive outcomes following pediatric cataract surgery with primary intraocular lens (IOL) implantation.

Materials and Methods: A retrospective review was conducted in children younger than 13 years who underwent cataract surgery with primary IOL implantation at Siriraj Hospital between 2000 and 2020, with a minimum follow-up of 5 years. Refractive data were converted to spherical equivalents. Linear mixed models were used to analyze refractive shifts across four age groups (1 to <2.5, 2.5 to <4, 4 to <7, and 7 to <13 years) and identify influencing factors.

Results: The study included 71 eyes of 46 children, with a mean follow-up of 8.74 ± 3.01 years. The mean final refractive change ranged from -5.47 D (95% CI: -7.93, -3.01) in children aged 1 to <2.5 years to -1.33 D (95% CI: -1.99, -0.67) in those aged 7 to <13 years. Overall, only 30.99% of eyes achieved a final refraction within ±1.00 D of emmetropia. Multivariate analysis identified preoperative axial length (P = 0.005) and follow-up duration (P = 0.003) as significant predictors of refractive change.

Conclusion: Younger age at surgery correlates with greater magnitude and variability of myopic shift. Standard guidelines should be adapted to target higher residual hyperopia to achieve optimal long-term emmetropic refraction.

Keywords: Cataract; pediatric ophthalmology; myopic shift (Siriraj Med J 2026;78(5):359-366)

INTRODUCTION

Childhood cataract remains a significant cause of visual impairment worldwide.[1,2] Its management presents a unique challenge: the implantation of a static intraocular lens (IOL) into a rapidly growing eye.[3] Clinicians must balance immediate visual rehabilitation with the long-term trajectory of ocular growth.[4] Accurate prediction of postoperative refractive changes is essential for appropriate initial IOL power selection. The literature consistently demonstrates substantial myopic shifts, particularly in children operated on at a younger age, leading to the development of various predictive guidelines.[5-9] Recent data from the Pediatric Eye Disease Investigator Group (PEDIG) highlight both the magnitude and variability of this shift in younger children.[10] Furthermore, *Lekskul et al.* reported high rates of late-onset myopia in Thai children, suggesting that current guidelines may be insufficient for this population.[11]

To address the need for population-specific data, this study evaluates refractive outcomes stratified by age at surgery and identifies factors associated with long-term refractive change following pediatric cataract surgery with primary IOL implantation.

MATERIALS AND METHODS

This retrospective study was approved by the Siriraj Institutional Review Board, Faculty of Medicine Siriraj Hospital (COA no. Si 696/2025), and was conducted in accordance with the tenets of the Declaration of Helsinki. The requirement for patient consent was waived.

We reviewed the medical records of children younger than 13 years who underwent cataract surgery with primary IOL implantation at Siriraj Hospital between 2000 and 2020, with a minimum follow-up of 5 years. Patients were identified using the ICD-10 code for infantile and juvenile cataract (H26.0). For bilateral cases, data from both eyes were included. Eyes with traumatic cataract, glaucoma-related conditions diagnosed at any stage, ocular comorbidities affecting development, or incomplete data were excluded.

Data collected included baseline demographics, surgical techniques, and postoperative refractive outcomes, including initial postoperative refraction within 6 months of surgery, 5-year refraction, defined as measurements obtained 4 to 6 years postoperatively, and final refraction, defined as the last recorded refraction before age 18. All refractive errors were converted to spherical equivalents (SE), calculated as the sphere plus half the cylinder, and reported in diopters (D). To account for inter-eye correlation in bilateral cases, Linear Mixed Models (LMMs) with a random patient intercept were used to calculate adjusted means and 95% confidence intervals (CI). Participants were stratified by age at surgery. Since no patients younger than 1 year were included, the cohort was stratified into four groups: 1 to <2.5 years, 2.5 to <4 years, 4 to <7 years, and 7 to <13 years. We also evaluated refractive changes based on the initial postoperative refractive status, classifying eyes as hyperopic or emmetropic (≥ 0.00 D) or myopic (< 0.00 D).

Predictors of final refractive change were assessed using LMMs. Covariates included age at surgery, preoperative axial length, average keratometry, early postoperative refraction, follow-up duration, and laterality; IOL fixation technique was excluded due to insufficient data. Variables

with P ≤ 0.10 in the univariate analysis were included in the multivariate model, with no multicollinearity observed (variance inflation factor < 2).

All statistical analyses were performed using SPSS software version 29.0 (SPSS Inc., Chicago, IL, USA), with significance defined as P < 0.05.

RESULTS

A total of 71 eyes from 46 children were included. The cohort was predominantly male (52.11%), with a mean age at surgery of 6.04 ± 3.06 years and a mean follow-up duration of 8.74 ± 3.01 years. Bilateral cataracts accounted for 73.24% of cases. The clinical characteristics of the cohort and each age group are shown in Table 1.

The magnitude of myopic shift was inversely associated with age at surgery (Table 1). The youngest cohort (1 to <2.5 years) demonstrated the largest myopic shift, with a mean 5-year refractive change of -3.20 D (95% CI: -5.66, -0.74) and final refractive change of -5.47 D (95% CI: -7.93, -3.01), resulting in a mean final refraction of

TABLE 1. Clinical characteristics by age group.

	Overall n = 71 (100%)	1 to <2.5 y n = 8 (11.27%)	2.5 to <4 y n = 14 (19.72%)	4 to <7 y n = 26 (36.62%)	7 to <13 y n = 23 (32.39%)
Age (y)[a]	6.04 (3.06)	1.88 (0.30)	3.42 (0.23)	5.32 (0.87)	9.70 (1.81)
Male[b]	37 (52.11%)	5 (62.50%)	11 (78.57%)	12 (46.15%)	9 (29.13%)
Bilateral cataract[b]	52 (73.24%)	5 (62.50%)	12 (85.71%)	20 (76.92%)	15 (65.22%)
Axial length (mm)[a]	23.15 (1.98)	22.87 (2.23)	21.77 (1.27)	23.17 (2.01)	23.90 (1.86)
Average K (D)[a]	44.32 (1.80)	45.03 (1.84)	44.37 (1.37)	44.20 (2.29)	44.16 (1.36)
IOL Power (D)[a]	20.38 (5.41)	18.25 (6.33)	23.68 (4.92)	20.56 (4.60)	19.30 (5.74)
IOL fixation					
Capsular bag[b]	63 (88.73%)	6 (75.00%)	11 (78.57%)	25 (96.15%)	20 (86.96%)
Sulcus[b]	8 (11.27%)	2 (25.00%)	1 (7.14%)	1 (3.85%)	3 (13.04%)
PCCC performed[b]	48 (67.61%)	8 (100%)	12 (85.71%)	20 (76.92%)	15 (65.22%)
Early postoperative refraction (D)[c]	0.58 (0.09, 1.07)	1.89 (0.50, 3.28)	1.96 (0.34, 3.59)	0.34 (-0.42, 1.11)	-0.45 (-1.05, 0.16)
5-year change of refraction (D)[c]	-1.71 (-2.32, -1.10)	-3.20 (-5.66, -0.74)	-2.5 (-4.27, -0.73)	-1.43 (-2.26, -0.60)	-1.02 (-1.68, -0.37)
5-year actual refraction (D)[c]	-1.13 (-1.62, -0.64)	-1.31 (-2.70, 0.08)	-0.54 (-2.16, 1.09)	-1.09 (-1.85, -0.32)	-1.47 (-2.07, -0.86)
Final change of refraction (D)[c]	-2.75 (-3.35, -2.14)	-5.47 (-7.93, -3.01)	-4.24 (-6.01, -2.47)	-2.35 (-3.18, -1.52)	-1.33 (-1.99, -0.67)
Final actual refraction (D)[c]	-2.16 (-2.66, -1.67)	-3.58 (-4.97, -2.19)	-2.28 (-3.90, -0.66)	-2.01 (-2.78, -1.24)	-1.78 (-2.38, -1.17)
Final refraction within ±2.00 D[a]	38 (53.52%)	4 (50.00%)	4 (28.57%)	13 (50.00%)	17 (73.91%)
Final refraction within ±1.00 D[a]	22 (30.99%)	2 (25.00%)	2 (14.29%)	8 (30.77%)	10 (43.48%)
Follow-up time (y)[a]	8.74 (3.01)	9.16 (4.41)	10.80 (3.47)	8.73 (2.71)	7.56 (1.93)
Age at final visit (y)[a]	14.78 (3.27)	11.04 (4.49)	14.22 (3.62)	14.05 (2.50)	17.26 (0.60)

[a]Mean (SD), [b]N (%), [c]Adjusted mean (95% confidence interval) by linear mixed model.
Abbreviations: y = year; mm = millimeter; K = keratometry; D = diopter; IOL = intraocular lens

-3.58 D (95% CI: -4.97, -2.19). In contrast, the oldest group (7 to <13 years) showed greater stability, with 5-year and final refractive changes of -1.02 D (95% CI: -1.68, -0.37) and -1.33 D (95% CI: -1.99, -0.67), respectively, and a final refraction of -1.78 D (95% CI: -2.38, -1.17). Overall, the mean final refraction was -2.16 D (95% CI: -2.66, -1.67). Only 53.52% and 30.99% of all eyes achieved final refractive outcomes within ±2.00 D and ±1.00 D of emmetropia, respectively. For bilateral cases, refractive changes and actual refractions at the 5-year and final follow-ups did not differ significantly between the first and second operated eyes (all P > 0.05, paired t-test). The distributions of postoperative refractive errors and postoperative refractive change across age groups are shown in Fig 1.

When stratified by early postoperative refraction (Table 2), eyes that were initially hyperopic or emmetropic demonstrated a significantly larger 5-year myopic shift compared with those that were initially myopic (-2.24 D vs. -1.25 D; P = 0.026). Despite slower progression, the

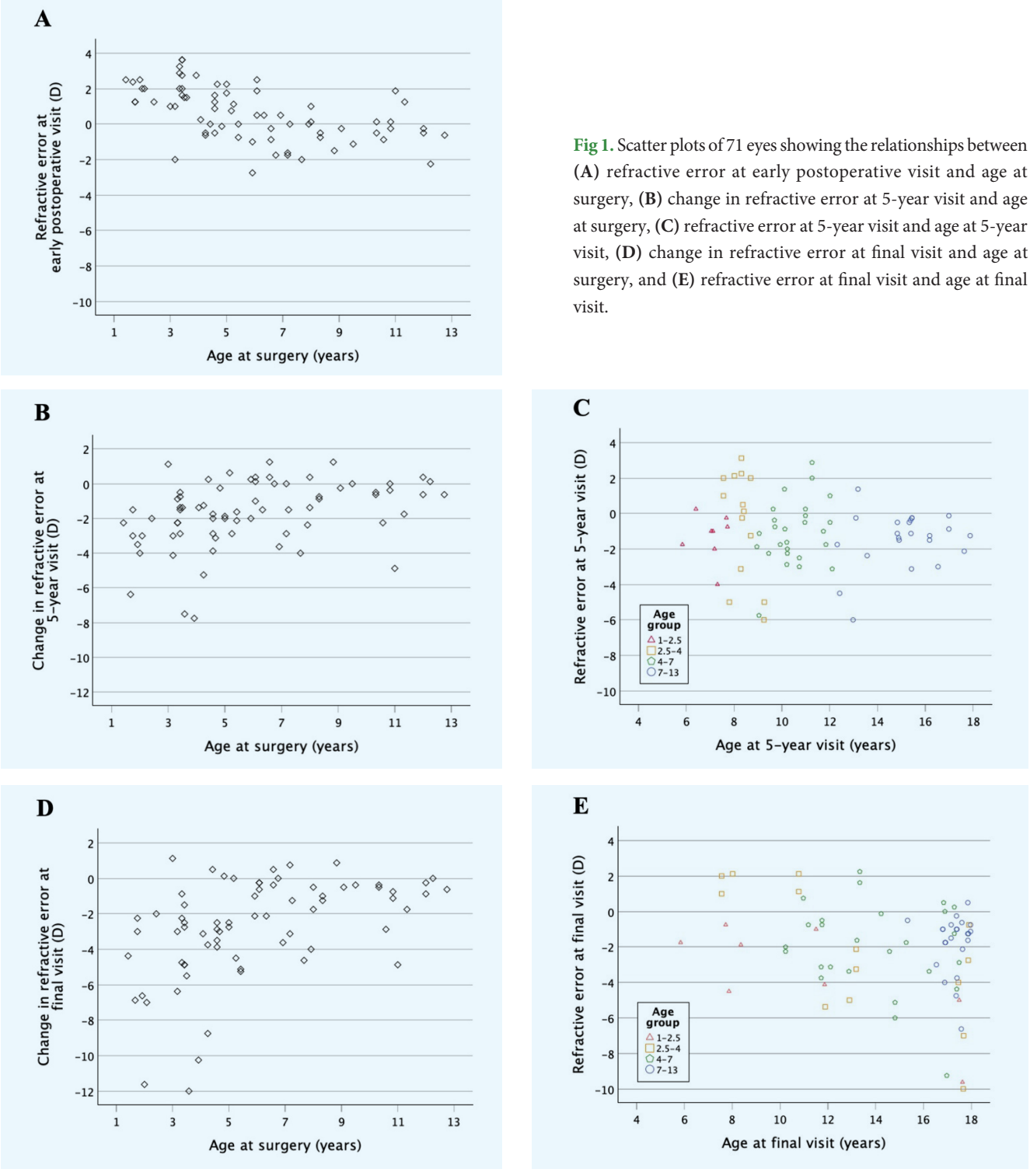

Fig 1. Scatter plots of 71 eyes showing the relationships between **(A)** refractive error at early postoperative visit and age at surgery, **(B)** change in refractive error at 5-year visit and age at surgery, **(C)** refractive error at 5-year visit and age at 5-year visit, **(D)** change in refractive error at final visit and age at surgery, and **(E)** refractive error at final visit and age at final visit.

TABLE 2. Refractive error according to early postoperative status.

	Hyperopia or Emmetropia n = 33 (46.48%)	Myopia n = 38 (53.52%)	P value[a]
5-year change of refraction (D)[a]	-2.24 (-2.87, -1.60)	-1.25 (-1.84, -0.66)	0.026
5-year actual refraction (D)[a]	-0.63 (-1.30, -0.05)	-1.56 (-2.19, -0.93)	0.047
Final change of refraction (D)[a]	-3.44 (-4.40, -2.49)	-2.16 (-3.05, -1.27)	0.054
Final actual refraction (D)[a]	-1.80 (-2.71, -0.89)	-2.48 (-3.33, -1.63)	0.28

[a]Adjusted mean (95% confidence interval) by linear mixed model.
Abbreviation: D = diopter.

initially myopic group remained more myopic at final follow-up (-2.48 D vs. -1.80 D); however, this difference was not statistically significant (P = 0.28).

Multivariate analysis (Table 3) identified preoperative axial length (P = 0.005) and follow-up duration (P = 0.003) as independent predictors of final refractive change. Although age at surgery and early postoperative refraction were significant in univariate analysis, they were not independently associated with final refractive change after multivariate adjustment.

DISCUSSION

This longitudinal analysis confirms that refractive stability following pediatric cataract surgery with primary IOL implantation is strongly age-dependent, with younger children manifesting significantly greater myopic shift. In children younger than 4 years, the mean early postoperative refraction was approximately +1.90 D; however, substantial myopic progression was observed by 5 years of follow-up. These findings suggest that the degree of initial hyperopic targeting in this age group may be insufficient to offset subsequent axial elongation. Our findings suggest that current recommendations may warrant adjustment, as reluctance to target sufficient hyperopia due to amblyopia concerns often results in pronounced adolescent myopia. Thus, surgical planning must carefully balance the immediate risk of amblyopia against the long-term consequences of axial elongation.

Our findings are consistent with several long-term studies. A recent PEDIG study[10] that followed 186 eyes

TABLE 3. Factors associated with final change in refractive error: linear mixed model analysis.

	Univariate			Multivariate		
	β	95%CI	P value	β	95%CI	P value
Age at surgery (y)	0.44	0.25, 0.64	<0.001	0.13	-0.11, 0.36	0.28
Axial length (mm)	0.76	0.45, 1.07	<0.001	0.48	0.15, 0.81	0.005
Average K (D)	-0.31	-0.69, 0.07	0.1	-0.04	-0.38, 0.30	0.82
Early postoperative refraction (D)	-0.69	-1.10, -0.27	0.002	-0.41	-0.90, 0.07	0.09
Follow-up time (y)	-0.45	-0.64, -0.25	<0.001	-0.32	-0.52, -0.12	0.003
Laterality (unilateral)	0.16	-1.36, 1.68	0.83	-	-	-

Abbreviations: CI = confidence interval; y = year; mm = millimeter; K = keratometry; D = diopter

over 5 years reported a mean 5-year refractive change of -2.16 D and confirmed the inverse relationship between age and myopic shift. While our 5-year myopic shifts were comparable, our final outcomes revealed continued progression, particularly in the youngest cohort. Notably, PEDIG reported 44% and 71% of eyes within ±1.00 D and ±2.00 D of emmetropia at 5 years, respectively, whereas our cohort achieved lower rates (30.99% and 53.52%, respectively). This difference likely stems from our longer follow-up duration and relatively less hyperopic postoperative refraction, resulting in greater residual myopia. *VanderVeen et al.*[9] analyzed 162 eyes with a median follow-up of 9.6 years and reported a clear age-dependent trend, with median final myopic shift ranging from -5.75 D in children aged 0–2 years to -1.00 D in those aged 8–10 years. In comparison, our patients aged 2.5 to <4 years demonstrated a larger myopic shift compared to the corresponding age group in their cohort. Furthermore, although infants younger than 1 were excluded from our study, our youngest group (1 to <2.5 years) still exhibited a myopic shift comparable to their 0-to 2-year group, suggesting that Asian populations may be predisposed to a more aggressive myopic shift.

Given the well-documented higher incidence of myopia in Asian populations,[12] recent studies have emphasized aggressive refractive changes in this demographic. *Li et al.*[13] retrospectively studied 126 children with unilateral cataract, reporting a mean myopic shift of -2.60 D over 3 years. They confirmed that younger age was strongly associated with greater change and proposed specific target refraction guidelines for unilateral cases. Similarly, *Lekskul et al.*[11] observed significant progression in 84 Thai eyes; despite adherence to standard undercorrection guidelines, 60.8% developed myopia, with a mean final error of -2.26 D among myopic eyes.

We observed that initial postoperative myopia was associated with a smaller subsequent myopic shift, aligning with the PEDIG study[10] and the myopic defocus theory.[14] This finding contrasts with previous reports that found no correlation between refractive target and refractive change.[15,16] However, despite exhibiting a smaller myopic shift, the early myopic group remained more myopic at final follow-up. Further longitudinal studies are warranted to confirm these associations.

In our multivariate analysis, preoperative axial length and follow-up duration were independent predictors of myopic shift, whereas age at surgery was not significant. This is likely due to strong biological collinearity. While chronological age serves as a generalized temporal proxy for ocular development, baseline axial length provides a precise anatomical measurement directly dictating the eye's optical mechanics and future refraction.[17] Although this differs from previous literature emphasizing age as the primary predictor, our results align with modern, biometry-driven models incorporating axial data. For instance, *Trivedi et al.* demonstrated that baseline axial length outweighs age in predicting postoperative ocular growth.[18] Furthermore, our finding that longer preoperative axial length correlates with reduced myopic shift parallels the PEDIG study.[10] Beyond axial length, *VanderVeen et al.*[9] noted that flatter baseline keratometry predicted greater myopic shift, advocating for higher hyperopic targets in such cases. Regarding laterality, previous studies[19,20] found that unilateral cases were associated with larger myopic shift compared with bilateral cases, particularly when interocular axial length differences were small.[13,21]

While infants under 1 year of age were excluded from this cohort, the profound and highly variable myopic shifts observed in our youngest patients (1 to <2.5 years) reinforce the rationale for delaying primary IOL implantation. Because the infant eye undergoes logarithmic axial elongation during the first 12 months, biometric prediction in this age group is exceptionally unpredictable. This cautious approach aligns with the long-term findings of the Infant Aphakia Treatment Study, which demonstrated that primary IOL implantation in infants under 6 months carries a significantly higher risk of adverse events and secondary intraocular surgeries without a corresponding long-term visual acuity benefit compared to aphakic contact lens correction.[22]

Based on our longitudinal data and observed final refractive change, more hyperopic refractive targets than those conventionally planned may be warranted.[5,9] Specifically, our findings support targeting approximately +5.0 to +6.0 D in children younger than 2.5 years, +3.5 to +4.5 D in those aged 2.5 to <4 years, +1.5 to +3.0 D in children aged 4 to <7 years, and +0.5 to +1.0 D in those aged 7 to <13 years. These targets represent a more hyperopic aim than commonly selected initial postoperative refractions across all age groups and reflect the magnitude of long-term myopic progression observed in our cohort. However, because these recommendations introduce a significant amblyopia risk during early visual development, a rigorous optical rehabilitation protocol is mandatory. This includes immediate correction of residual hyperopia with spectacles or contact lenses, potentially adding bifocals at school age. Furthermore, strict occlusion therapy and frequent refractions are required to titrate the hyperopic correction as the eye elongates.

This study has several limitations inherent to its retrospective design. First, the relatively small sample

size limited detailed subgroup analysis. Notably, infants younger than 1 year were not included, reflecting our institutional preference for aphakic spectacle correction in this age group. Second, the 20-year study duration introduces potential heterogeneity in surgical techniques and IOL selection. Third, although records of intended refractive targets were incomplete, early postoperative outcomes indicate a preference for conservative targeting to optimize immediate vision. Consequently, the final myopia in our cohort resulted from these conservative initial targets confronting accelerated axial growth. Finally, data regarding compliance with postoperative refractive correction were unavailable. Future studies should prospectively validate the proposed age-specific refractive nomogram in Asian children using standardized surgical and biometric protocols. Multicenter collaboration will be essential to confirm its generalizability and refine target refraction based on axial growth patterns. In addition, emerging strategies such as adjustable intraocular lenses or planned secondary IOL exchange may offer promising solutions to mitigate long-term myopic shift while minimizing early amblyopia risk.

CONCLUSIONS

In conclusion, age at surgery remains the primary predictor of myopic shift, with the greatest magnitude and variability observed in the youngest group. Given the profound myopic shift in Asian eyes, further studies are warranted to determine if targeting higher residual hyperopia is necessary to achieve optimal long-term emmetropia.

Data Availability Statement

The data supporting the findings of this study are available from the corresponding author upon reasonable request.

ACKNOWLEDGEMENT

The authors thank Julaporn Pooliam for assistance with statistical analysis.

DECLARATIONS

Grants and Funding Information

None.

Conflict of Interest

None.

Registration Number of Clinical Trial

None.

Author Contributions

Conceptualization and methodology, A.L. and T.S. ; Investigation, A.L. ; Formal analysis, A.L. ; Visualization and writing – original draft, A.L. ; Writing – review and editing, A.L. and T.S. ; Supervision, T.S. All authors have read and agreed to the final version of the manuscript.

Use of Artificial Intelligence

During preparation of the manuscript, the authors used ChatGPT 5.3 to refine grammar and improve wording.

REFERENCES

1. Rahi JS, Dezateux C, British Congenital Cataract Interest G. Measuring and interpreting the incidence of congenital ocular anomalies: lessons from a national study of congenital cataract in the UK. Invest Ophthalmol Vis Sci. 2001;42(7):1444–8.
2. Kim DG, Lee DY, Woo SJ, Park KH, Park SJ. Nationwide incidence of congenital and infantile cataract requiring surgery in Korea. Sci Rep. 2024;14(1):5251.
3. Weakley DR, Jr., Lynn MJ, Dubois L, Cotsonis G, Wilson ME, Buckley EG, et al. Myopic Shift 5 Years after Intraocular Lens Implantation in the Infant Aphakia Treatment Study. Ophthalmology. 2017;124(6):822–7.
4. Repka MX, Dean TW, Kraker RT, Li Z, Yen KG, de Alba Campomanes AG, et al. Visual Acuity and Ophthalmic Outcomes 5 Years After Cataract Surgery Among Children Younger Than 13 Years. JAMA Ophthalmol. 2022;140(3):269–76.
5. Enyedi LB, Peterseim MW, Freedman SF, Buckley EG. Refractive changes after pediatric intraocular lens implantation. Am J Ophthalmol. 1998;126(6):772–81.
6. Plager DA, Kipfer H, Sprunger DT, Sondhi N, Neely DE. Refractive change in pediatric pseudophakia: 6-year follow-up. J Cataract Refract Surg. 2002;28(5):810–5.
7. Crouch ER, Crouch ER, Jr., Pressman SH. Prospective analysis of pediatric pseudophakia: myopic shift and postoperative outcomes. J AAPOS. 2002;6(5):277–82.
8. Orazbekov L, Smagulova S, Ruslanuly K. Long-term Results of Congenital Cataract Surgery with Primary Intraocular Lens Implantation: A Case-Control Study of Three Age Groups. J Curr Ophthalmol. 2022;34(3):290–6.
9. VanderVeen DK, Oke I, Nihalani BR. Deviations From Age-Adjusted Normative Biometry Measures in Children Undergoing Cataract Surgery: Implications for Postoperative Target Refraction and IOL Power Selection. Am J Ophthalmol. 2022;239:190–201.
10. Pediatric Eye Disease Investigator G, de Alba Campomanes AG, Repka MX, Hatt SR, Sutherland DR, Leske DA, et al. Myopic Shift over 5 Years after Pediatric Lensectomy with Primary Intraocular Lens Implantation. Ophthalmology. 2025;132(3):290–8.
11. Lekskul A, Chuephanich P, Charoenkijkajorn C. Long-term outcomes of intended undercorrection intraocular lens implantation in pediatric cataract. Clin Ophthalmol. 2018;12:1905–11.
12. Wu PC, Huang HM, Yu HJ, Fang PC, Chen CT. Epidemiology of Myopia. Asia Pac J Ophthalmol (Phila). 2016;5(6):386–93.
13. Li Y, Jin G, Tan Y, Chen H, Jin J, Luo L, et al. Myopic shift after primary intraocular lens implantation in unilateral cataract children and its association with preoperative ocular parameters. J Cataract Refract Surg. 2025;51(1):53–9.

14. Troilo D, Wallman J. The regulation of eye growth and refractive state: an experimental study of emmetropization. Vision Res. 1991;31(7-8):1237–50.
15. Lambert SR, Archer SM, Wilson ME, Trivedi RH, del Monte MA, Lynn M. Long-term Outcomes of Undercorrection Versus Full Correction After Unilateral Intraocular Lens Implantation in Children. Am J Ophthalmol. 2012;153(4):602–8, 8 e1.
16. Valeina S, Heede S, Erts R, Sepetiene S, Skaistkalne E, Radecka L, et al. Factors influencing myopic shift in children after intraocular lens implantation. Eur J Ophthalmol. 2020;30(5):933–40.
17. Surachatkumtonekul T, Jaruniphakul P. Prevalence, Predictive Factors, and Surgical Outcomes of Strabismus in High Myopia. Siriraj Med J. 2026;78(3):175–84.
18. Trivedi RH, Barnwell E, Wolf B, Wilson ME. A Model to Predict Postoperative Axial Length in Children Undergoing Bilateral Cataract Surgery With Primary Intraocular Lens Implantation. Am J Ophthalmol. 2019;206:228–34.
19. Gouws P, Hussin HM, Markham RH. Long term results of primary posterior chamber intraocular lens implantation for congenital cataract in the first year of life. Br J Ophthalmol. 2006;90(8):975–8.
20. Hoevenaars NE, Polling JR, Wolfs RC. Prediction error and myopic shift after intraocular lens implantation in paediatric cataract patients. Br J Ophthalmol. 2011;95(8):1082–5.
21. Trivedi RH, Wilson ME, Jr. Changes in interocular axial length after pediatric cataract surgery. J AAPOS. 2007;11(3):225–9.
22. Infant Aphakia Treatment Study Group, Lambert SR, Lynn MJ, et al. Comparison of contact lens and intraocular lens correction of monocular aphakia during infancy: a randomized clinical trial of HOTV optotype acuity at age 4.5 years and clinical findings at age 5 years. JAMA Ophthalmol. 2014;132(6):676-82.

Digital Reference Frame Anchored to the Pedicle Screw–rod Construct for O-arm–Assisted Pedicle Screw Insertion: A Pilot Study

Korawish Mekariya, M.D.[1], Chonlatid Ruangsangthong, M.D.[1], Dollaporn Anopas, Ph.D.[2], Chatupon Chotigavanichaya, M.D.[1], Ekkapoj Korwutthikulrangsri, M.D.[1], Sirichai Wilartratsami, M.D.[1], Werasak Sutipornpalangkul, M.D.[1], Panya Luksanapruksa, M.D.[1], Monchai Ruangchainikom, M.D.[1,*]

[1]*Department of Orthopaedic Surgery, Faculty of Medicine Siriraj Hospital, Mahidol University, Bangkok, Thailand,* [2]*Biodesign Innovation Center and Siriraj Integrative Center for Neglected Parasitic Diseases, Department of Parasitology, Faculty of Medicine Siriraj Hospital, Mahidol University, Bangkok, Thailand.*

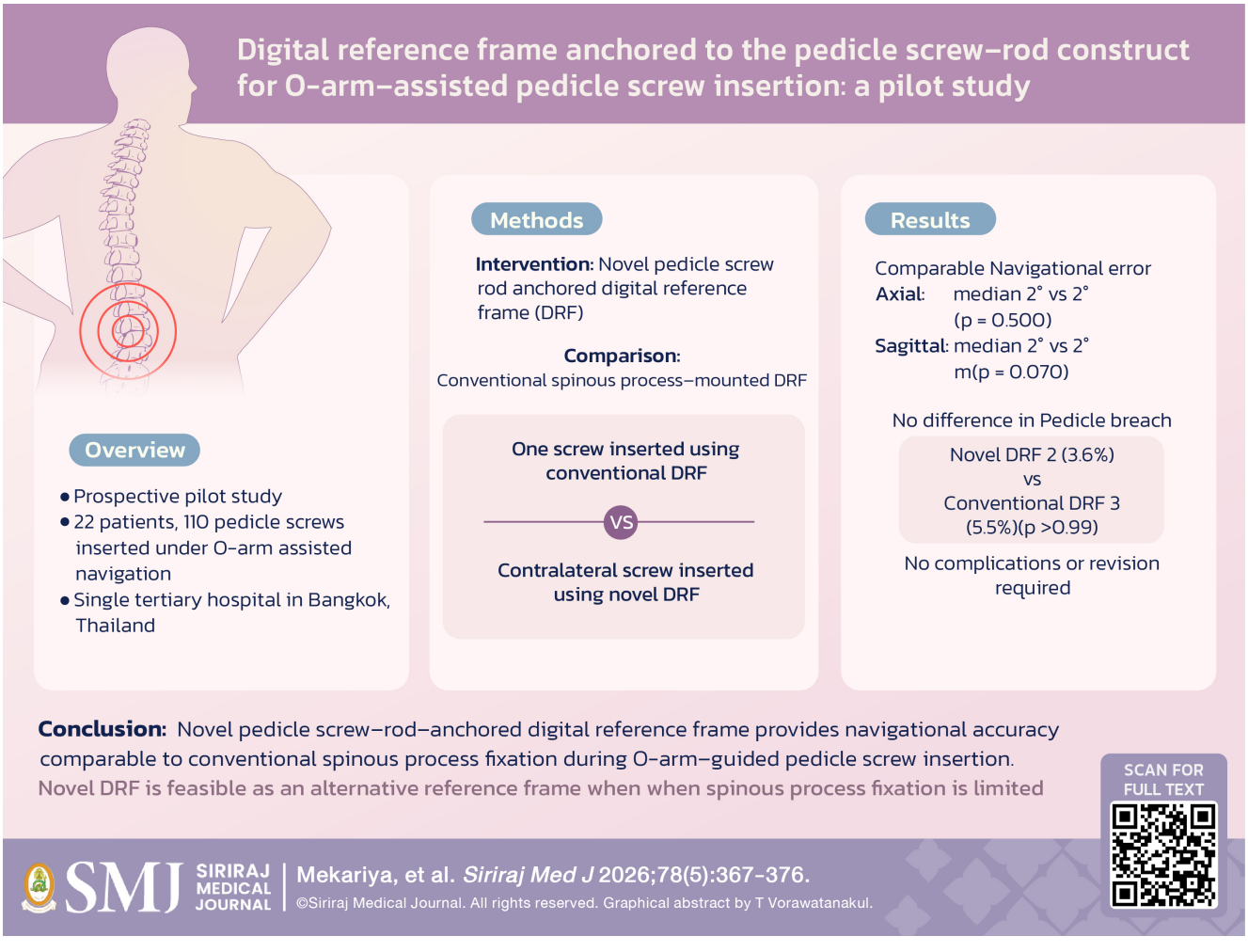

*Corresponding author: Monchai Ruangchainikom
E-mail: monchai.ortho@gmail.com
Received 14 October 2025 Revised 5 March 2026 Accepted 8 March 2026
ORCID ID: http://orcid.org/0000-0003-0525-6390
https://doi.org/10.33192/smj.v78i5.278286

All material is licensed under terms of the Creative Commons Attribution 4.0 International (CC-BY-NC-ND 4.0) license unless otherwise stated.

ABSTRACT

Objective: Accurate pedicle screw placement reduces neurological injury and complications. Although O-arm navigation improves precision, navigation error and digital reference frame (DRF) instability persist. This study aims to develop and evaluate a novel DRF anchored to the pedicle screw–rod construct as an alternative to spinous process–based attachment for O-arm–assisted pedicle screw insertion.

Materials and Methods: This pilot study enrolled patients undergoing O-arm–assisted thoracolumbar pedicular screw instrumentation between November 2024 and February 2025. At each instrumented level, one pedicle screw was placed using the conventional DRF, and the contralateral pedicle screw was placed using the novel pedicle screw–rod–anchored DRF. We compared the 2 DRF systems within each level. Navigational error was defined as the angular deviation between the intraoperative virtual trajectory and the screw position on postoperative computed tomography. Pedicle breaches were identified and graded.

Results: Twenty-two patients (110 pedicle screws) were included. The median navigational error did not differ between novel and conventional DRF in axial (2°, $P = 0.500$) or sagittal (2°, $P = 0.070$) planes. Subgroup analyses by level and pathology (degenerative, tumor, trauma) showed no significant differences. Minor pedicle breaches (< 2 mm) occurred in 2 screws with the novel DRF and 3 screws with the conventional DRF, all mid-thoracic and without clinical complications.

Conclusions: The novel pedicle screw–rod–anchored DRF provides navigational accuracy comparable to the conventional system. These findings support its feasibility as an alternative reference frame for O-arm–guided spinal procedures when spinous process fixation is limited.

Keywords: Digital reference frame; O-arm navigation; pedicle screw placement; pilot study; spinal surgery (Siriraj Med J 2026;78(5):367-376)

INTRODUCTION

Pedicle screws are the cornerstone of modern spinal fixation and are used extensively across degenerative disease, deformity correction, and spinal trauma. Instrumentation with a pedicle screw–rod system improves construct strength and fusion rates in spinal fusion surgery.[1,2] The use of pedicle screws has increased markedly over recent decades.

Accurate pedicle screw placement with optimal pedicle purchase is essential to prevent neurologic injury and instrumentation failure. Traditional techniques report misplacement rates as high as 15% - 40%[3,4], leading to nerve root injury, vascular or visceral damage, and reoperation for pedicle breaches.[5] To address these risks, guidance strategies include C-arm fluoroscopy, 3-dimensional (3D) O-arm navigation, and robotic-assisted methods.[4,6] Among these, 3D O-arm navigation is widely accepted. It has been used in Thailand for more than 10 years and yields superior accuracy, faster insertion, and lower complication rates compared to conventional methods.[7]

The 3D O-arm navigation system integrates real-time intraoperative 3D imaging with trajectory guidance for pedicle screw placement. Intraoperative 3D images are obtained using 2 components: a digital reference frame (DRF) attached to the patient for automated registration and the O-arm system (Medtronic Surgical Technologies, Louisville, CO, USA), which generates computed tomographic–like images. The navigation platform then processes these images, enabling simultaneous visualization of screw trajectories and spinal anatomy during surgery.

Despite the high accuracy of O-arm–assisted techniques, navigational error and pedicle screw misplacement persist in up to 3% of cases.[8,9] These events are often attributed to "navigation drift"—a deviation of the navigated trajectory from the true pedicle path—reported particularly in deformity surgery.[10] Contributing factors include increased DRF–to–instrumented-level distance, DRF displacement, inadequate neuromuscular blockade with patient movement, and obstruction between the DRF and the optical tracking cameras.[10-12] Conventional DRF fixation—typically to the spinous process or, via an additional incision, to the iliac bone—faces additional challenges in specific contexts. These include pediatric cases with small, unstable spinous processes; scoliosis procedures requiring intraoperative neuromonitoring without muscle relaxation; and revision surgery when the spinous process has been removed.[13]

To address these limitations, we developed a novel DRF for O-arm navigation that attaches directly to the

pedicle screw–rod construct to improve stability. We hypothesized that this design would deliver navigational accuracy comparable to, or greater than, traditional DRF systems. This pilot study evaluated the novel DRF with a modified attachment mechanism in patients undergoing elective surgery for degenerative and deformity conditions of the spine.

MATERIALS AND METHODS

Study design and registration

This single-center pilot study was conducted at a tertiary hospital in Bangkok, Thailand, from November 1, 2024 to February 28, 2025. The protocol received Institutional Review Board approval before enrollment. The trial was registered with the Thai Clinical Trials Registry (TCTR20250506005). All participants provided written informed consent after receiving detailed study information.

Participants and eligibility

Adults aged > 18 years who underwent open posterior thoracolumbar instrumentation requiring 3D O-arm–navigated pedicle screw insertion were eligible. The exclusion criteria were spinal infection (e.g., spondylodiscitis or spinal epidural abscess), revision spine surgery, pedicle screw insertion extending to the cervical level, or planned pelvic fixation. Baseline demographics and clinical characteristics were recorded after enrollment.

Development and design of the novel DRF

The novel DRF was manufactured from certified medical-grade titanium (Orthopesia Co., Bangkok, Thailand), similar to the conventional DRF. Instead of a claw-tooth spinous process clamp, the device uses a straight, rod-shaped lower base, 5.0-6.0 mm in diameter, that connects to polyaxial or monoaxial pedicle screw heads. The connection is secured when the screw nut is tightened (Figs 1, 2). Standard sterilization protocols were applied to the DRF set before surgery.

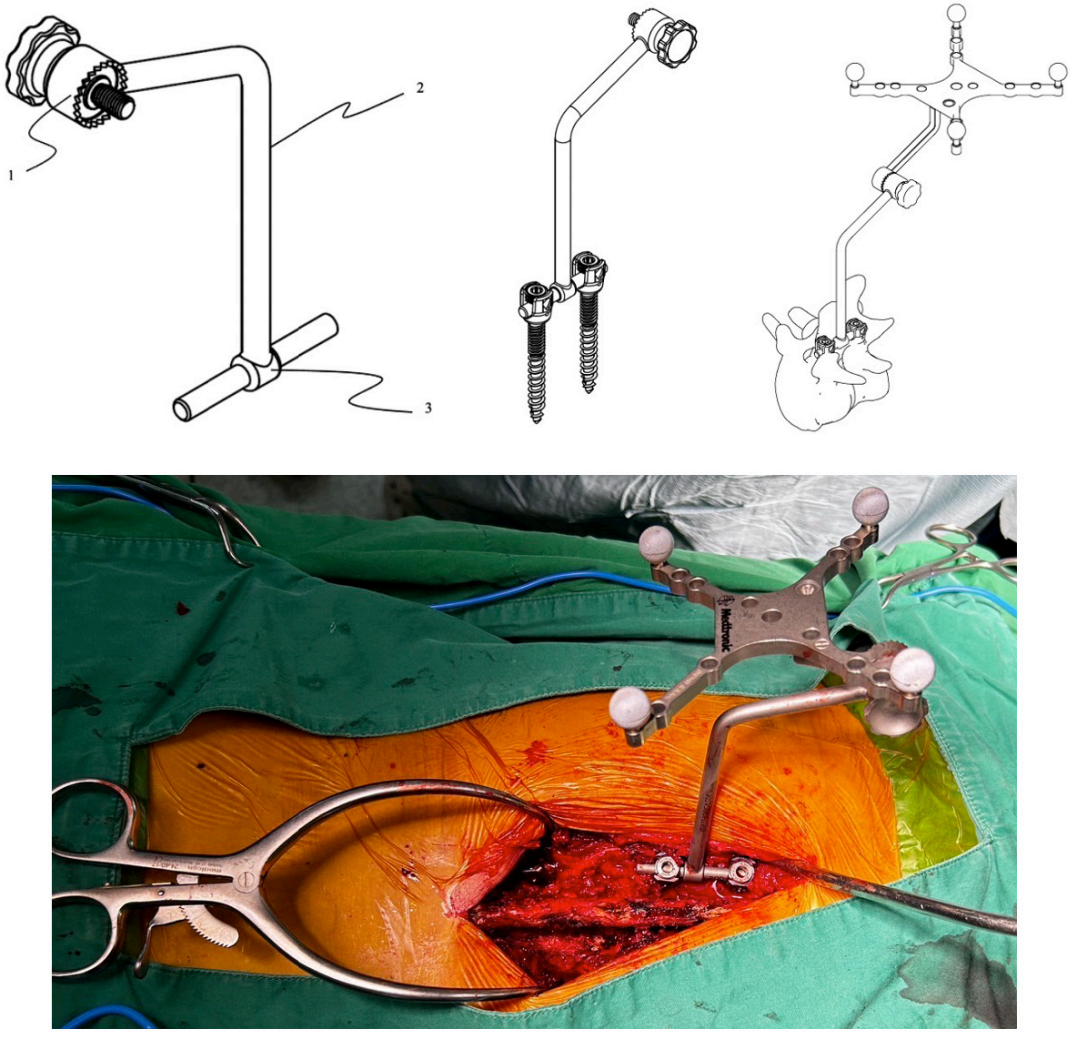

Fig 1. Design and Dimensions of the Novel Digital Reference Frame (DRF) with a Straight Rod-Like Base Attachment for Pedicular Screw head. The novel dynamic reference frame (DRF) consists of three main components: (1) A Hirth joint connector with tapered teeth, designed to connect with standard reference markers (light-reflecting spheres). (2) An arm of the DRF angled at 110°. (3) A rod-shaped base connector that attaches to pedicle screw heads.

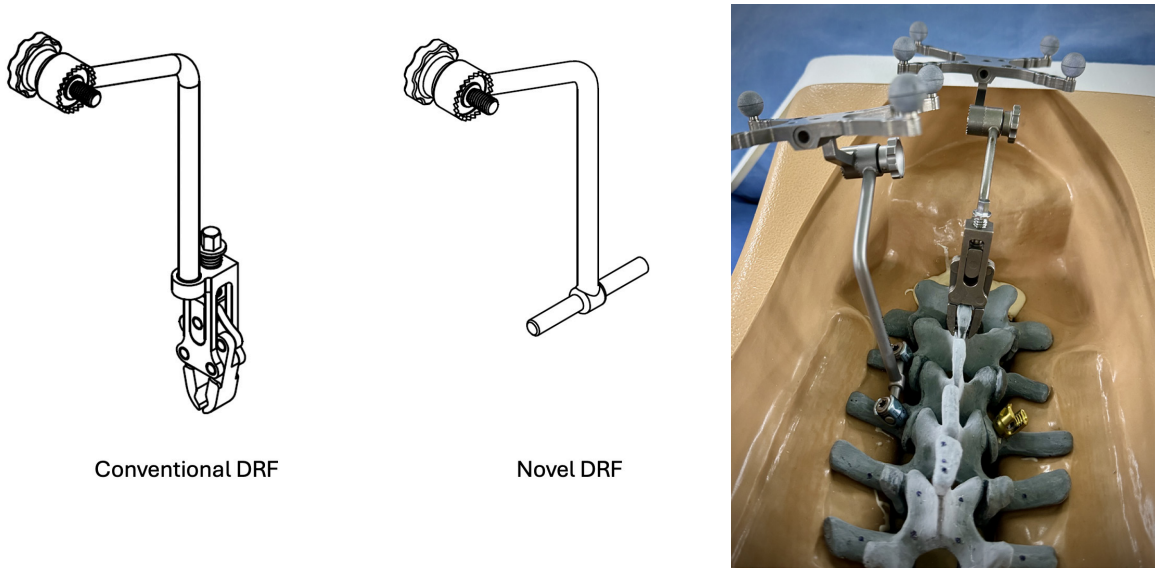

Fig 2. Comparison Between the Conventional Digital Reference Frame (DRF) Using Spinous Process Attachment and the Novel DRF Using Pedicular Screw Attachment.

Surgical procedure

All patients underwent open posterior surgery with 3D O-arm–navigated guidance. After induction of general anesthesia, patients were positioned prone on a Jackson frame. The operative field was prepped and draped, followed by a midline longitudinal incision and subperiosteal detachment of paraspinal musculature. The index level was confirmed with C-arm fluoroscopy. Dissection proceeded to the spinous process, lamina, and facet joints. A conventional DRF was attached to the spinous process 1–2 levels adjacent to the planned instrumented level. The O-arm and StealthStation navigation system (Medtronic Navigation, Louisville, CO, USA) were used.

Imaging, registration, and accuracy verification

After the first intraoperative computed tomography, scan image processing and instrument registration were performed. Accuracy was verified with a navigated light-reflecting ball probe pointing to 8 anatomical landmarks: superior and inferior spinous processes; superior laminar borders (left/right); inferior laminar borders (left/right); transverse processes (left/right). The probe's true position was compared with the navigation display. If the discrepancy was > 1 mm, registration was deemed unsuccessful ("not passed"), and image acquisition and registration were repeated.

DRF allocation, pedicle screw insertion, and surgical procedure

After passing accuracy verification, half of the planned pedicle screws were inserted under guidance from the conventional DRF. The conventional DRF was removed, and the novel DRF was attached to the inserted screws nearest the spinous process previously used for conventional attachment. A second intraoperative scan and registration were performed using the novel DRF as the reference, and the remaining pedicle screws were inserted. Final intraoperative computed tomography was obtained to assess pedicle screw position. Based on the preoperative plan and the patient's diagnosis, the procedures after pedicle screw insertion were done as indicated, including laminectomy, posterior spinal fusion, or interbody fusion.

Navigational error and pedicle breaches

Two spine surgeons evaluated navigational error and pedicle breaches for the conventional and novel DRF. The navigational error angle was defined as the angular difference between the StealthStation navigation system's virtual screw trajectory and the actual pedicle screw trajectory shown on postoperative computed tomography at each vertebral level (Fig 3). On axial images, the angle was measured between the screw axis and the midsagittal vertebral axis (Figs 3A, B).[14] The midsagittal axis is a line that bisects the vertebral body and aligns with the laminar base and spinous process. On sagittal images, the angle was measured between the screw axis and the superior endplate of the corresponding vertebral body (Figs 3C, D). Pedicle breaches were identified on the final computed tomographic images. Each screw was assessed by perforation direction in 6 anatomical categories: anterior, lateral, medial, inferomedial, inferolateral, and superior. Pedicle breach severity was graded as follows: Grade 0, no breach (0 mm); Grade 1, > 0 mm and ≤ 2 mm; Grade 2, > 2 mm and ≤ 4 mm; and Grade 3, > 4 mm.[15]

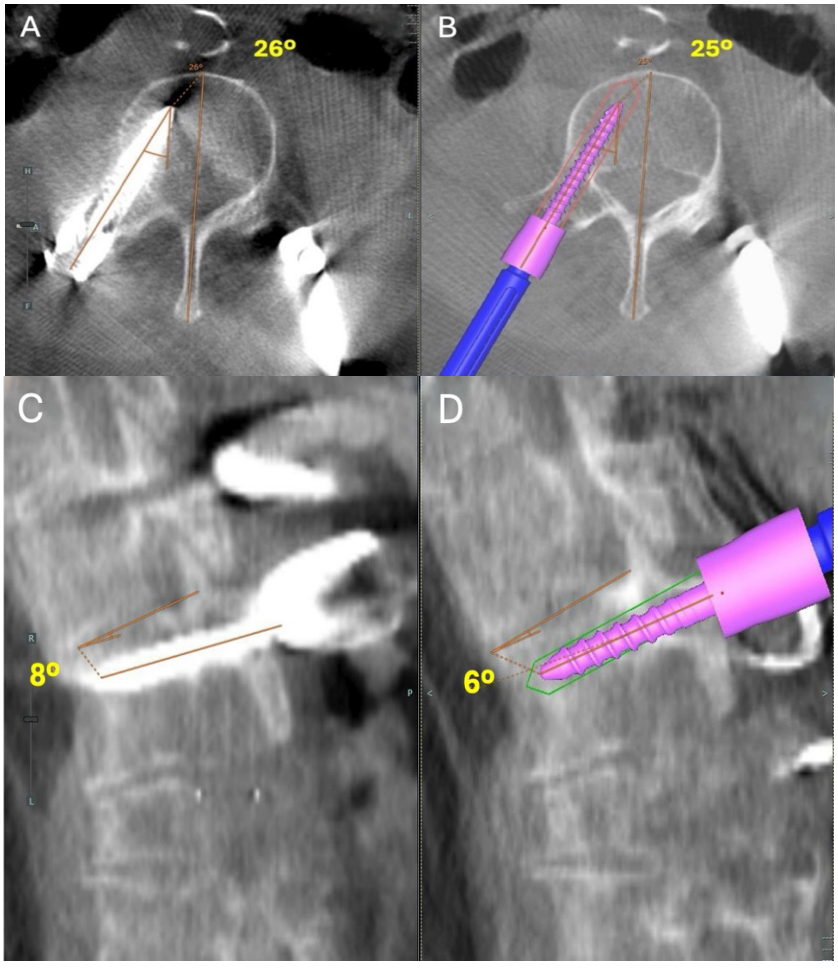

Fig 3. Measurement of navigational error in axial and sagittal planes.

Angles are measured in degrees. Navigational error is the absolute angular difference between the navigated and postoperative CT angles. Actual postoperative screw angle relative to the midsagittal vertebral axis (A) and the corresponding O arm–navigated trajectory (B). The axial navigational error in this example is 1°. Actual postoperative screw angle relative to the superior endplate (C) and the navigated trajectory (D). The sagittal navigational error in this example is 2°.

Statistical analysis

Data were analyzed with Stata version 17 (StataCorp LLC, College Station, TX, USA). Categorical variables were summarized as frequencies and percentages. Normality was assessed with the Shapiro–Wilk test. Continuous variables were summarized as means with standard deviations or medians with interquartile ranges, as appropriate. Group comparisons used the independent *t* test or the Mann–Whitney *U* test, as appropriate. All tests were two-sided, and $P < 0.05$ denoted statistical significance.

Sample size calculation

The sample size for this pilot study was determined according to the guidelines proposed by Viechtbauer et al..[16] Assuming a true event rate of 10% and a 90% confidence interval for identifying issues in navigation accuracy, a total of 22 participants was required.

RESULTS

Characteristics of participants

Twenty-four participants were enrolled; 2 were excluded for spondylodiscitis, leaving 22 eligible. Table 1 presents their demographic and clinical characteristics. Most participants (77.3%) underwent surgery for degenerative conditions—spondylolisthesis, spinal stenosis, or adult spinal deformity correction. Three (13.6%) had spinal tumors, and 2 (9.1%) had thoracolumbar fractures. A total of 110 pedicle screws within 55 levels of vertebral bodies were inserted—55 guided by the novel DRF and 55 by the conventional DRF—across different spinal levels. Distribution by level was thoracic 30 (27.3%) and lumbosacral 80 (72.7%).

Comparison of novel versus conventional DRF

Table 2 summarizes the navigational errors for the novel versus the conventional DRF. In the axial view, the median error was 2° for both systems—novel range 0°–6°, conventional range 0°–5°; $P = 0.500$. In the sagittal view, the median error was 2° for both systems—novel range 0°–4°, conventional range 0°–5°; $P = 0.070$. Subgroup analyses by spinal level and patient's diagnosis showed no significant differences in navigational error between the DRF systems. Five Grade 1 pedicle breaches occurred (5/110; 4.5%) with no significant difference between groups (Table 4). In the novel DRF group, there was one 1-mm anterior perforation and one lateral breach. In the conventional DRF group, there were two 1-mm anterior perforations and one 1.5-mm lateral breach. All breaches occurred at mid-thoracic levels (T3–T10); no complications or revisions were required.

TABLE 1. Baseline demographics and characteristics of the participants (n=22, 110 pedicle screw).

Baseline characteristics	N (%)/ Median (Q1, Q3)
Male	13 (59.1)
Age (years) [median (Q1, Q3)]	63.5 (56.3, 71.3)
Body mass index (kg/m^2) [median (Q1, Q3)]	22.4 (20.0, 25.7)
<18.5	4 (18.2)
18.5-22.9	8 (36.4)
≥23.0	10 (45.5)
Medical comorbidities	
Hypertension	11 (50.0)
Diabetes	6 (27.3)
Dyslipidemia	5 (22.7)
Patient's diagnosis	
Degenerative disease	17 (77.3)
Tumor	3 (13.6)
Fracture	2 (9.1)
Level of screw placement (n=110)	
Thoracic	30 (27.3)
Lumbosacral	80 (72.7)

TABLE 2. Comparison of navigation error between novel and conventional digital reference frame (DRF) (total n=110 screws)

Plane of measurement	Novel DRF (n=55)			Conventional DRF (n=55)			*p*-value[a]
	Navigation angle (°) median (Q1, Q3)	Real angle (°) median (Q1, Q3)	Navigation error (°) median (min-max)	Navigation angle (°) median (Q1, Q3)	Real angle (°) median (Q1, Q3)	Navigation error (°) median (min-max)	
Axial	12 (7, 19)	11 (6, 17)	2 (0, 6)	10 (7, 17)	10 (6, 17)	2 (0, 5)	0.500
Sagittal	4 (2, 6)	3 (2, 4)	2 (0, 4)	4 (2, 6)	2 (2, 6)	2 (0, 5)	0.070

[a] Navigation errors between novel and conventional DRF screw placements were compared using Mann–Whitney U test

TABLE 3. Subgroup analysis of navigation error between novel and conventional digital reference frame (DRF) by screw placement and patient's diagnosis (N=110 screws)

Characteristics	No. of compared screws	Novel DRF (n=55)			Conventional DRF (n=55)			*p*-value[a]
		Navigation angle (°)	Real angle (°)	Navigation error (°)	Navigation angle (°)	Real angle (°)	Navigation error (°)	
		median (Q1, Q3)		median (min-max)	median (Q1, Q3)		median (min-max)	
Level of screw placement								
Thoracic level								
Axial	30	7 (6, 9.5)	7.5 (5, 10)	2 (0, 4)	7.5 (6, 9.5)	6.5 (4.5, 9)	1 (0, 4)	0.359
Sagittal		3.5 (2, 5)	2 (1, 3)	2 (0, 3)	3 (2, 4)	2 (1, 2)	2 (0, 3)	0.703
Lumbosacral level								
Axial	80	15 (8, 20)	14 (8, 19)	2 (0, 6)	12 (8, 19)	14 (7, 19)	2 (0, 5)	0.169
Sagittal		4 (3, 6)	3 (2, 6)	2 (0, 4)	4 (2, 6)	3 (2, 6)	2 (0, 5)	0.070
Patient's diagnosis								
Degenerative								
Axial	90	14 (8, 19)	13 (7, 17)	2 (0, 6)	10 (8, 17)	13 (7, 17)	2 (0, 5)	0.458
Sagittal		4 (3, 6)	3 (2, 6)	2 (0, 4)	4 (3, 6)	3 (2, 6)	2 (0, 5)	0.070
Tumor								
Axial	12	7 (6, 12)	7 (6, 8)	1 (0, 4)	7.5 (6, 8)	5 (4, 6)	2 (0, 3)	0.625
Sagittal		3 (2, 4)	1 (1, 2)	2 (0, 3)	2.5 (1, 3)	0.5 (0, 6)	2 (0, 3)	>0.999
Fracture								
Axial	8	16.5 (7.5, 26)	16.5 (5.5, 28)	2 (2, 4)	17.5 (5, 32.5)	16.5 (3.5, 30)	1.5 (1, 4)	0.500
Sagittal		1.5 (1, 4)	1 (1, 2)	0.5 (0, 3)	1.5 (0.5, 3.5)	1 (0.5, 1.5)	0.5 (0, 3)	>0.999

[a] Navigation errors between novel and conventional DRF screw placements were compared using Mann–Whitney U test

TABLE 4. Incidence of pedicle breaches between novel and conventional digital reference frame (DRF)

Pedicle breaches (No. of screws)	Novel DRF (n=55) n (%)	Conventional DRF (n=55) n (%)	*p*-value[a]
Grade I (≤2mm)	2 (3.6%)	3 (5.5%)	*p*>0.999
Grade II and above (>2mm)	0 (0)	0 (0)	-

[a] Fisher's exact test was used to compare the incidence of pedicle breeches between novel and conventional DRF screw placements

DISCUSSION

This pilot study demonstrated the feasibility of a novel DRF attachment for O-arm–assisted pedicle screw insertion. By fixing the DRF to the screw–rod construct rather than the spinous process, accuracy remained comparable to the conventional approach without increasing navigational error.

The median navigational error was 2° in both axial and sagittal planes for the novel and conventional DRF. These values are consistent with prior O-arm–assisted pedicle screw insertion studies. Oertel et al reported a mean navigational error of 2.8° ± 1.9°.[8] Mathew et al evaluated 104 screws during L4–5 fusion and found mean deviations of 2.31° and 3.11° in the axial and sagittal planes, respectively.[17] Comparable performance was reported for computer-assisted placement using preoperative computed tomography, with a mean angular deviation of 2.28° ± 1.92°.[18] Our minor anterior perforation rate (2.7%) and lateral pedicle breach rate (1.8%) align with prior O-arm navigation studies reporting breach rates of 1.0%–3.2%.[8,9,17] Collectively, these data support the conclusion that O-arm navigation improves screw placement accuracy and reduces misplacement compared with conventional freehand techniques.[9]

Intraoperative computed tomography with O-arm navigation provides precise visualization of spinal anatomy in the surgical position, enabling real-time, image-guided instrumentation. However, because the DRF is mounted intraoperatively, the mounting process can introduce navigational error. Deviations between planned and actual screw trajectories—termed navigational error or the "drift phenomenon"—have been reported in up to 16.7% of O-arm–guided cases.[10] Contributing factors include reference frame–to–target level distance due to intervertebral flexibility, movement due to inadequate neuromuscular blockade or respiration, and DRF displacement.[10-12] To mitigate these issues, we developed a DRF that attaches to the screw–rod construct to enhance intraoperative stability and aim reduce error sources.

In the present study, navigational error and pedicle breach rates did not differ significantly between the novel and conventional DRF in either plane. This finding likely reflects that conventional spinous process clamp fixation may provide sufficient stability for accurate tracking in our cohort, which predominantly comprised adult degenerative, trauma, and tumor cases. In this population, residual navigational error may be driven primarily by factors other than DRF attachment, including intrinsic system-related error during image acquisition, processing, or tracking, as well as iatrogenic micro-movement during instrumentation. Therefore, a construct-based DRF may not confer a measurable advantage in standard anatomy where conventional fixation performs reliably. Notably, the absence of a significant difference may also represent a Type II error given the pilot design and the limited proportion of highly complex cases in which dynamic shift is more pronounced and DRF instability is most problematic. Future studies should therefore focus on higher-complexity cohorts, such as severe scoliosis or high-grade spondylolisthesis, to more definitively evaluate whether construct-based fixation provides a stability-related benefit. In addition, the numerical differences in median angular error between groups were small, and modest reductions may not translate into clinically meaningful differences in routine adult anatomy. Nevertheless, even minor angular deviations may be more consequential in high-risk settings, such as severe scoliosis with narrow or dysplastic pedicles or patients with compromised bone quality, underscoring the need for targeted evaluation in these populations.

Although conventional fixation appeared adequate in our cohort, traditional spinous process attachment poses limitations, particularly in revision surgery where a laminectomy has removed suitable bony landmarks. In such settings, surgeons may secure the DRF at a distant level with an intact spinous process, which increases navigational error. Alternatively, iliac fixation can be used, but it requires an additional incision. One feasibility of the novel DRF design is that it permits DRF attachment through existing pedicle screws, avoiding the need for additional incisions with comparable accuracy.

Similarly, pediatric deformity surgery poses challenges for conventional DRF fixation because spinous processes are often small or underdeveloped, limiting stable DRF fixation and increasing intraoperative motion that can cause navigational error. Prior O-arm navigation studies in this population report malposition rates of 8.5%–9.8% in complex deformity and scoliosis, with a tracker placement of more than 3 levels from the target identified as a notable risk factor.[19,20] One study documented Grade 2–3 pedicle breaches in up to 21% of patients with dystrophic scoliosis secondary to neurofibromatosis type 1.[20] Although multiple factors contribute—including small, rotated, dysplastic pedicles and optical tracking signal deviation—we hypothesize that instability of DRF attachment is a key driver of navigational error in this cohort. A stronger, screw–rod–anchored DRF reduces susceptibility to displacement from patient movement or inadvertent instrument contact.[21] To our knowledge, this is the first study to evaluate DRF fixation through pedicle screws. Although our cohort did not include pediatric deformity cases, the comparable accuracy observed in

typical adult indications might support the feasibility of construct-based fixation and provide a rationale for future evaluation in pediatric and complex deformity in which conventional placement is difficult or unfeasible.

Nonetheless, several limitations must be acknowledged. First, as a pilot investigation, this study was designed to assess feasibility and characterize navigational accuracy rather than to demonstrate the superiority of the novel DRF over conventional attachment. Accordingly, the findings primarily inform sample size calculations for adequately powered comparative studies. Second, although the device targets challenging scenarios, such as revision surgery and pediatric deformity, our cohort predominantly comprised degenerative, tumor, and trauma indications only. Consequently, performance of the device in more complex settings remains unvalidated, and navigational accuracy may be lower with higher pedicle breach rates in such populations. Third, the study had limited ability to evaluate differences in the most clinically consequential safety outcome. Specifically, no Grade II or higher pedicle breaches (>2 mm) occurred in either group, resulting in a very low event rate and minimal statistical power to detect between-group differences in clinically significant breaches. Therefore, the absence of severe breaches difference and any potential safety benefit of this pilot study should be interpreted cautiously. Finally, we did not evaluate the biomechanical stability of the DRF under dynamic loading. Future cadaveric or benchtop biomechanical studies could quantify stability, characterize failure modes, and define any mechanical advantages in simulated surgical environments.

CONCLUSIONS

This pilot study demonstrates that a novel DRF attached to the pedicle screw–rod construct achieves navigational accuracy comparable to a conventional spinous process–mounted DRF during O-arm–assisted pedicle screw insertion. These results provide a foundation for future trials and support continued development of alternative DRF strategies, particularly for complex spinal deformity surgery and revision cases.

Data Availability Statement

The data that support the findings of this study are available from the corresponding author upon reasonable request. The data are not publicly available due to privacy or ethical restrictions.

ACKNOWLEDGEMENT

The authors thank Miss Pinprapha Boonhyad of the Orthopaedic Research Unit of the Department of Orthopaedic Surgery, Faculty of Medicine Siriraj Hospital, Mahidol University, Bangkok, Thailand, for her assistance with data documentation, archiving, and statistical analysis.

DECLARATIONS

Grants and Funding Information

This research project is supported by Siriraj research development fund, Grant number (IO) R016738002, Faculty of Medicine Siriraj Hospital, Mahidol University.

Conflict of Interest

The authors declare that there are no conflicts of interest. No financial support was received from companies that produce or distribute the drugs, devices, or materials described in this report.

Registration Number of Clinical Trial

The trial was registered with the Thai Clinical Trials Registry (TCTR20250506005).

Author Contributions

KM: Conceptualization, Project administration, Writing – original draft, Investigation, Formal analysis, Writing – review & editing; PL: Conceptualization, Project administration, Writing – original draft, Investigation; DA: Conceptualization, Project administration, Writing – original draft, Formal analysis; MR: Conceptualization, Project administration, Writing – original draft, Investigation, Formal analysis, Writing – review & editing; CR: Investigation, Formal analysis; EK: Investigation; CC: Investigation; SW: Investigation; WS: Investigation.

Ethics approval and consent to participate

This prospective cohort study was approved by the Siriraj Institutional Review Board (COA no. Si 610/2024). All methods were performed in accordance with relevant guidelines and regulations. Written informed consent was obtained from all participants.

Use of Artificial Intelligence

None.

Abbreviations

3D: 3-dimensional
DRF: Digital reference frame

REFERENCES

1. Cho W, Cho SK, Wu C. The biomechanics of pedicle screw-based instrumentation. J Bone Joint Surg Br. 2010;92-B(8):1061-5.
2. Rose PS, Lenke LG, Bridwell KH, Mulconrey DS, Cronen

GA, Buchowski JM, et al. Pedicle Screw Instrumentation for Adult Idiopathic Scoliosis. Spine. 2009;34(8):852-7.
3. Amiot L-P, Lang K, Putzier M, Zippel H, Labelle H. Comparative Results Between Conventional and Computer-Assisted Pedicle Screw Installation in the Thoracic, Lumbar, and Sacral Spine. Spine. 2000;25(5):606-14.
4. Gelalis ID, Paschos NK, Pakos EE, Politis AN, Arnaoutoglou CM, Karageorgos AC, et al. Accuracy of pedicle screw placement: a systematic review of prospective in vivo studies comparing free hand, fluoroscopy guidance and navigation techniques. Eur Spine J. 2012;21(2):247-55.
5. Hicks JM, Singla A, Shen FH, Arlet V. Complications of Pedicle Screw Fixation in Scoliosis Surgery. Spine. 2010;35(11):E465-E70.
6. Alomari S, Lubelski D, Lehner K, Tang A, Wolinsky J-P, Theodore N, et al. Safety and Accuracy of Freehand Pedicle Screw Placement and the Role of Intraoperative O-arm: A Single Institution Experience. Spine. 2022.
7. Sun J, Wu D, Wang Q, Wei Y, Yuan F. Pedicle Screw Insertion: Is O-Arm–Based Navigation Superior to the Conventional Freehand Technique? A Systematic Review and Meta-Analysis. World Neurosurg. 2020;144:e87-e99.
8. Oertel MF, Hobart J, Stein M, Schreiber V, Scharbrodt W. Clinical and methodological precision of spinal navigation assisted by 3D intraoperative O-arm radiographic imaging. J Neurosurg Spine. 2011;14(4):532-6.
9. Silbermann J, Riese F, Allam Y, Reichert T, Koeppert H, Gutberlet M. Computer tomography assessment of pedicle screw placement in lumbar and sacral spine: comparison between free-hand and O-arm based navigation techniques. Eur Spine J. 2011;20(6):875-81.
10. Zhao J, Jiang H, Zhuge Y, Gao R, Wang C, Ma J, et al. Risk Factors for the Drift Phenomenon in O-arm Navigation-Assisted Pedicle Screw Placement during Spinal Deformity Surgery. Orthop Surg. 2023;15(1):118-23.
11. Guha D, Jakubovic R, Gupta S, Fehlings MG, Mainprize TG, Yee A, et al. Intraoperative Error Propagation in 3-Dimensional Spinal Navigation From Nonsegmental Registration: A Prospective Cadaveric and Clinical Study. Global Spine J. 2019;9(5):512-20.
12. Tauchi R, Imagama S, Sakai Y, Ito Z, Ando K, Muramoto A, et al. The correlation between cervical range of motion and misplacement of cervical pedicle screws during cervical posterior spinal fixation surgery using a CT-based navigation system. Eur Spine J. 2013;22(7):1504-8.
13. Roberts SB, Tsirikos AI. Paediatric Spinal Deformity Surgery: Complications and Their Management. Healthcare (Basel). 2022;10(12):2519.
14. Kotani Y, Abumi K, Ito M, Takahata M, Sudo H, Ohshima S, et al. Accuracy analysis of pedicle screw placement in posterior scoliosis surgery: comparison between conventional fluoroscopic and computer-assisted technique. Spine. 2007;32(14):1543-50.
15. Mirza SK, Wiggins GC, Kuntz Iv C, York JE, Bellabarba C, Knonodi MA, et al. Accuracy of thoracic vertebral body screw placement using standard fluoroscopy, fluoroscopic image guidance, and computed tomographic image guidance: a cadaver study. Spine. 2003;28(4):402-13.
16. Viechtbauer W, Smits L, Kotz D, Budé L, Spigt M, Serroyen J, et al. A simple formula for the calculation of sample size in pilot studies. J Clin Epidemiol. 2015;68(11):1375-9.
17. Mathew JE, Mok K, Goulet B. Pedicle violation and Navigational errors in pedicle screw insertion using the intraoperative O-arm: A preliminary report. Int J Spine Surg. 2013;7:e88-94.
18. Kamimura M, Ebara S, Itoh H, Tateiwa Y, Kinoshita T, Takaoka K. Accurate pedicle screw insertion under the control of a computer-assisted image guiding system: laboratory test and clinical study. J Orthop Sci. 1999;4(3):197-206.
19. Jin M, Liu Z, Qiu Y, Yan H, Han X, Zhu Z. Incidence and risk factors for the misplacement of pedicle screws in scoliosis surgery assisted by O-arm navigation-analysis of a large series of one thousand, one hundred and forty five screws. Int Orthop. 2017;41(4):773-80.
20. Jin M, Liu Z, Liu X, Yan H, Han X, Qiu Y, et al. Does intraoperative navigation improve the accuracy of pedicle screw placement in the apical region of dystrophic scoliosis secondary to neurofibromatosis type I: comparison between O-arm navigation and free-hand technique. Eur Spine J. 2016;25(6):1729-37.
21. Rivkin MA, Yocom SS. Thoracolumbar instrumentation with CT-guided navigation (O-arm) in 270 consecutive patients: accuracy rates and lessons learned. Neurosurg Focus. 2014;36(3):E7.

Is Erythema Toxicum Neonatorum in Neonates Associated with Atopic Diseases?

Suthida Chaithirayanon, M.D.[1,*], Napat Chaimongkol[1], Nyda Yotsaranphorn Songkiatkul[1], Siripa Satianvatidkul[1], Suphatsorn Charoenkitmongkol[1], Arpanun Nitayamekin[1], Arucha Treesirichod, M.D.[1], Vorasith Siripornpanich, M.D., Ph.D.[2]

[1]*Department of Pediatrics, Faculty of Medicine, Srinakharinwirot University, Nakhon Nayok 26120, Thailand,* [2]*Research Center for Neuroscience, Institute of Molecular Biosciences, Mahidol University, Nakhon Pathom 73170, Thailand.*

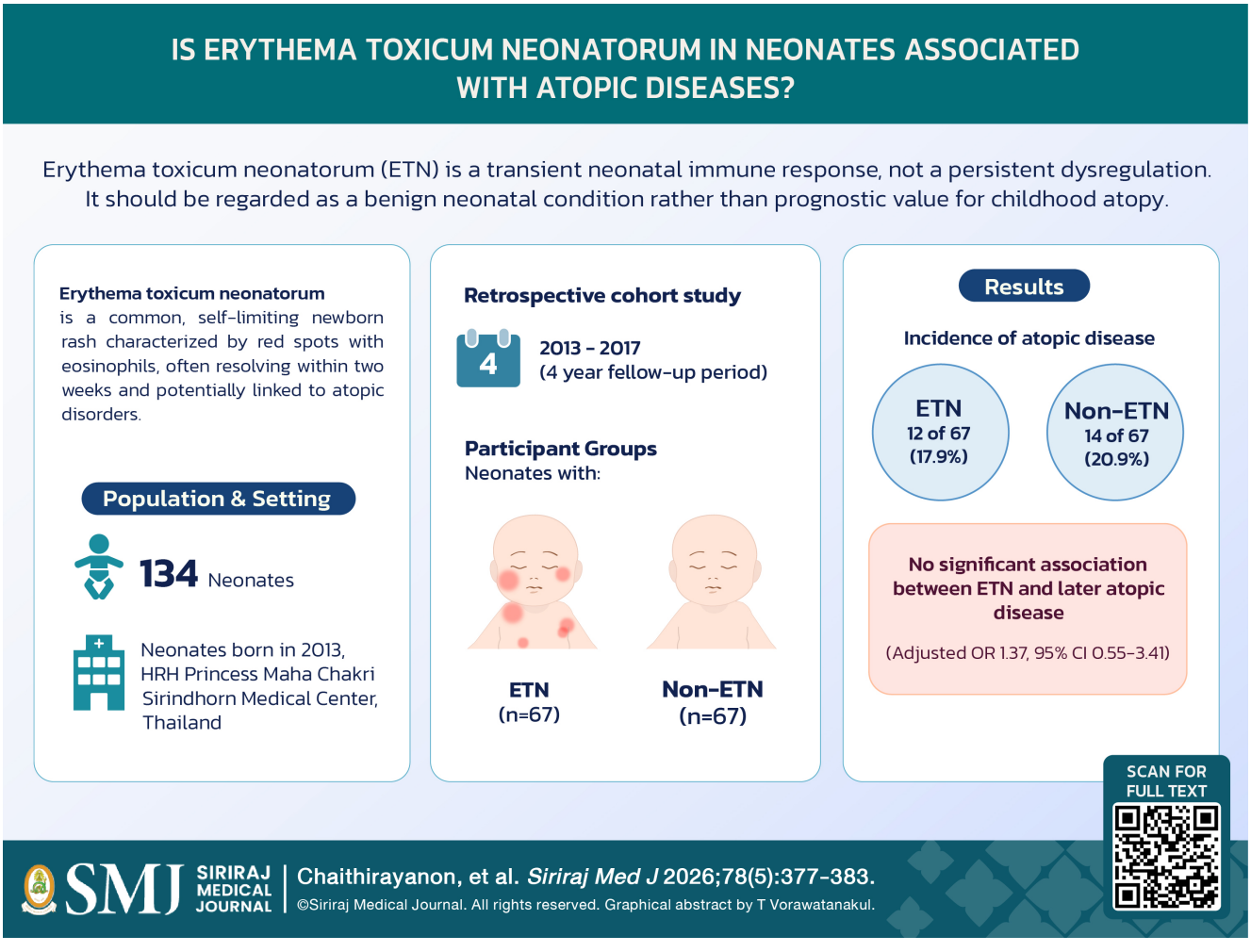

*Corresponding author: Suthida Chaithirayanon
E-mail: suthidachaithirayanon@gmail.com
Received 19 February 2026 Revised 18 March 2026 Accepted 1 April 2026
ORCID ID: http://orcid.org/0009-0000-5734-9850
https://doi.org/10.33192/smj.v78i5.280505

All material is licensed under terms of the Creative Commons Attribution 4.0 International (CC-BY-NC-ND 4.0) license unless otherwise stated.

ABSTRACT

Objective: Erythema toxicum neonatorum (ETN) is a benign rash commonly observed in newborns, typically resolving spontaneously within one to two weeks. The lesions are characterized by multiple erythematous macules containing eosinophils and are known to be associated with peripheral eosinophilia, a condition commonly seen in atopic diseases. Therefore, the presence of ETN may be associated with the subsequent development of atopic diseases. This study aimed to determine the prevalence of atopic diseases in newborns with and without ETN and to evaluate the association between the presence of ETN and the manifestation of atopic diseases during childhood.

Materials and Methods: This retrospective cohort study utilized electronic medical records and telephone interviews of subjects born at HRH Princess Maha Chakri Sirindhorn Medical Center in 2013. Participants were divided into two groups: newborns with ETN and those without ETN. The follow-up period for diagnosing atopic diseases extended to four years after birth (2017).

Results: A total of 134 newborns were included in the study (67 with ETN and 67 without ETN). During the follow-up period, 12 of 67 newborns with ETN and 14 of 67 newborns without ETN developed atopic diseases. Statistical analysis revealed that the presence of ETN was not associated with an increased risk of developing atopic diseases (adjusted odds ratio (OR) 1.37; 95% CI 0.55-3.41). However, a significant association was found between a family history of atopic diseases and the development of atopic conditions in the children.

Conclusions: The presence of ETN does not increase the risk of developing atopic diseases during childhood.

Keywords: Atopic diseases; erythema toxicum neonatorum; newborn; rash (Siriraj Med J 2026;78(5):377-383)

INTRODUCTION

Erythema toxicum neonatorum (ETN) is a benign, self-limited skin condition seen in newborns. ETN is a relatively common skin lesion, affecting approximately 16% to 30% of neonates.[1,2]

It typically presents as erythematous macules, often accompanied by small, white-yellow papules or pustules measuring approximately 1–3 mm in diameter. These lesions are commonly distributed over the trunk, thighs, and buttocks, while the palms and soles are rarely affected. ETN usually appears within the first 2 to 4 days of life and resolves spontaneously within one week without leaving any residual marks.[2]

The reported incidence of ETN ranges from 21% to 41% across studies. The wide variation in incidence is likely due to differences in the timing of neonatal skin assessments among studies.[3] Diagnosis of ETN is primarily clinical, based on its characteristic presentation. In certain cases, the microscopic examination of ETN with Wright stain can be performed, which reveals eosinophils in the superficial layers of the skin[4], particularly near the entrances of subcutaneous ducts. This observation may help explain the absence of lesions on the palms and soles. Additionally, peripheral eosinophilia may be detected in approximately 15% of affected neonates.[3]

To date, the precise etiology of ETN remains unclear. Several hypotheses have been proposed, including allergic reactions, a graft-versus-host-like response, and mechanisms involving the innate antimicrobial barrier.[5] Nonetheless, various studies have examined risk factors associated with ETN. These include increased gestational age at birth, vaginal delivery, higher birth weight, and male sex.[6]

Atopic diseases refer to a group of hereditary allergic disorders characterized by an exaggerated immune response to typically harmless environmental antigens. These diseases are of significant clinical importance due to their high prevalence and substantial impact on quality of life.[7] The prevalence of atopic diseases in children is estimated to range from approximately 10% to 30%, depending on the specific condition.[8,9] This hypersensitivity is mediated through immunoglobulin E (IgE). All atopic diseases fall under the category of Type I hypersensitivity reactions, which occur when an antigen binds to IgE receptors on mast cells, triggering the release of inflammatory mediators such as histamine, proteases, and leukotrienes. These mediators contribute to the characteristic allergic inflammation. The most common atopic diseases consist of asthma, atopic conjunctivitis, allergic rhinitis, atopic dermatitis, and food allergy. The presence of one atopic condition increases the risk of developing additional atopic diseases. Interestingly, recent studies have demonstrated an association between eosinophils and three major atopic diseases: atopic dermatitis, allergic rhinitis, and asthma.[10]

There is currently no clear association between ETN and atopic diseases. While some studies have suggested a link between ETN and an increased risk of developing

atopic conditions later in life, others have found no such association. This study aimed to determine whether ETN in newborns is associated with the development of atopic diseases in childhood.

MATERIALS AND METHODS

Participants

This study was reviewed and approved by the Institutional Review Board for Clinical Research in Humans of Srinakharinwirot University with CoA SWUEC/E/M-024/2566E. Informed consent was obtained from the parents and/or legal guardians of subjects by means of a voluntary written agreement form. The calculation of the sample size for this research was based on a study by Odelram et al.[11] exploring the relationship between eosinophils and atopic disease manifestation. Thus, a total of 134 neonates at HRH Princess Maha Chakri Sirindhorn Medical Center (MSMC) of Srinakharinwirot University, Ongkharak, Thailand from 2013 to 2017 were recruited. These were healthy individuals not admitted to neonatal intensive care unit (NICU), and whose mothers had previously received care at the MSMC antenatal clinic (ANC).

Research design

This study was designed as a retrospective cohort study by analyzing data previously collected from 2013 to 2017, categorizing neonates into either of the two categories – ETN and non-ETN. Children with a history of ETN were identified from the hospital medical database during the aforementioned period, whereas the control group without a history of ETN was randomly selected from infants born at MSMC within the same period. Details of data collection included gender of neonate, date of birth, gestational age, birthweight, mode of delivery, family history of atopy, and smoking in household.

Data collection

Neonates were evaluated by pediatricians or pediatrics residents at MSMC. The data collection form was reviewed by a pediatric dermatologist and a pediatric allergist before being implemented for patient data collection to ensure that all essential information was adequately obtained. Non-invasive full body examinations were carried out and the presence of rash, or the lack thereof, was documented accordingly using the form previously drafted which classified skin manifestations into different categories; Mongolian spot; salmon patch; hemangioma; port wine stain; cytomegalovirus (CMV) rash; Café au lait macule; sebaceous hyperplasia; erythema toxicum neonatorum; milia; desquamation; miliaria; collodion membrane; Epstein pearls; subcutaneous fat necrosis; cutis marmorata; bullous diseases; angel kiss. Neonates were allowed more than one category if presented with several skin manifestations. In addition to the type of rash, other information was noted namely gestational age, date of birth, birth body weight, mode of delivery and maternal underlying diseases. In addition, diagnosis of atopic diseases was performed by experienced pediatricians at MSMC based on clinical manifestations and investigations.

Statistical analyses

Statistical analyses were performed using Statistical Package for the Social Sciences (SPSS) version 22. Frequency data were expressed as percentages (%). For univariate analysis, Chi-square tests were used to compare birth body weight, gender, family history of atopy, and household smoking. For multivariate analysis, adjusted odds ratios (ORs) were calculated from crude odds ratios using the Hosmer-Lemeshow method, accounting for other variables. A p-value < 0.05 was considered statistically significant.

RESULTS

There were 134 participants, of whom 69 (51.5%) were male. Most participants (98.5%) were term newborns. In the ETN group, 35 participants were female (52.2%) and 32 were male (47.8%). Twelve participants with ETN were diagnosed with atopic disease in childhood, in which 7 of them had allergic rhinitis, 8 had atopic dermatitis, 1 had asthma, and none had food allergy. It should also be noted that some individuals may present with multiple atopic diseases. There were 5 participants with a family history of atopic diseases and 6 lived in households with smoking.

In the non-ETN group, there were 30 female participants (44.77%) and 37 male participants (55.22%). Fourteen of the participants without ETN had atopy, with 9 of them had allergic rhinitis, 2 had atopic dermatitis, 4 had asthma and 2 had food allergy. Three participants revealed family history of atopic diseases, and 2 of total non-ETN participants' households had smoking. All information was presented in Tables 1 & 2.

A chi-square test of independence was performed to examine the association between ETN and the development of atopic diseases later in life, as shown in Table 3. Multivariate analysis results are presented in Table 4. In this study, the presence of atopic diseases was the outcome variable, while the exposures included ETN in newborns, gender, household smoking, and family history of atopy. Our results showed that only 17.9% of newborns with ETN developed atopic diseases later in

TABLE 1. Demographic and clinical information between ETN and Non-ETN groups.

Clinical information	ETN (n = 67)	Non-ETN (n = 67)
Gender		
Female	35	30
Male	32	37
Atopic diseases		
Presence	12	14
Absence	55	53
Family history of atopy		
Presence	5	3
Absence	62	64
History of smoking in the family		
Presence	6	2
Absence	61	65

TABLE 2. Type of atopic diseases between ETN and non-ETN group.

Type of atopic diseases	ETN (n = 12)	Non-ETN (n =14)
Allergic rhinitis	7*	9
Atopic dermatitis	8	2
Asthma	1	4
Food allergy	-	2

*Within the data, two participants presented with allergic rhinitis as well as asthma and 4 participants presented with allergic rhinitis as well as atopic dermatitis.

TABLE 3. Chi-square test for factors associated with atopic disease.

Clinical Parameters	Presence of atopic disease				X^2 (df)	p-value
	Presence		Absence			
	N	(%)	N	(%)		
Presence of ETN					0.191 (1)	.662
Yes	12	17.9	55	82.1		
No	14	20.9	53	79.1		
Gender					0.072 (1)	.789
Female	12	18.5	53	81.5		
Male	14	20.3	55	79.7		
Family history of atopic diseases					10.105 (1)	.001
Yes	5	62.5	3	37.5		
No	21	16.7	105	83.3		
Smoking in the household					1.782 (1)	.182
Yes	3	37.5	5	62.5		
No	23	18.3	103	81.7		

TABLE 4. Crude and adjusted odds ratios for the multivariate analysis.

Covariates	Unadjusted Model			Adjusted Model	
	OR	95% CI	p-value	OR	95% CI
Presence of ETN					
ETN	0.83	0.35-1.95	.662	1.37	0.55-3.41
Non-ETN	1.00	-		1.00	-
Gender					
Female	0.89	0.38-2.01	.789	1.11	0.45-2.73
Male	1.00	-		1.00	-
Family history of atopic diseases					
Yes	8.33	1.85-37.58	.001	0.13	0.03-0.63
No	1.00	-		1.00	-
Smoking in the household					
Yes	2.69	0.60-12.06	.182	0.73	0.12-4.53
No	1.00	-		1.00	-

life (Table 3), with an adjusted OR for newborns with ETN was 1.37 (95% CI 0.55-3.41) (Table 4). However, this finding also did not reach statistical significance. Therefore, no significant association was found between the presence of ETN in newborns and the subsequent development of atopic diseases.

The proportion of participants with atopic diseases did not differ significantly by gender or household smoking. However, a significant association was found between a family history of atopy and the development of atopic diseases. Among those with a positive family history, 62.5% developed atopic diseases (Table 3). In the multivariate analysis, a family history of atopy was significantly associated with the development of atopic diseases. The crude odds ratio (OR) was 8.33 (95% CI 1.85–37.58), whereas the adjusted OR was 0.126 (95% CI 0.03–0.63) (Table 4).

DISCUSSION

This study explored the relationship between the presence of ETN at birth and the development of atopic diseases during childhood. Other factors, such as gender, household smoking, and family history of atopy, were also examined. No significant association was found between ETN and atopic diseases. In contrast, participants with a family history of atopy were approximately eight times more likely to develop atopic diseases based on crude OR. The association between family history of atopy and the development of atopic diseases was statistically significant in the current study.

The association between ETN and atopic diseases has been hypothesized based on the presence of eosinophils in ETN skin lesions, as well as the occurrence of eosinophilia in individuals with atopic diseases. Previous studies have shown that blood eosinophil levels are associated with the severity of atopic dermatitis. Specifically, individuals with atopic dermatitis who also have a family history of respiratory atopic diseases were found to have higher peripheral eosinophil counts compared to those without such a family history.[12] Moreover, research has indicated that neonates with elevated eosinophil counts or total IgE levels in cord blood have an increased risk of developing atopic diseases.[13] Another study by Witmer and colleagues reported that neonates with ETN have an increased risk of developing eosinophilic esophagitis, with an odds ratio of 3.52.[14]

Based on these findings, elevated eosinophil levels appear to be associated with the development of atopic diseases such as allergic rhinitis, asthma, and atopic dermatitis. Given that ETN is also characterized by the presence of eosinophils in skin lesions, these observations form the basis of the present research hypothesis: that ETN in infancy may be associated with an increased risk of developing atopic diseases later in life. However, our results from univariate analysis did not reveal that ETN was associated with an increased risk of atopic diseases. On the contrary, it suggested that the presence of ETN rash at birth might be a protective factor against atopic diseases (OR=0.826), compared to the control group (neonates without ETN). Compared with the prospective

study by Gonzalez Echeverría[4] in 1997 in which the most common atopic manifestation with ETN as a possible risk factor was atopic dermatitis, the results of this study were similar as atopic dermatitis was the most common in the ETN sample group. However, this information could not be reliably concluded due to the insignificant *p*-values, which could be a result of a small sample size, and unadjusted confounding factors. This warrants the need to include a larger sample size to further study the relationships.

With regard to gender, females were 20% less likely to develop atopic diseases than males (p=.889), but there was no statistical significance. In other studies, male was three times more likely to develop asthma than female pre-puberty. However, there were no difference in the prevalence and severity of allergic dermatitis and allergic rhinitis in both genders.[15,16] With respect to smoking exposure, neonates exposed to household smoke exhibited a higher likelihood of developing atopic diseases compared with unexposed neonates; however, this association did not reach statistical significance. This finding is partly consistent with the systematic review and meta-analysis by Kantor et al., which demonstrated that both passive and active smoking are associated with an increased prevalence of allergic dermatitis.[17]

Due to the insignificant results in this study, there is no definite conclusion on the relationships between the development of atopic diseases from both factors, sex and smoking in household. The only statistically significant factor associated with the development of atopic diseases in this study was a family history of atopy. However, a discrepancy was observed between the crude and adjusted odds ratios. Specifically, the crude OR indicated that neonates with a family history of atopy were more likely to develop atopic diseases (OR 8.33, 95% CI 1.85–37.58), whereas the adjusted OR suggested an inverse association (OR 0.126, 95% CI 0.03–0.63), representing a reversal in the direction of effect. The authors postulate that this inconsistency may be attributable to the small sample size, which can introduce unmeasured confounding and lead to model instability during multivariate adjustment. In addition, when considering the existing literature, most studies consistently demonstrate that a family history of atopy is a significant risk factor for the development of atopic diseases. Previous studies have identified family history of atopy as one of the most important predisposing factors for atopy in childhood, with one atopic parent conferring approximately a 25% risk, and two atopic parents increasing the risk to around 50%.[18,19] Therefore, based on the crude OR and clinical plausibility, a family history of atopy is more likely to be a risk factor for the development of atopic diseases rather than a protective factor, as suggested by the adjusted OR.

The clinical implication of this study is that physicians may reassure parents about ETN in the neonatal period is unlikely to be associated with the subsequent development of atopic diseases. Nevertheless, obtaining a family history of atopy remains important for guiding anticipatory counseling and early preventive strategies in infant care to reduce the risk of atopic diseases in childhood.

Limitation

The main limitation of this study is the low statistical power. The sample size was 67 participants per group, which is considered rather small and could make it difficult to detect true effects or relationships of ETN and the development of atopy. Apart from this, due to the nature of this study being a retrospective cohort study, there is potential for recall bias and inaccurate data collection. However, this bias was minimized by double-checking the electronic medical records of each participant.

CONCLUSION

In conclusion, the relationship between ETN rash at birth and the development of atopy in childhood is inconclusive. The only statistically significant predisposing factor in this study is family history of atopy. This is largely due to inadequate sample size. Further study is needed to include larger and more representative sample size for meaningful and trustworthy scientific contribution.

Data Availability Statement

Data will be made available on request.

ACKNOWLEDGEMENTS

The authors would like to express their sincere gratitude to all patients and their parents/guardians who participated in this study. The authors also sincerely thank the medical records staff for their assistance in coordinating patient data. The authors gratefully acknowledge the research grant provided by HRH Princess Mahachakri Sirindhorn Medical Center, Faculty of Medicine, Srinakharinwirot University.

DECLARATIONS

Grants and Funding Information

This study was supported by a research grant from HRH Princess Mahachakri Sirindhorn Medical Center, Faculty of Medicine, Srinakharinwirot University (Contract No 400/2567).

Conflict of Interest

All authors declare no conflicts of interest.

Registration Number of Clinical Trial

None.

Author Contributions

Conceptualization and methodology, S.C.1 and A.T.; Data collection, N.C., N.S., S.S., S.C.2, and A.N.; Formal analysis, N.C., N.S., S.S., S.C.2, and A.N.; Manuscript writing (first draft), N.C., N.S., S.S., S.C.2, and A.N.; Writing – review and editing, S.C.1, A.T., and V.S.; Supervision, V.S.; All authors have read and agreed to the final version of the manuscript.

Use of Artificial Intelligence

ChatGPT (OpenAI) was used solely for language editing of complex sentences. All AI-assisted content was carefully reviewed, validated, and approved by the authors to ensure accuracy and adherence to academic and ethical standards.

REFERENCES

1. Chang MW, Jiang SB, Orlow SJ. Atypical erythema toxicum neonatorum of delayed onset in a term infant. Pediatr Dermatol. 1999;16(2):137-41.
2. Monteagudo B, Labandeira J, Cabanillas M, Acevedo A, Toribio J. Prospective study of erythema toxicum neonatorum: epidemiology predisposing factors. Pediatr Dermatol. 2012;29(2):166-8.
3. Eichenfield LF, Frieden IJ, Esterly NB. Neonatal Dermatology. 2nd ed. Philadelphia: Saunders, 2008.
4. González Echeverría F, Martínez Rodríguez J, Ancín Chandía T, Córdoba Iturriaga A. Is neonatal toxic erythema a risk factor in the development of allergy in childhood? An Esp Pediatr. 1997;47(5):515-20.
5. Boralevi F. Erythema toxicum neonatorum: Still a Problem in 2005? Dermatology (Basel). 2005;210(4):257-8.
6. Liu C, Feng J, Qu R, Zhou H, Ma H, Niu X, et al. Epidemiologic study of the predisposing factors in erythema toxicum neonatorum. Dermatology (Basel). 2005;210(4):269-72.
7. Monti F, Agostini F, Gobbi F, Neri E, Schianchi S, Arcangeli F. Quality of life measures in Italian children with atopic dermatitis and their families. Ital J Pediatr. 2011;37:59.
8. Thomsen SF. Epidemiology and natural history of atopic diseases. Eur Clin Respir J. 2015;2:10.3402.
9. Puangpet P, Boonpuen N, Saipornchai K, Suchaoin R, Poompakdeepan P, McFadden J. Patch testing of Thai children with eczema. Siriraj Med J. 2023;75(2):70-5.
10. Martin LB, Kita H, Leiferman KM, Gleich GJ. Eosinophils in allergy: role in disease, degranulation, and cytokines. Int Arch Allergy Immunol. 1996;109(3):207-15.
11. Odelram H, Björkstén B, Leander E, Kjellman NI. Predictors of atopy in newborn babies. Allergy. 1995;50(7):585-92.
12. Uehara M, Izukura R, Sawai T. Blood eosinophilia in atopic dermatitis. Clin Exp Dermatol. 1990;15(4):264-6.
13. Crnković HT, Bendelja K, Šimić Klarić A, Tomić Rajić M, Drkulec V, Aberle N. Family history and cord blood eosinophil count as predictors for atopic manifestations. Cent Eur J Public Health. 2019;27(4):267-71.
14. Witmer CP, Susi A, Min SB, Nylund CM. Early infant risk factors for pediatric eosinophilic esophagitis. J Pediatr Gastroenterol Nutr. 2018;67(5):610-5.
15. Herr M, Clarisse B, Nikasinovic L, Foucault C, Le Marec AM, Giordanella JP, et al. Does allergic rhinitis exist in infancy? Findings from the PARIS birth cohort. Allergy. 2011;66(2):214-21.
16. Ong PY, Boguniewicz M. Atopic dermatitis. Prim Care. 2008;35(1):105-17, vii.
17. Kantor R, Kim A, Thyssen JP, Silverberg JI. Association of atopic dermatitis with smoking: A systematic review and meta-analysis. J Am Acad Dermatol. 2016;75(6):1119-25.e1.
18. Thomsen SF. Epidemiology and natural history of atopic diseases. Eur Clin Respir J. 2015;2.
19. Ravn NH, Halling AS, Berkowitz AG, Rinnov MR, Silverberg JI, Egeberg A, Thyssen JP. How does parental history of atopic disease predict the risk of atopic dermatitis in a child? A systematic review and meta-analysis. J Allergy Clin Immunol. 2020;145(4):1182-93.

The Outcomes of Siriraj's Classification for Giant Inguinal Hernia: A Literature Review and Meta-analysis

Watsaphon Tangkullayanone, M.D., Chawisa Nampoolsuksan, M.D., Thikamporn Tawantanakorn, M.D., Tharathorn Suwatthanarak, M.D., Nicha Sriworanan, M.D., Voraboot Taweerutchana, M.D., Thammawat Parakonthun, M.D., Chinarong Phalanusitthepha, M.D., Jirawat Swangsri, M.D., Thawatchai Akaraviputh, M.D., Asada Methasate, M.D., Vitoon Chinswangwattanakul, M.D., Atthaphorn Trakarnsanga, M.D.*

Minimally Invasive Surgery Unit, Department of Surgery, Faculty of Medicine Siriraj Hospital, Mahidol University, Bangkok, Thailand.

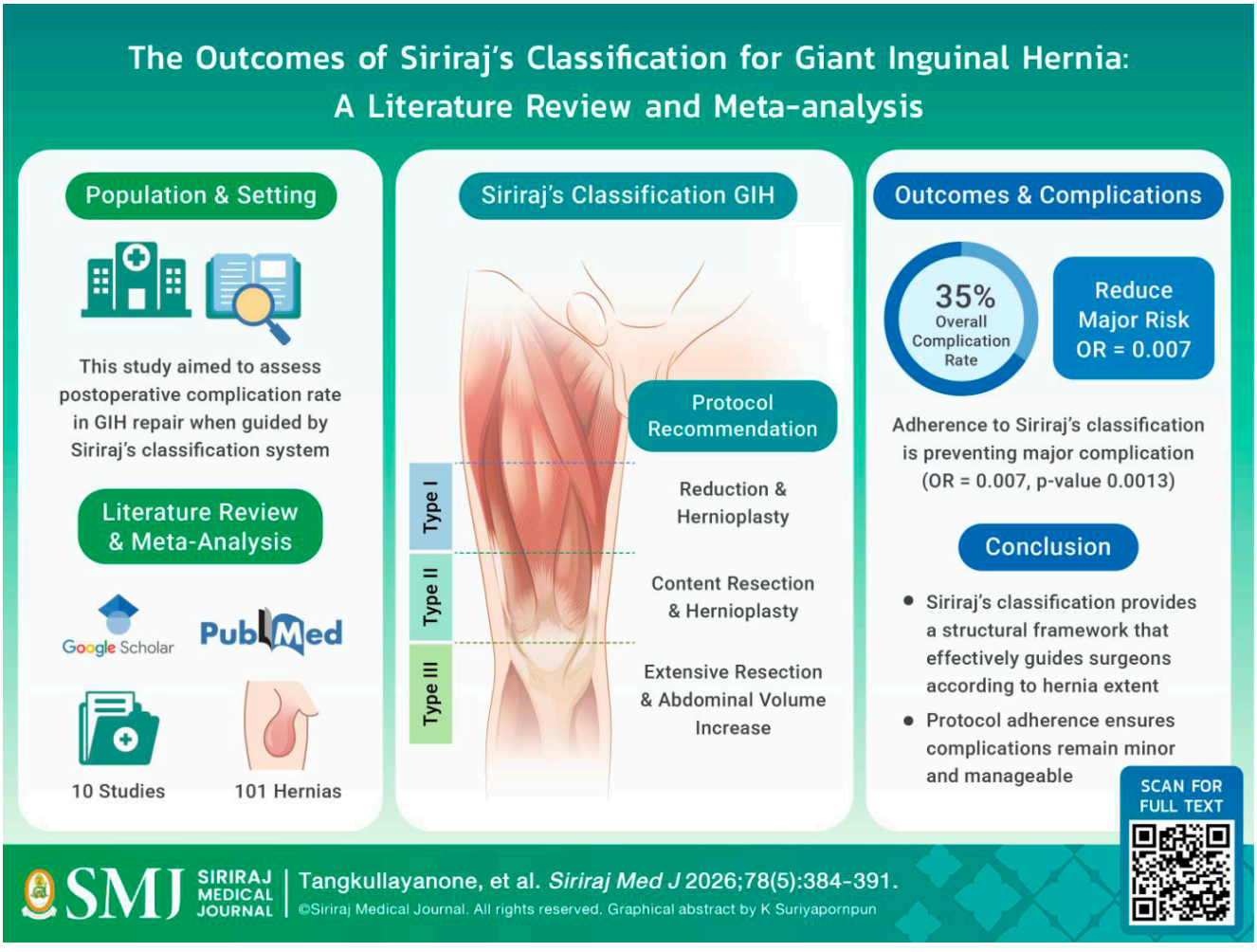

*Corresponding author: Atthaphorn Trakarnsanga
E-mail: atthaphornt@gmail.com
Received 19 February 2026 Revised 2 March 2026 Accepted 11 March 2026
ORCID ID: http://orcid.org/0000-0002-1980-7782
https://doi.org/10.33192/smj.v78i5.280511

All material is licensed under terms of the Creative Commons Attribution 4.0 International (CC-BY-NC-ND 4.0) license unless otherwise stated.

ABSTRACT

Objective: Giant inguinal hernia is a rare condition associated with high perioperative morbidity. Siriraj's classification was developed to guide surgical management according to hernia extent; however, clinical outcome data remain limited. This study aimed to evaluate postoperative complications associated with giant inguinal hernia repair according to Siriraj's classification.

Materials and Methods: A literature review and proportion meta-analysis were conducted to assess the surgical outcomes of giant inguinal hernia repair. PubMed and Google Scholar were systematically searched for studies reporting surgical management and complications of giant inguinal hernia. Studies were included if the hernia type could be classified according to Siriraj's classification or sufficient clinical information was available. The primary outcome was postoperative complications. Pooled complication rates with 95% confidence intervals (CI) were calculated using fixed- or random-effects models based on heterogeneity.

Results: Ten studies involving 101 giant inguinal hernias were included in the meta-analysis. The overall postoperative complication rate was 35% (95% CI: 0.17–0.59). Type I giant inguinal hernia showed a complication rate of 43%, while non-Type I hernias demonstrated a complication rate of 37%. Although overall complication rates were comparable, major complications were predominantly observed in cases not adhering to Siriraj's classification. Protocol adherence was significantly associated with reduced risk of major complications (odds ratio 0.007, 95% CI: 0.0003–0.142; p=0.0013).

Conclusion: Siriraj's classification provides a practical framework for guiding surgical management of giant inguinal hernia and may reduce major postoperative complications. Further large-scale studies are required to validate these findings.

Keywords: Giant inguinal hernia; hernia repair; surgical outcomes; postoperative complications; classification; meta-analysis (Siriraj Med J 2026;78(5):384-391)

INTRODUCTION

Indirect inguinal hernia is one of the most common surgical problems, characterized by a protruding mass from the deep inguinal ring. The pooled prevalence of inguinal hernia is 7.7%.[1] In contrast, a giant inguinal hernia, defined as a hernia extending below the midpoint of the inner thigh in the standing position, is less commonly found. The prevalence of giant inguinal hernia is very low, less than 5% in developed countries.[2] In 2014, our institute proposed a classification system for giant inguinal hernias, consisting of three types as demonstrated in Fig 1.[3]:

- **Type I**: Giant inguinal hernia where the sac extends between the mid-inner thigh and an imaginary line midway between the mid-inner thigh and the suprapatellar level.

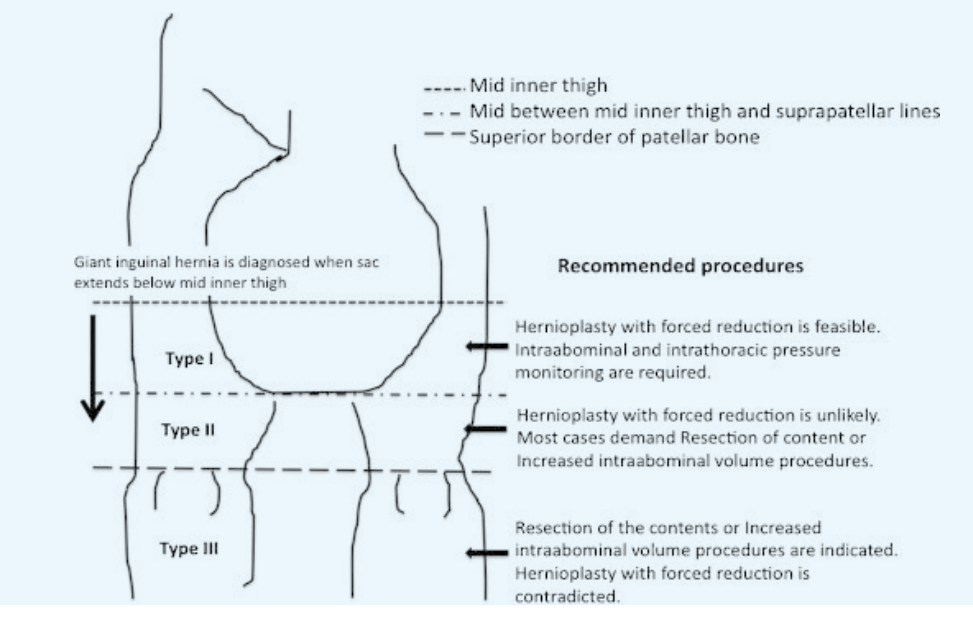

Fig 1. Siriraj's classification of giant inguinal hernia and recommended procedures.[3]

- **Type II:** Hernia where the sac extends beyond the imaginary line but does not exceed the superior border of the patellar bone.
- **Type III:** The most extended type, where the sac extends below the superior border of the patellar bone.

The purpose of describing this classification is to suggest appropriate surgical treatments. The principle of treatment for all types is the reduction of the hernia contents and hernioplasty. This standard procedure is sufficient for Type I giant inguinal hernia when combined with intraoperative or postoperative intra-abdominal pressure monitoring. In cases where the sac is larger, as in Type II, hernioplasty and content reduction alone might not be safe due to the risk of abdominal hypertension, thus necessitating content resection. Furthermore, for Type III giant inguinal hernia, which has the largest sac volume, hernioplasty and content reduction are contraindicated. This type requires at least extensive content resection and is usually combined with procedures to increase abdominal volume.

MATERIALS AND METHODS

Study design and reporting standards

This study was conducted as a literature review with a proportion meta-analysis to evaluate the surgical outcomes of giant inguinal hernia repair according to Siriraj's classification. The study methodology was designed in accordance with the Preferred Reporting Items for Systematic Reviews and Meta-Analyses (PRISMA) guidelines where applicable.

Search strategy

A systematic literature search was performed in PubMed and Google Scholar from database inception to November 2023. The search strategy included the following terms: ("adult" OR "adult*") AND ("giant inguinal hernia" OR "giant inguinoscrotal hernia"). Reference lists of relevant articles and citation tracking were also performed to identify additional eligible studies.

Eligibility criteria

Studies were included if they:

1. Reported surgical management of a giant inguinal hernia,
2. Provided sufficient clinical information to classify hernia type according to Siriraj's classification or explicitly used this classification,
3. Reported postoperative outcomes or complications.
4. Studies were excluded if they were non-operative studies, non-English publications, lacked sufficient clinical detail for classification, or used alternative classification systems.

Study selection

Two investigators independently screened titles, abstracts, and full texts for eligibility. Disagreements were resolved through discussion.

Data extraction

Data extracted included patient demographics, hernia type, diagnostic investigations, surgical approach, adherence to Siriraj's classification, and postoperative complications.

Outcome measures

The primary outcome was postoperative complication rate. Secondary outcomes included severity of complications and the association between protocol adherence and major complications.

Protocol registration

This study was conducted based on a predefined research protocol. The review protocol was not prospectively registered due to its retrospective design, but followed established literature review methodology.

Ethics statement

This study involved secondary analysis of previously published data. Ethical approval and informed consent were not required.

RESULTS

The search was conducted in November 2023. The database and manual search yielded 142 articles. After removing 31 duplicates, 111 articles were reviewed based on their abstracts. Following abstract screening, 70 articles were selected for full-text review. Ultimately, 37 articles met the inclusion criteria for an in-depth review. Ten of these articles[4-13], which met the criteria for meta-analysis, were analyzed, while the remaining 27 articles were assessed and categorized by each individual type as shown in Fig 2.[14-40]

We derived the pooled prevalence with a 95% confidence interval (CI) of the complications of procedures conducted on giant inguinal hernias. The I^2 statistic was used to determine the heterogeneity of the gathered data. A random-effects model was used when I^2 was >50%, and a fixed-effects model was used when I^2 was <50%.

Of the 10 publications, there were 99 male patients and 101 giant inguinal hernias. The mean age was 61.2 years. Type I giant inguinal hernias accounted for 68 hernias,

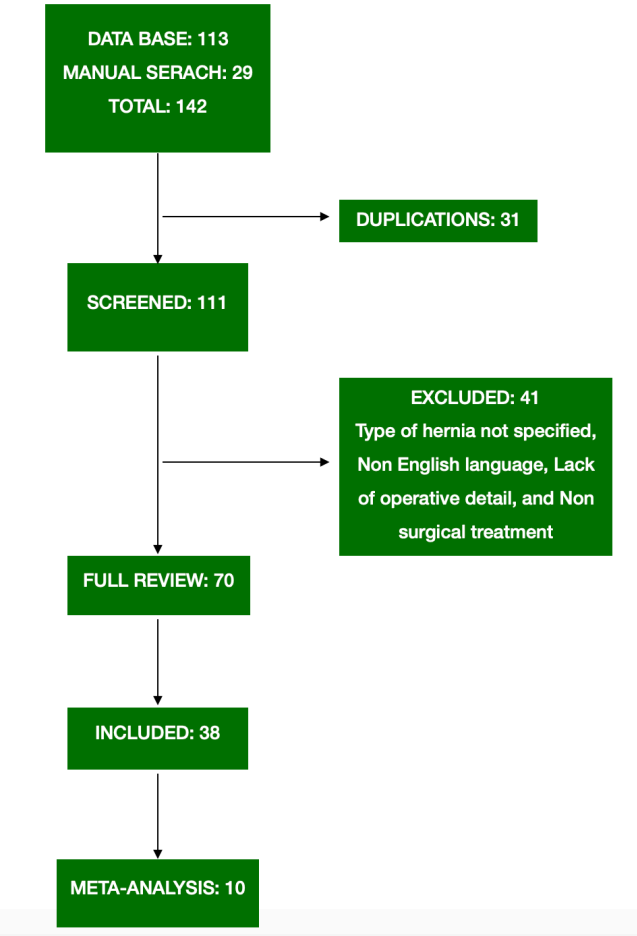

Fig 2. The flow diagram of the literature review.

and non-Type I giant inguinal hernias accounted for 33 hernias. The most common investigation performed prior to specific surgical treatment was computed tomography (CT), particularly in non-Type I giant inguinal hernias. In contrast, only 11.8% (8 hernias) of Type I giant inguinal hernia cases underwent CT scans, with the majority needing only physical examination to determine the hernia type.

The surgical approach for Type I giant inguinal hernia was predominantly laparoscopic in 91.2% (62 hernias) of cases, with the open approach used in 8.8% (6 hernias). For non-Type I giant inguinal hernias, the open approach was used in 69.7% (23 hernias). The most common technique for laparoscopic repair was transabdominal preperitoneal (TAPP) hernioplasty. Various techniques were used for open approaches, including Lichtenstein, retrorectus, or preperitoneal hernioplasty.

In the case of Type I giant inguinal hernia, all 68 hernias in five publications followed Siriraj's classification. Fourteen complications were reported, but all were minor. The complication rate for Type I giant inguinal hernia was 43% (95% CI: 0.09-0.85) with a random effects model (I^2 = 81.03%) (Fig 3).

Since there was only one publication reporting on Type III giant inguinal hernia treatment and complications, five publications with Type II and Type III giant inguinal hernias were categorized into the non-Type I giant inguinal hernia group. Out of 33 hernias in this group, complications were reported in 11 hernias. The overall complication rate was 37% (95%CI: 0.21-0.55). When subgrouped by adherence to Siriraj's classification, as shown in Fig 4, the complication rate for non-Type I giant inguinal hernia cases that followed the protocol and non-followed the protocol were 36% (95% CI: 0.16-0.62) and 36% (95% CI: 0.14-0.66), respectively. In non-followed protocol article[9], four major complications were noted, including abdominal compartment syndrome and abdominal hypertension, while only minor complications were found in the followed protocol subgroup.[4,7,8,11] Although overall complication rates were comparable, major complications occurred predominantly in non-protocol cases.

Out of 99 patients, complications were found in 25 patients. According to the Clavien-Dindo classification[41], serious complications (grade IIIb-V) were found in 4 patients, including abdominal hypertension and pulmonary embolism. Minor complications (grade I-IIIa) consisted of seroma, hematoma, surgical site infection, and abscess.

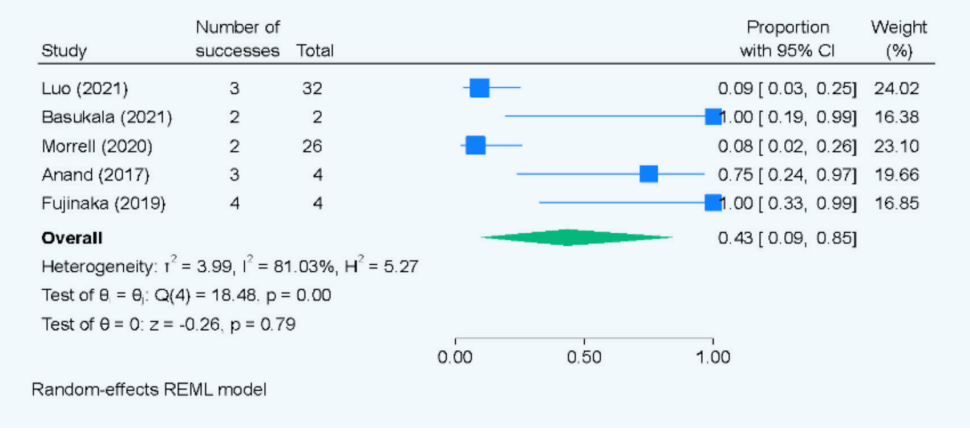

Fig 3. Complications of type I giant inguinal hernia.

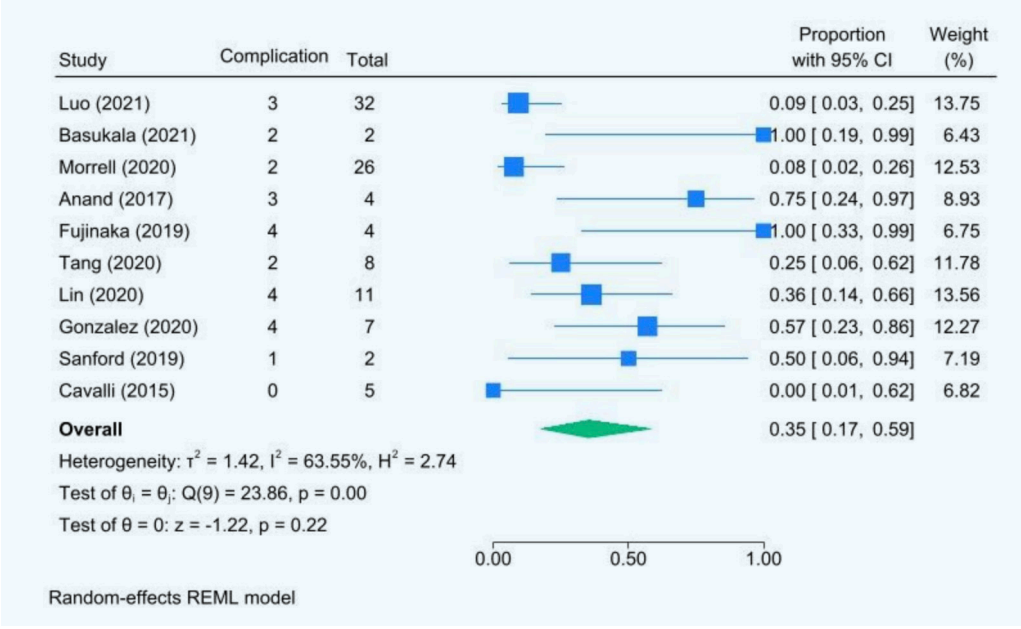

Fig 4. Overall complications.

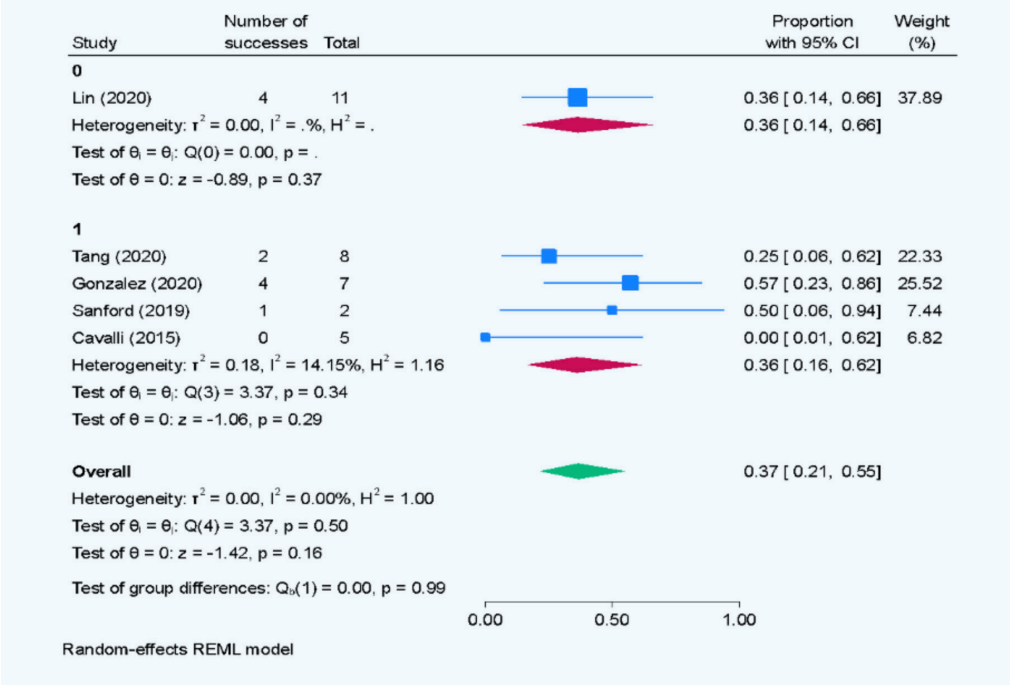

Fig 5. Complications of non-type I giant inguinal hernia.

The overall complication rate was 35% (95% CI: 0.17-0.59) based on a random effects model (I^2 = 63.55%) (Fig 2). Focusing on Siriraj's classification and surgical complications, the odds of major complications in the protocol group and odds of major complications in the non-protocol group were calculated. Fisher's Exact test was used to determine nonrandom associations between two categorical variables. The odds ratio (OR) was 0.007 (95% CI: 0.0003-0.142, p-value 0.0013), which means adhering to the protocol is highly effective in preventing major complications.

DISCUSSION

Inguinal hernia repairs typically exhibit overall complication rates ranging from 2.9% to 8%, commonly involving bleeding, wound infection, and cardiovascular or pulmonary complications. However, giant inguinal hernias are associated with higher complication rates. Previous systematic reviews have reported an overall complication rate of 39% for giant inguinal hernias, with more severe complications such as abdominal compartment syndrome, bowel injury, or Fournier's gangrene. To mitigate these hazardous events, surgical

protocols tailored to the type of giant inguinal hernia are imperative.

Type I giant inguinal hernias are often diagnosed by clinical examination or simple investigations such as CT scans. Our protocol suggests that this type requires content reduction, intraoperative intraabdominal pressure monitoring, and hernioplasty. Surgical approaches can be achieved through either open or laparoscopic methods. From our review, 91.2% of Type I cases were managed laparoscopically, mainly via transabdominal preperitoneal hernia repair (TAPP). Despite the higher number of complications compared to non-giant inguinal hernias, all complications were minor and treatable with conservative treatment.

Type II giant inguinal hernias pose greater surgical challenges and typically require CT scans to determine the extent of visceral involvement. Approaches may include open, laparoscopic, or hybrid methods. Forceful reduction of the hernia contents is often difficult and can lead to abdominal hypertension, thus organ resection might be unavoidable. Commonly removed contents from the hernia sac include the greater omentum, orchidectomy, or bowel segments. Alternatively, increasing intra-abdominal volume through progressive pneumoperitoneum in the first stage, followed by content reduction with hernioplasty in the second stage, may be performed without extensive organ resection.

Massive inguinal hernias, such as type III, require at least a CT scan and abdominal CT volumetry to assess for loss of domain. Hernioplasty and forceful reduction are contraindicated due to the risk of fatal complications. To mitigate abdominal compartment syndrome or respiratory failure, extensive organ resection may be necessary, possibly combined with progressive pneumoperitoneum. Prediction of abdominal hypertension through preoperative CT volumetry, using the ratio of hernia sac volume divided by abdominal cavity volume ≤ 0.25, is crucial. If prediction methods such as the Tanaka or Sabbagh method indicate the possibility of abdominal hypertension, procedures to increase abdominal volume are warranted. Additionally, perioperative and postoperative intraabdominal pressure monitoring must be mandatory.

Limitations

This study has several limitations. Firstly, it is not a systematic review but rather a literature review, and the search strategy was not as strict as systematic review guidelines. Specific inclusion criteria were set only for Siriraj's classification. Secondly, due to the rarity of this condition, many publications are case reports, case series, or retrospective studies, which may have impacted the power of our meta-analysis. Lastly, a significant number of studies did not include follow-up protocols or have significant follow-up periods, thus limiting the collection of data on recurrence rates among giant hernia types, which is a crucial long-term outcome of treatment.

CONCLUSION

The classification and management of giant inguinal hernia remain heterogeneous and technically demanding. This study suggests that Siriraj's classification provides a practical, structured framework to guide operative strategy according to hernia extent. While overall complication rates were comparable, adherence to classification-guided management was associated with a significant reduction in major postoperative complications. In particular, Type I giant inguinal hernias may be safely managed with reduction and hernioplasty—predominantly via laparoscopic TAPP with intra-abdominal pressure monitoring—whereas non–Type I hernias frequently require adjunctive procedures to prevent abdominal compartment syndrome.

Although limited by a small sample size and substantial heterogeneity, these findings offer clinically relevant preliminary guidance in an area lacking standardized management algorithms. Further prospective, large-scale studies are warranted to validate these recommendations and refine operative strategies for each hernia type.

Data Availability Statement

The data that support the findings of this study are available from the corresponding author upon reasonable request. Most of the relevant references are already cited and available in the bibliography.

ACKNOWLEDGEMENTS

The authors thank all individuals and departments who contributed to this study and we would like to express our gratitude to Doctor Roongnapa Khampang (R.K.) and Juthamas Prawjaeng (J.P.) from Siriraj Health Policy Unit for their valuable contributions to the search strategy and the proportion meta-analysis. Their expertise and support were essential to the successful completion of this study.

DECLARATIONS

Grants and Funding Information

This research did not receive any specific grant from funding agencies in the public, commercial, or not-for-profit sectors.

Conflict of Interest

The authors declare no competing interests.

Registration Number of Clinical Trial

Not applicable.

Author Contributions

Conceptualization and methodology, W.T., A.T., T.A., A.M., and V.C. ; Developed the review article, W.T. and A.T. ; Formal analysis, W.T., R.K., and J.P. ; Visualization and writing – original draft, W.T. and A.T. ; Writing – review and editing, W.T. and A.T. ; Supervision, A.T. All authors have read and agreed to the final version of the manuscript.

Use of Artificial Intelligence

No artificial intelligence tools or technologies were utilized in the writing, analysis, or development of this research.

REFERENCES

1. Abebe MS, Tareke AA, Alem A, Debebe W, Beyene A. Worldwide magnitude of inguinal hernia: Systematic review and meta-analysis of population-based studies. SAGE Open Med. 2022;10: 20503121221139150.
2. Menenakos C, Albrecht HC, Gretschel S. Bilateral giant inguinoscrotal hernia. Presentation of a novel combined two-stage repair approach. J Surg Case Rep. 2020;2020(3):rjaa012.
3. Trakarnsagna A, Chinswangwatanakul V, Methasate A, Swangsri J, Phalanusitthepha C, Parakonthun T, et al. Giant inguinal hernia: Report of a case and reviews of surgical techniques. Int J Surg Case Rep. 2014;5(11):868-72.
4. Cavalli M, Biondi A, Bruni PG, Campanelli G. Giant inguinal hernia: the challenging hug technique. Hernia. 2015;19(5):775-83.
5. Anand M, Hajong R, Naku N, Hajong D, Singh KL. Giant Inguinal Herniae Managed by Primary Repair: A Case Series. J Clin Diagn Res. 2017;11(2):PR01-PR02.
6. Fujinaka R, Urade T, Fukuoka E, Murata K, Mii Y, Sawa H, et al. Laparoscopic transabdominal preperitoneal approach for giant inguinal hernias. Asian J Surg. 2019;42(1):414-9.
7. Sanford Z, Weltz AS, Singh D, Hanley R, Todd D, Belyansky I. Minimally Invasive Multidisciplinary Approach to Chronic Giant Inguinoscrotal Hernias. Surg Innov. 2019;26(4):427-31.
8. Gonzalez-Urquijo M, Estrada-Cortinas OJ, Rodarte-Shade M, Bermea-Mendoza JH, Gil-Galindo G. Preoperative progressive pneumoperitoneum: The answer for treating giant inguinal hernias while avoiding morbidities? Hernia. 2020;24(4):781-6.
9. Lin R, Lu F, Lin X, Yang Y, Chen Y, Huang H. Transinguinal preperitoneal repair of giant inguinoscrotal hernias using Kugel mesh. J Visc Surg. 2020;157(5):372-7.
10. Morrell AC, Morrell ALG, Malcher F, Morrell AG, Morrell-Junior AC. Primary Abandon-of-the-Sac (Pas) Technique: Preliminary Results of a Novel Minimally Invasive Approach for Inguinoscrotal Hernia Repair. Arq Bras Cir Dig. 2020;33(2):e1519.
11. Tang FX, Zong Z, Xu JB, Ma N, Zhou TC, Chen S. Combination of Preoperative Progressive Pneumoperitoneum and Botulinum Toxin A Enables the Laparoscopic Transabdominal Preperitoneal Approach for Repairing Giant Inguinoscrotal Hernias. J Laparoendosc Adv Surg Tech A. 2020;30(3):260-6.
12. Basukala S, Rijal S, Pathak BD, Gupta RK, Thapa N, Mishra R. Bilateral giant inguinoscrotal hernia: A case report. Int J Surg Case Rep. 2021;88:106467.
13. Luo H, Zhang H, Sun J, Chen Y, Qi X, Wang H, et al. Laparoscopic transabdominal preperitoneal approach with negative pressure drainage for giant inguinal hernia. J Laparoendosc Adv Surg Tech A. 2021;31(8):931-6.
14. Monestiroli UM, Bondurri A, Gandini F, Lenna G, Vellini S, Danelli P. Giant inguinoscrotal hernia. Tech Coloproctol. 2007;11(3): 283-4.
15. Tahir M, Ahmed FU, Seenu V. Giant inguinoscrotal hernia: case report and management principles. Int J Surg. 2008;6(6): 495-7.
16. Vasiliadis K, Knaebel HP, Djakovic N, Nyarangi-Dix J, Schmidt J, Büchler M. Challenging surgical management of a giant inguinoscrotal hernia: report of a case. Surg Today. 2010;40(7): 684-7.
17. Gaedcke J, Schüler P, Brinker J, Quintel M, Ghadimi M. Emergency repair of giant inguinoscrotal hernia in a septic patient. J Gastrointest Surg. 2013;17(4):837-9.
18. Karthikeyan VS, Sistla SC, Ram D, Ali SM, Rajkumar N. Giant inguinoscrotal hernia--report of a rare case with literature review. Int Surg. 2014;99(5):560-4.
19. Lajevardi SS, Gundara JS, Collins SA, Samra JS. Acute Gastric Rupture in a Giant Inguinoscrotal Hernia. J Gastrointest Surg. 2015;19(12):2283-5.
20. Tarchouli M, Ratbi MB, Bouzroud M, Aitidir B, Ait-Ali A, Bounaim A, Sair K. Giant inguinoscrotal hernia containing intestinal segments and urinary bladder successfully repaired by simple hernioplasty technique: a case report. J Med Case Rep. 2015;9:276.
21. Sahsamanis G, Samaras S, Basios A, Katis K, Dimitrakopoulos G. Treatment of a half century year old giant inguinoscrotal hernia. A case report. Int J Surg Case Rep.2016;25:51-4.
22. Prochotsky A, Dolak S, Minarovjech V, Medzo I, Hutan M, Mifkovic A. Giant inguinoscrotal hernia repair. Bratisl Lek Listy. 2017;118(8):472-8.
23. Staubitz JI, Gassmann P, Kauff DW, Lang H. Surgical treatment strategies for giant inguinoscrotal hernia - a case report with review of the literature. BMC Surg. 2017;17(1):135.
24. Aguirre JE, Ruiz-Niño H, Maria M, Jose A, Jorge JJACES. Case report: preoperative progressive pneumoperitoneum in giant inguinoscrotal hernia. Arch Clin Exp Surg. 2018;7(2): 84-8.
25. Hever P, Dhar M, Cavale N. Loss of domain leading to intra-operative cardiorespiratory arrest during open repair of a giant inguinoscrotal hernia and hydrocele. JPRAS Open. 2018;16:1-5.
26. Sprunger H, Carbonell AM, Marguet CG, Cobb WS, Warren JA, Flanagan WF. Staged Management of Giant Inguinoscrotal Hernia. Am Surg. 2018;84(3):e114-e6.
27. Caruso R, Vicente E, Quijano Y, D'Ovidio A, Ielpo B, Ferri VJIJoSCR. Review with video of a laparoscopic transabdominal preperitoneal (TAPP) repair for giant inguinoscrotal hernia. Int J Surg Case Rep. 2020;76:549-51.
28. Lin M, Long G, Chen M, Chen W, Mo J, Chen N. Giant recurrent left inguinal hernia with femoral nerve injury: a report of a rare case. BMC Surg. 2020;20(1):123.

29. Voravisutthikul P. Case report: multi-stage operation for giant inguinoscrotal hernia repair. Mahasarakham Hospital Journal. 2020;17(2):142-8.
30. Porfidia R, Grimaldi S, Picarella P, Ciolli M, Romano AJAICMCA-Da. Giant Inguinoscrotal Hernia: Single-Stage Repair Using Posterior Component Separation Technique and Transversus Abdominis Release. Annals of International Clinical and Medical Case Reports. 2020;11. Available from: https://www.sergiogrimaldi.it/wp-content/uploads/2022/02/Ernia-Inguinoscrotale-2020.pdf
31. Brandt ASV, Tastesen J, Sværdborg M, Kirkeby HJ. Joint venture surgery of a giant inguinoscrotal hernia in a patient suffering from trisomy 21 and Eisenmenger's syndrome. Urol Case Rep. 2021;39:101757.
32. Cubero JÁO, Soto-Bigot M, Chaves-Sandí M, Méndez-Villalobos A, Martínez-Hoed JJIJoAW, Surgery H. Surgical treatment for inguinoscrotal hernia with loss of dominion with preoperative progressive pneumoperitoneum and botulinum toxin: Case report and systematic review of the literature. International Journal of Abdominal Wall and Hernia Surgery. 2021;4(4):156-65.
33. Davis T, Vivens M, Barghuthi L, Ismael H. Giant sliding inguinal hernia requiring intraoperative aspiration of fluid: a case report and literature review. J Surg Case Rep. 2021;2021(8):rjab340.
34. Ilma W. Hernia Inguinalis Permagna: Laporan Kasus. Medula. 2021;11(1):151-6.
35. Olaogun JG, Ige JT, Kadiri IA, Wuraola OK. Giant Inguinal Hernia: Two Case Reports and Literature Review. 2021. Available from: https://www.researchgate.net/publication/367793887_Giant_Inguinal_Hernia_Two_Case_Reports_and_Literature_Review
36. Polat FR. Bilateral giant inguinoscrotal hernia with hydrocele. A case report. J Surg Arts. 2021;14(2):82-5.
37. Quarto G, D'Amore A, Vertaldi S, Anoldo P, Benassai G, De Palma GD, et al. A giant inguinal hernia in a patient with Ehlers-Danlos syndrome. Ann Ital Chir. 2021;10:S2239253X21034770.
38. Sewalia P, Chawla AS, Sangtam LT, Mandalapu H, Kumar H, Kaur A, et al. Repair of giant inguino-scrotal hernia with loss of domain using minimally invasive anterior component separation technique combined with Lichtenstein tension-free mesh hernioplasty. International Surgery Journal. 2021;8(1):406-10.
39. Nakamura K, Shibasaki S, Takenaka M, Serizawa A, Akimoto S, Nakauchi M, et al. Orchiectomy due to delayed severe scrotal hematocele after laparoscopic transabdominal preperitoneal repair for a giant inguinoscrotal hernia: a case report. Surg Case Rep. 2022;8(1):222.
40. Goroeasem S, Vijayalakshmi V, Farook M. Role of progressive preoperative pneumoperitoneum in the management of giant inguinoscrotal hernia-case report. International Surgery Journal. 2023;10(2):315-8.
41. Dindo D, Demartines N, Clavien PA. Classification of surgical complications: a new proposal with evaluation in a cohort of 6,336 patients and results of a survey. Ann Surg. 2004;240(2):205-13.

Bispecific Protein Engager-Armed T Cells (BATs): Next-Generation Platforms for Precision Cancer Immunotherapy

Pa-thai Yenchitsomanus, Ph.D.

Siriraj Center of Research Excellence for Cancer Immunotherapy (SiCORE-CIT), and Division of Molecular Medicine, Research Department, Faculty of Medicine Siriraj Hospital, Mahidol University, Bangkok 10700, Thailand.

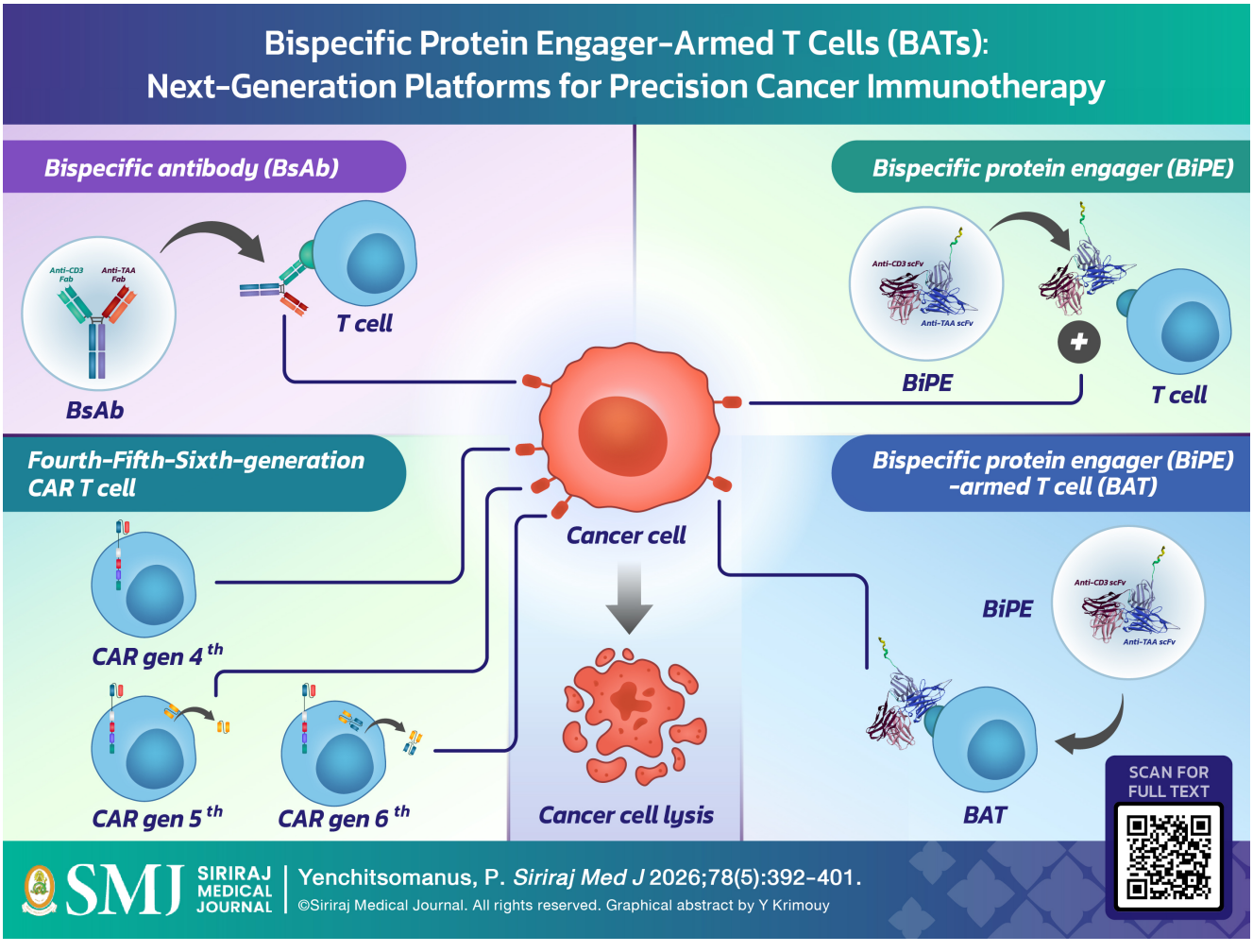

Corresponding author: Pa-thai Yenchitsomanus
E-mail: pathai.yen@mahidol.ac.th; ptyench@gmail.com
Received 7 April 2026 Revised 17 April 2026 Accepted 21 April 2026
ORCID ID: http://orcid.org/0000-0001-9779-5927
https://doi.org/10.33192/smj.v78i5.281440

All material is licensed under terms of the Creative Commons Attribution 4.0 International (CC-BY-NC-ND 4.0) license unless otherwise stated.

ABSTRACT

Chimeric antigen receptor (CAR) T-cell therapy and CD3-directed bispecific T-cell engagers (BiTEs) have transformed cancer immunotherapy, particularly for relapsed or refractory hematologic malignancies. However, CAR T-cell therapy remains constrained by complex genetic engineering, individualized manufacturing, specialized infrastructure, high cost, limited accessibility, and treatment-related toxicities such as cytokine release syndrome (CRS) and immune effector cell–associated neurotoxicity syndrome (ICANS). In contrast, soluble BiTEs frequently require repeated dosing or continuous infusion because of their short serum half-life and may also induce CRS and neurotoxicity. To address these limitations, our research group at the Siriraj Center of Research Excellence for Cancer Immunotherapy (SiCORE-CIT) developed bispecific protein engager (BiPE)–armed T cells (BATs), a non-genetically modified and adaptable platform that combines BiPE-mediated tumor targeting with the intrinsic cytotoxic activity of activated T cells. This review positions BATs within the broader evolution of cancer immunotherapy—including monoclonal antibodies (mAbs), antibody–drug conjugates (ADCs), CAR T cells, bispecific antibodies (BsAbs), and BiTEs—and summarizes their structure and mechanism of action. BATs mediate major histocompatibility complex (MHC)-independent T-cell activation, promote immune synapse formation, and enable efficient tumor cell lysis. Clinical studies of bispecific antibody–armed T cells (BsAb-Ts), the closest clinical analogs of BATs, demonstrate feasibility, a consistent absence of dose-limiting toxicities (DLTs), and preliminary biological and clinical activity. Building on this foundation, next-generation BAT platforms targeting tumor-associated antigens and immune checkpoint molecules—including BCMA, CD138, integrin αvβ6, and PD-L1—have shown promising preclinical activity in multiple myeloma, breast cancer, and cholangiocarcinoma. Collectively, BATs represent a flexible, scalable, and potentially safer platform for next-generation precision T-cell immunotherapy.

Keywords: Cancer immunotherapy; bispecific protein engager-armed T cells (BATs); bispecific antibodies; chimeric antigen receptor (CAR) T cells; tumor-associated antigens (Siriraj Med J 2026;78(5):392-401)

INTRODUCTION

Cancer comprises heterogeneous diseases driven by dysregulated proliferation, invasion, and metastasis, ultimately causing organ failure and death if untreated. At the molecular level, oncogenesis arises from the progressive accumulation of genomic and epigenetic alterations that confer hallmark capabilities, including immune evasion.[1] Globally, cancer accounted for approximately 20 million new cases and 9.7 million deaths in 2022, and demographic shifts are projected to increase annual incidence substantially to 35 million new cases by 2050, disproportionately affecting low- and middle-income countries where access to effective prevention and therapies remains limited.[2,3] Immune surveillance can eliminate transformed cells; however, antitumor immunity is often compromised by aging, immunosuppression, and tumor-mediated evasion mechanisms, including the expression of immune checkpoint proteins.[4] These insights form the foundation of modern immunotherapy, which aims to restore, amplify, or redirect immune responses to achieve durable tumor control.

Development of Cancer Immunotherapy

The development of cancer immunotherapy has progressed through a series of pivotal milestones. Early observations in the late 19th century by William B. Coley demonstrated that bacterial infections could induce tumor regression, leading to the development of "Coley's toxins," which stimulate antitumor immune responses.[5] This was followed by the identification of tumor antigens and advances in monoclonal antibody technology in the 1970s–1990s, enabling targeted therapies such as rituximab. The discovery of immune checkpoint pathways, particularly CTLA-4 and PD-1, led to the development of checkpoint inhibitors that revolutionized cancer treatment by overcoming tumor-induced immune suppression.[4,6] Immunotherapy has expanded from therapeutic monoclonal antibodies to antibody-drug conjugates (ADCs), vaccines, and adoptive cell transfer (ACT). ACT approaches, including tumor-infiltrating lymphocytes (TILs) and chimeric antigen receptor (CAR) T cells, enable ex vivo expansion and/or functional programming of immune cells for enhanced tumor recognition and cytotoxicity.[7,8] CAR T-cell therapy has achieved high response rates in several hematologic malignancies, establishing immune cell redirection as a powerful paradigm.[8-10] Together, these sequential breakthroughs have transformed immunotherapy into a central pillar of modern oncology.

Monoclonal Antibodies and Antibody-Drug Conjugates

Therapeutic monoclonal antibodies (mAbs) were among the earliest widely adopted targeted immunotherapies. Their specificity enables selective targeting with reduced off-target damage, and mechanisms include blockade of oncogenic signaling, antibody-dependent cellular cytotoxicity (ADCC), complement-dependent cytotoxicity (CDC), and immune checkpoint modulation.[11] Antibody-drug conjugates (ADCs) extend mAb functionality by linking a tumor-targeting antibody to a potent cytotoxic payload. After binding and internalization, payload release can kill tumor cells while reducing systemic exposure compared with conventional chemotherapy.[12,13]

Chimeric Antigen Receptor T Cells

Chimeric antigen receptor (CAR) T-cell therapy enables patient-derived T cells to recognize and kill tumor cells in a major histocompatibility complex (MHC)-independent manner. First-generation CARs fused an antibody-derived single-chain variable fragment (scFv) to CD3ζ but showed limited persistence and activity, prompting iterative improvements.[8,9] Second-generation CARs incorporate one costimulatory domain (e.g., CD28 or 4-1BB) and underpin most approved products, while later-generation constructs add signaling modules and/or inducible payloads to enhance function and modulate the tumor microenvironment.[14]

Our research group developed a stepwise CAR generation platform (CAR4, CAR5, and CAR6) (Fig 1), first in hematologic malignancies and then in solid tumors. In B-cell malignancies, CD19-CAR4 T cells incorporating CD28, 4-1BB (CD137), and CD27 costimulatory domains demonstrated potent antigen-specific cytotoxicity against CD19-positive leukemia/lymphoma cells with preserved proliferative capacity and reduced inflammatory cytokine production, supporting improved safety and persistence.[15] Fifth-generation CAR5 designs were engineered to overcome checkpoint suppression via local secretion of anti-PD-L1 scFv, enabling effective killing of CD19-positive/PD-L1high leukemia cells and restoring activity under PD-L1-mediated inhibition.[16,17] Translating to solid tumors, CAR4 T cells targeting CD133 and MUC1 in cholangiocarcinoma and FRα and Trop2 in breast cancer showed strong antigen-dependent cytotoxicity and T helper 1-type effector responses, including in three-dimensional spheroid models.[18-21] Incorporation of checkpoint blockade in CAR5 constructs (e.g., BCMA-CAR5; αvβ6-CAR5, FRα-CAR5) enhanced cytotoxicity against

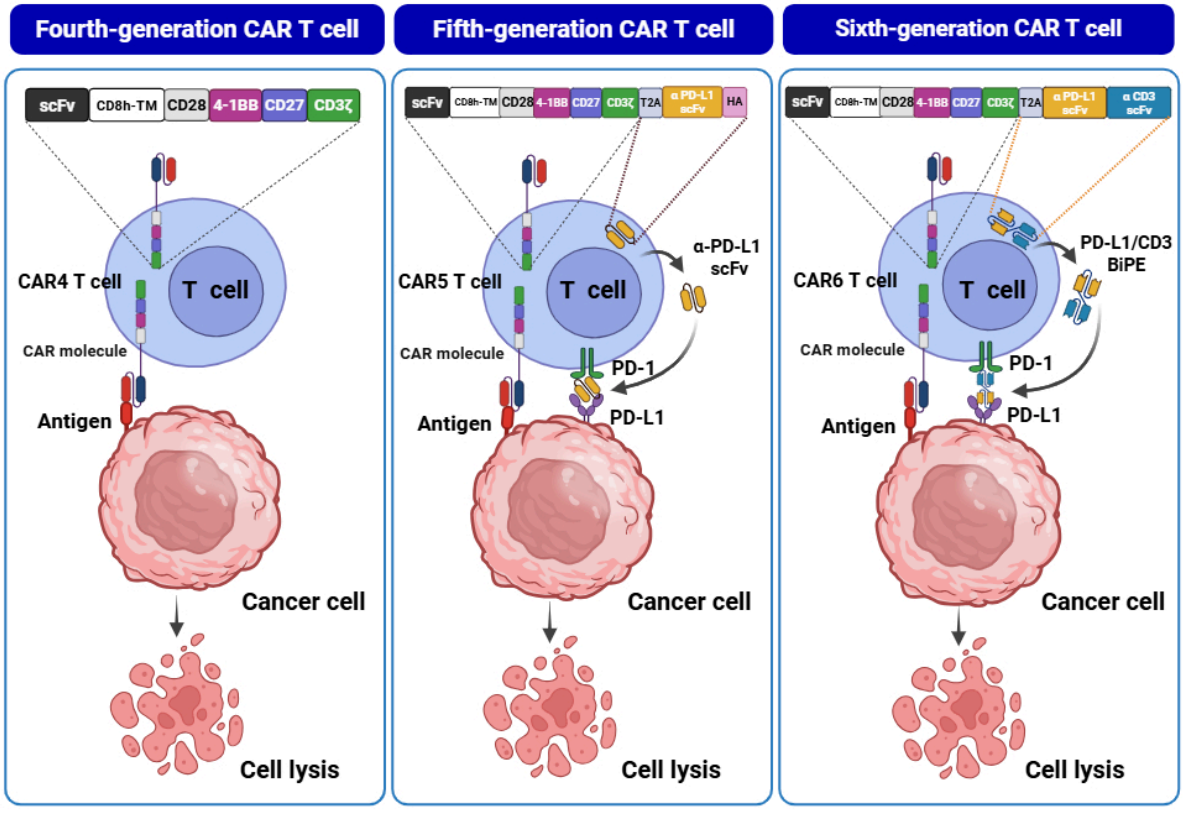

Fig 1. Chimeric antigen receptor (CAR) T-cell platforms developed at the Siriraj Center of Research Excellence for Cancer Immunotherapy (SiCORE-CIT), including fourth-generation (CAR4), fifth-generation (CAR5), and sixth-generation (CAR6) constructs. CAR4 T cells incorporate multiple costimulatory domains—CD28, 4-1BB (CD137), and CD27—linked to the CD3ζ signaling domain. CAR5 T cells retain the CAR4 architecture and are additionally engineered to secrete anti-PD-L1 single-chain variable fragments (scFv). CAR6 T cells are based on the CAR4/5 framework and are further designed to secrete anti-PD-L1 × anti-CD3 bispecific protein engagers (BiPEs).

PD-L1high targets and improved spheroid infiltration and control.[17,22,23] Sixth-generation CAR6 T cells were designed to secrete an αPD-L1 × αCD3 bispecific engager, combining localized checkpoint blockade with bystander T-cell recruitment and amplifying antitumor responses in PD-L1-positive cholangiocarcinoma models.[24]

Clinically, CD19-targeted CAR T-cell therapies have achieved high remission rates in relapsed/refractory B-cell acute lymphoblastic leukemia (B-ALL) and large B-cell lymphomas, while BCMA-directed CAR T cells show remarkable efficacy in multiple myeloma.[9,10] However, their therapeutic activity in solid tumors remains limited because of antigen heterogeneity, inadequate T-cell trafficking and infiltration, and the presence of immunosuppressive microenvironments. Consequently, next-generation strategies, including multi-target and armored CAR T cells, are actively being developed to overcome these barriers.[14] Despite their substantial clinical promise, CAR T-cell therapies remain constrained by complex and time-consuming manufacturing processes, high treatment costs, and risks of CRS/ICANS that require specialized management. Standardized toxicity assessment has been improved through the consensus grading criteria established by the American Society for Transplantation and Cellular Therapy (ASTCT).[25]

Bispecific Antibodies and Bispecific Antibody-Armed T Cells

Bispecific antibodies (BsAbs) bind two distinct antigens or epitopes and can redirect immune effector cells. A key oncologic application is T-cell redirection: one arm binds a tumor-associated antigen (TAA) and the other engages CD3, enforcing proximity, immune synapse formation, activation, and tumor lysis in an MHC-independent manner[26-29] (Fig 2). Early BsAbs generated by chemical conjugation or quadroma technology were limited by heterogeneity and purification challenges. Modern engineering platforms, including knobs-into-holes, CrossMab, and common light chain/Fc engineering, support scalable production and improved stability and pharmacokinetics.[30-34]

Bispecific antibody-armed T cells (BsAb-Ts), regarded as first-generation "BATs", are activated T cells transiently coated *ex vivo* with anti-CD3 × anti-TAA antibodies, thereby redirecting cytotoxicity without permanent genetic modification.[35-40] Across early-phase studies in diverse malignancies, BsAb-Ts have shown feasibility, a reproducible safety profile with a consistent absence of dose-limiting toxicities (DLTs), and early activity signals such as immune activation, partial responses, and prolonged stable disease in subsets[35-40] (Table 1).

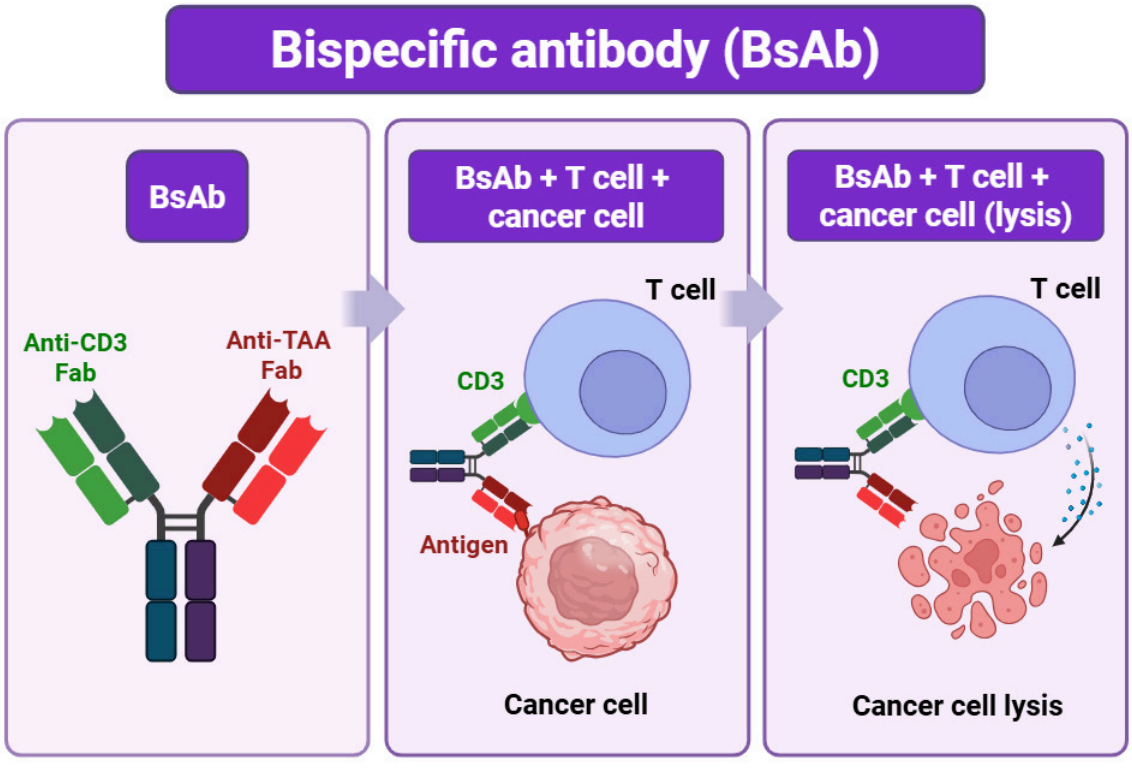

Fig 2. Structure and mechanism of action of bispecific antibodies (BsAbs). BsAbs contain two distinct antigen-binding fragments (Fabs): one recognizing CD3 on T cells and the other targeting a tumor-associated antigen (TAA) on cancer cells. By simultaneously binding both cells, BsAbs bring T cells and tumor cells into close proximity, promoting immune synapse formation, T-cell activation, and targeted tumor cell lysis in a major histocompatibility complex (MHC)–independent manner.

TABLE 1. Summary of clinical investigations of BsAb-Ts (representative examples).[35-40]

Target antigen	Cancer indication	Trial phase / design	Maximum BAT dose tested	Key safety findings	DLTs	Signals of efficacy / immune activity
GD2 (GD2-BATs)	Neuroblastoma, osteosarcoma, desmoplastic small round cell tumor	Phase I/II, 3+3 escalation (n=12)	160×10^6 cells/kg/ infusion	Mild CRS (fever, chills), minimal GD2-related pain	None	Partial response, prolonged stable disease, increased IFN-γ ELISpot, T helper 1 cytokines[35]
EGFR (EGFR-BATs)	Grade 4 astrocytoma	Phase I, escalation plus expansion (n=10)	Total 80×10^9 cells (study-defined)	No CRS; transient cytokine changes	None	Induced systemic antitumor immunity[36]
HER2 (HER-BATs)	Metastatic breast cancer (HER2-low/ negative)	Phase II (immune consolidation) (n=32)	20×10^9 BATs per infusion (total 80×10^9 BATs)	Grade 1-2 infusion reactions	None	Stable disease; immune activation[37]
HER2+ PD-1 (HER2-BATs)	Metastatic castration-resistant prostate cancer	Phase II combination (n=14)	Up to 10^{10} BATs/infusion (twice per week for 4 weeks) in combination with pembrolizumab	Manageable infusion reactions	None	Progression-free and overall survival signals in subsets[38]
EGFR (EGFR-BATs)	Pancreatic cancer	Early-phase plus translational (n=7)	$10\text{-}40\times10^9$ BATs/infusion	Well tolerated	None	Anti-cancer responses, and tumor chemosensitization; killing of resistant cells[39]
CD20 (targeting CD138-negative precursors)	Multiple myeloma (peri-ASCT)	Phase Ib (n=12)	2 doses of 10^{10} BATs	Safe in the peri-transplant setting	None	Reduced clonogenic cells; transferable anti-myeloma immunity[40]

CD3-Engaging Bispecific T-Cell Engagers / Bispecific Protein Engagers

CD3-engaging bispecific proteins redirect endogenous T cells toward malignant cells. "BiTE" is trademarked; here "BiPE" is used as a broader descriptor. These molecules typically comprise two linked scFvs: one binds CD3ε and the other recognizes a TAA, bridging T cells and tumor cells to drive synapse formation, T-cell activation/proliferation, and perforin/granzyme-mediated cytotoxicity in an MHC-independent manner[26-28,41] (Fig 3). Clinically, blinatumomab (anti-CD19 × anti-CD3) improved outcomes in relapsed/refractory B-ALL and gained approvals including for minimal residual disease (MRD)-positive disease.[42-44] In multiple myeloma, anti-BCMA × anti-CD3 bispecific antibodies such as teclistamab and elranatamab show substantial activity in relapsed/refractory settings.[45,46] In solid tumors, redirection is complicated by antigen heterogeneity and on-target/off-tumor risks; however, tebentafusp (anti-gp100-derived peptide presented on HLA-A*02:01 × anti-CD3) demonstrated an overall survival benefit in metastatic uveal melanoma, validating the strategy in selected solid tumors.[47,48]

Despite promise, key constraints of many bispecific formats include short half-life, frequent dosing or continuous infusion requirements, and CRS/neurotoxicity risks; mitigation strategies include half-life extension, step-up dosing, and rational combinations.[26-28,34]

Bispecific Protein Engager-Armed T Cells

CAR T cells and soluble CD3-engaging BiTEs/BiPEs can be highly effective but face practical and safety limitations, including manufacturing complexity and CRS/ICANS for CAR T cells, and frequent dosing and CRS/neurotoxicity for soluble engagers.[8-10,25-28] BATs combine the targeting precision of BiPEs with the intrinsic cytotoxic capacity of activated T cells, aiming to preserve potency while improving manufacturability and pharmacodynamic control.[49-52]

BATs are non-genetically modified T cells armed ex vivo with BiPEs, typically scFv-scFv constructs binding CD3ε and a TAA. After infusion, BiPE-armed T cells are bridged to tumor targets, inducing antigen-specific activation, immune synapse formation, and MHC-independent cytotoxicity[26-28,49-52] (Fig 4). Transient surface arming enables controllable activity without genomic modification, potentially simplifying manufacturing relative to gene-modified products.[49-52]

BAT efficacy depends on stable immune synapse formation. BiPE-mediated CD3-TAA crosslinking enforces close contact and triggers spatial reorganization of signaling and adhesion components, including clustering of the T-cell receptor (TCR)/CD3 complex, recruitment of proximal kinases, and organization of central and peripheral supramolecular activation cluster (cSMAC/pSMAC) structures supported by adhesion molecules.[53-56] Downstream signaling drives Ca^{2+} influx, mitogen-activated

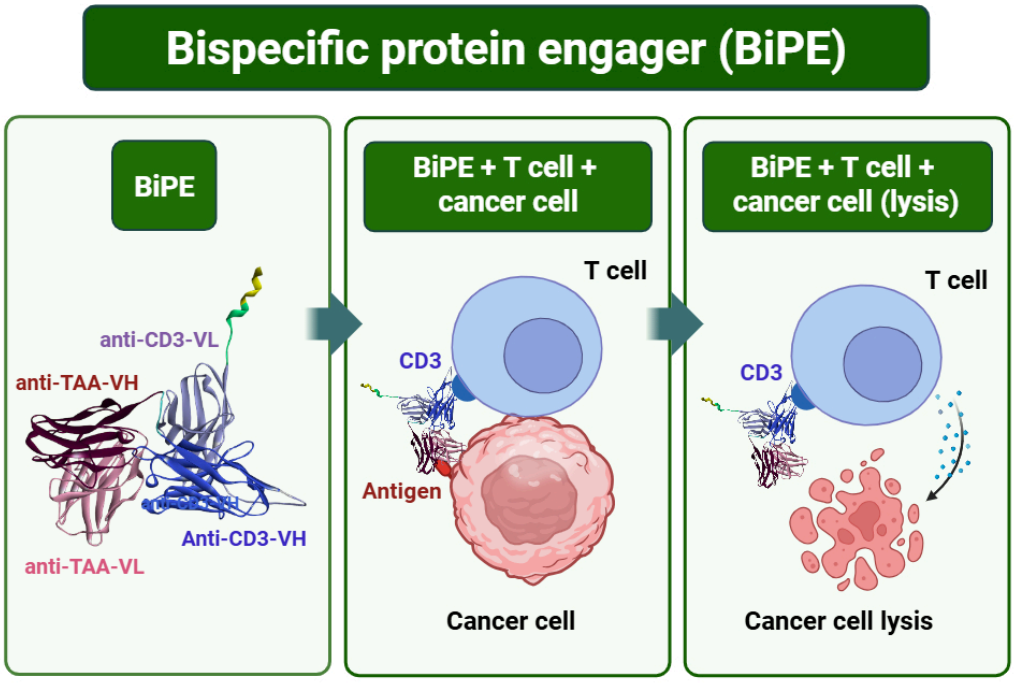

Fig 3. Structure and mechanism of action of bispecific protein engagers (BiPEs). BiPEs consist of two linked single-chain variable fragments (scFvs): one binds CD3ε on T cells and the other recognizes a tumor-associated antigen (TAA) on cancer cells. By simultaneously engaging both targets, BiPEs bridge T cells and tumor cells, promoting immune synapse formation, T-cell activation and proliferation, and perforin/granzyme-mediated cytotoxicity in a major histocompatibility complex (MHC)–independent manner.

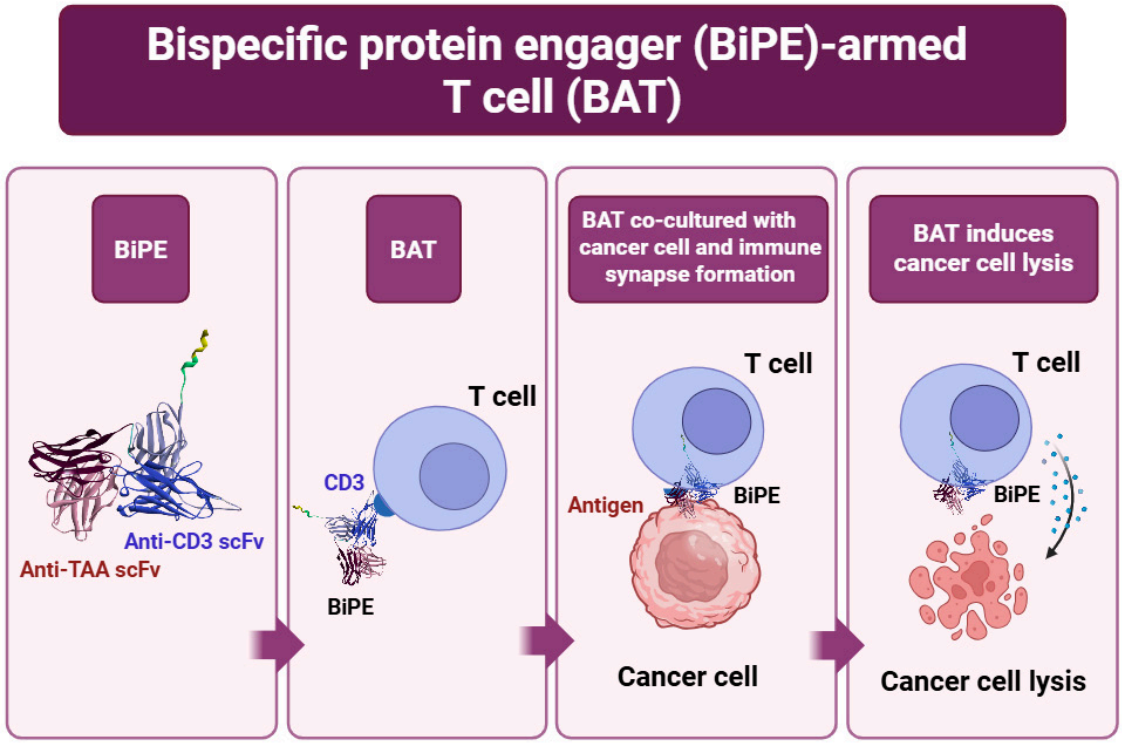

Fig 4. Structure and mechanism of action of bispecific protein engager (BiPE)–armed T cells (BATs). BATs are non-genetically modified T cells armed ex vivo with BiPEs, typically composed of scFv–scFv constructs that bind CD3ε on T cells and a tumor-associated antigen (TAA) on cancer cells. Following infusion, the BiPE molecules bridge BATs to tumor cells, promoting antigen-specific activation, immune synapse formation, perforin and granzyme release, and major histocompatibility complex (MHC)–independent tumor cell killing.

protein kinase activation, cytoskeletal remodeling, and microtubule-organizing center reorientation to deliver lytic granules.[53-55] Perforin enables granzyme entry, notably granzyme B, to trigger apoptosis and cancer cell lysis (Fig 4); Fas/FasL can contribute in parallel.[53-55,57]

Development of BATs at SiCORE-CIT

SiCORE-CIT has established BATs as a versatile platform targeting multiple antigens and immune checkpoints across hematologic and solid tumors. In multiple myeloma, anti-BCMA × anti-CD3 BATs promoted antigen-specific activation, proliferation, and cytotoxicity with robust effector cytokines and limited interleukin-6 (IL-6) induction.[50] CD138-specific BATs showed strong and selective killing of CD138-positive myeloma cells with induction of cytolytic mediators including perforin, granzymes, soluble Fas ligand, and tumor necrosis factor-α (TNF-α), together with low levels of selected pro-inflammatory cytokines, supporting a potentially favorable safety profile.[51] To overcome checkpoint-mediated suppression, anti-PD-L1 × anti-CD3 BATs efficiently lysed PD-L1-expressing breast cancer cells in two-dimensional and three-dimensional models and retained function after cryopreservation.[49] In cholangiocarcinoma, A20/anti-CD3 BATs targeting integrin αvβ6 enhanced activation, proliferation, effector-memory differentiation, and cytotoxicity, including against spheroids, supporting activity in complex tumor models.[52] Chemotherapy can also modulate tumor immune susceptibility. For example, gemcitabine has been shown to upregulate PD-L1 expression in cholangiocarcinoma cells, creating an opportunity to exploit this adaptive change using anti-PD-L1 × anti-CD3 BiPEs to enhance T-cell-mediate cytotoxicity.[58] Accordingly, BATs can be effectively integrated with chemotherapy. Combination strategies may leverage therapy-induced PD-L1 upregulation: for instance, anti-PD-L1 × anti-CD3 BATs combined with low-dose bortezomib demonstrated enhanced cytotoxic activity against multiple myeloma cells in preclinical models where bortezomib increased PD-L1 expression.[59]

Advantages of BATs over CAR T Cells and Soluble BiPEs

BATs offer several potential advantages: *(i)* simplified manufacturing without genetic modification or vector production; *(ii)* shorter timelines and potentially lower cost using transient arming with relatively small amounts of BiPE; *(iii)* localized pharmacodynamic engagement with reduced dependence on continuous infusion; and *(iv)* potential safety advantages via controllable arming density and transient activity.[25-28,49-52]

Preclinical BAT studies consistently show antigen-

specific cytotoxicity in hematologic and solid tumor models.[49-52] Supportive translational evidence comes from BsAb-T trials, which demonstrate feasibility and a consistent absence of DLTs, with biological activity signals across indications.[35-40]

The immunosuppressive tumor microenvironment limits many immunotherapies. BATs may partially mitigate these barriers through localized, engager-mediated activation and by modular targeting, including checkpoint ligands such as PD-L1, to address heterogeneity and immune escape.[26-28,49-52]

Translation requires good manufacturing practice (GMP)-compliant BiPE production, validated arming conditions, and standardized potency/stability assays with defined release criteria.[49-52] BATs share class risks of redirected T-cell activation, including CRS and less commonly neurotoxicity, and ASTCT grading provides standardized toxicity assessment.[25] Antigen selection and affinity tuning remain essential to reduce on-target/off-tumor toxicity.[26-28]

Compared with CAR T cells and continuous-infusion BiTE therapies, BATs may reduce complexity and improve accessibility, particularly if workflows become standardized and scalable.[49-52]

Future Directions and Innovations

Next steps include dual- or multi-target BiPEs/BATs to reduce antigen escape, incorporation of costimulatory engagement or checkpoint blockade to enhance persistence and limit T-cell exhaustion, and development of off-the-shelf approaches, including allogeneic strategies, while addressing rejection, persistence, and safety.[14,60-63] Beyond oncology, CD19- or BCMA-directed redirection strategies may be adaptable to selected antibody-mediated autoimmune diseases driven by pathogenic B cells or plasma cells, but will require stringent safety controls.[64,65]

CONCLUSION

BATs integrate bispecific targeting with T-cell cytotoxicity to enable MHC-independent tumor killing while potentially improving manufacturability and pharmacodynamic control relative to CAR T cells and soluble bispecific proteins. Accumulating preclinical evidence, supported by BsAb-T clinical experience, suggests BATs can deliver adaptable antitumor activity with a promising safety profile, but successful translation will require standardized GMP workflows, validated potency and safety testing, and rigorous clinical evaluation.[35-40,49-52]

Data Availability Statement

The data that support the findings of this study are available from the corresponding author upon reasonable request.

ACKNOWLEDGMENTS

The author sincerely thanks Miss Pucharee Songprakhon for preparing all the figures presented in this article. The author gratefully acknowledges the colleagues and staff members at the Siriraj Center of Research Excellence for Cancer Immunotherapy (SiCORE-CIT) and the Division of Molecular Medicine (DMM), including Professor Chanitra Thuwajit, Associate Professor Peti Thuwajit, Associate Professor Mutita Junking, Dr. Jatuporn Sujjitjoon, Dr. Piriya Luangwattananun, Dr. Kamonlapat Supimon, Dr. Thanich Sangsuwannukul, Dr. Chalermchai Somboonpatarakun, Dr. Kwanpirom Suwanchiwasiri, Miss Nunghathai Sawasdee, Miss Pucharee Songprakhon, and Miss Thanyaporn Dechtawewat for their efforts and valuable contributions to the development and evaluation of the BAT platform. The author also sincerely appreciates the continuing collaboration and contributions of Professor Aussara Panya, Department of Biology, Faculty of Science, Chiang Mai University, Chiang Mai, Thailand, and Assistant Professor Chutamart Thepmalee, Division of Biochemistry, School of Medical Sciences, University of Phayao, Phayao, Thailand. The SiCORE-CIT was financially supported by the Siriraj Research Fund (grant number R016737004).

DECLARATIONS

Conflicts of Interest

The author declares no conflicts of interest related to this review.

Grants and Funding Information

This review article did not receive any external funding.

Use of Artificial Intelligence

The author declares that artificial intelligence (AI) tools were used to assist with literature searching and English-language editing, and to improve writing clarity. The author retains full responsibility for the originality, conceptualization, structure, scientific content, and integrity of the article.

REFERENCES

1. Hanahan D. Hallmarks of cancer: New dimensions. Cancer Discov. 2022;12(1):31-46.
2. Bray F, Laversanne M, Sung H, Ferlay J, Siegel RL, Soerjomataram I, et al. Global cancer statistics 2022: GLOBOCAN estimates of incidence and mortality worldwide for 36 cancers in 185 countries. CA Cancer J Clin. 2024;74(3):229-63.

3. International Agency for Research on Cancer. Cancer Tomorrow. Lyon: International Agency for Research on Cancer; 2024.
4. Pardoll DM. The blockade of immune checkpoints in cancer immunotherapy. Nat Rev Cancer. 2012;12(4):252-64.
5. McCarthy EF. The toxins of William B. Coley and the treatment of bone and soft-tissue sarcomas. Iowa Orthop J. 2006;26:154-8.
6. Hodi FS, O'Day SJ, McDermott DF, Weber RW, Sosman JA, Haanen JB, et al. Improved survival with ipilimumab in patients with metastatic melanoma. N Engl J Med. 2010;363(8):711-23.
7. Rosenberg SA, Restifo NP. Adoptive cell transfer as personalized immunotherapy for human cancer. Science. 2015;348(6230): 62-8.
8. June CH, O'Connor RS, Kawalekar OU, Ghassemi S, Milone MC. CAR T cell immunotherapy for human cancer. Science. 2018;359(6382):1361-5.
9. Maude SL, Frey N, Shaw PA, Aplenc R, Barrett DM, Bunin NJ, et al. Chimeric antigen receptor T cells for sustained remissions in leukemia. N Engl J Med. 2014;371(16):1507-17.
10. Neelapu SS, Locke FL, Bartlett NL, Lekakis LJ, Miklos DB, Jacobson CA, et al. Axicabtagene ciloleucel CAR T-cell therapy in refractory large B-cell lymphoma. N Engl J Med. 2017; 377(26):2531-44.
11. Scott AM, Wolchok JD, Old LJ. Antibody therapy of cancer. Nat Rev Cancer. 2012;12(4):278-87.
12. Beck A, Goetsch L, Dumontet C, Corvaïa N. Strategies and challenges for the next generation of antibody-drug conjugates. Nat Rev Drug Discov. 2017;16(5):315-37.
13. Drago JZ, Modi S, Chandarlapaty S. Unlocking the potential of antibody-drug conjugates for cancer therapy. Nat Rev Clin Oncol. 2021;18(6):327-44.
14. Rafiq S, Hackett CS, Brentjens RJ. Engineering strategies to overcome the current roadblocks in CAR T cell therapy. Nat Rev Clin Oncol. 2020;17(3):147-67.
15. Wutti-in Y, Sujjitjoon J, Sawasdee N, Kongkhla K, Choomee K, Phanthaphol N, et al. Development of a novel anti-CD19 CAR containing a fully human scFv and three costimulatory domains. Front Oncol. 2022;11:802876.
16. Yuti P, Wutti-in Y, Sawasdee N, Kongkhla K, Phanthaphol N, Choomee K, et al. Anti-CD19 chimeric antigen receptor T cells secreting anti-PD-L1 single-chain variable fragment attenuate PD-L1-mediated T cell inhibition. Int Immunopharmacol. 2022;113(Pt B):109442.
17. Yuti P, Sawasdee N, Natungnuy K, Rujirachaivej P, Luangwattananun P, Sujjitjoon J, et al. Enhanced antitumor efficacy, proliferative capacity, and alleviation of T cell exhaustion by fifth-generation chimeric antigen receptor T cells targeting B-cell maturation antigen in multiple myeloma. Biomed Pharmacother. 2023; 168:115691.
18. Sangsuwannukul T, Supimon K, Sujjitjoon J, Phanthaphol N, Chieochansin T, Poungvarin N, et al. Anti-tumour effect of the fourth-generation chimeric antigen receptor T cells targeting CD133 against cholangiocarcinoma cells. Int Immunopharmacol. 2020;89(Pt A):107069.
19. Supimon K, Sangsuwannukul T, Sujjitjoon J, Phanthaphol N, Chieochansin T, Poungvarin N, et al. Anti-mucin 1 chimeric antigen receptor T cells for adoptive T cell therapy of cholangiocarcinoma. Sci Rep. 2021;11(1):6276.
20. Luangwattananun P, Junking M, Sujjitjoon J, Wutti-in Y, Poungvarin N, Thuwajit C, et al. Fourth-generation chimeric antigen receptor T cells targeting folate receptor alpha antigen expressed on breast cancer cells for adoptive T cell therapy. Breast Cancer Res Treat. 2021;186(1):25-36.
21. Somboonpatarakun C, Phanthaphol N, Suwanchiwasiri K, Ramwarungkura B, Yuti P, Poungvarin N, et al. Cytotoxicity of fourth-generation anti-Trop2 CAR-T cells against breast cancer. Int Immunopharmacol. 2024;129:111631.
22. Phanthaphol N, Somboonpatarakun C, Suwanchiwasiri K, Yuti P, Chieochansin T, Junking M, et al. Enhanced cytotoxicity against cholangiocarcinoma by fifth-generation chimeric antigen receptor T cells targeting integrin αvβ6 and secreting anti-PD-L1 scFv. J Transl Med. 2025;23:308.
23. Wutti-In Y, Luangwattananun P, Sawasdee N, Vongchan P, Yenchitsomanus PT, Panya A. Engineering a fifth-generation CAR T cells to overcome PD-L1-mediated immunosuppression in lung cancer. Biomed Pharmacother. 2026 Feb;195:118967.
24. Somboonpatarakun C, Phanthaphol N, Suwanchiwasiri K, Ramwarungkura B, Yenchitsomanus PT, Junking M. Next-generation CAR T cells targeting integrin αvβ6 and PD-L1 to enhance immunotherapy for cholangiocarcinoma. Biomed Pharmacother. 2025; 193:118806.
25. Lee DW, Santomasso BD, Locke FL, Ghobadi A, Turtle CJ, Brudno JN, et al. ASTCT consensus grading for cytokine release syndrome and neurologic toxicity associated with immune effector cells. Biol Blood Marrow Transplant. 2019;25(4):625-38.
26. Mack M, Riethmüller G, Kufer P. A small bispecific antibody construct expressed as a functional single-chain molecule with high tumor cell cytotoxicity. Proc Natl Acad Sci U S A. 1995;92(15): 7021-5.
27. Bargou R, Leo E, Zugmaier G, Klinger M, Goebeler M, Knop S, et al. Tumor regression in cancer patients by very low doses of a T cell-engaging antibody. Science. 2008;321(5891):974-7.
28. Kontermann RE. Bispecific antibodies. Drug Discov Today. 2015;20(7):838-47.
29. Segal DM , Weiner GJ , Weiner LM . Bispecific antibodies in cancer therapy. Curr Opin Immunol 1999;11(5):558-62.
30. Ridgway JBB, Presta LG, Carter P. 'Knobs-into-holes' engineering of antibody CH3 domains for heavy chain heterodimerization. Protein Eng. 1996;9(7):617-21.
31. Schaefer W, Regula JT, Bähner M, Schanzer J, Croasdale R, Dürr H, et al. Immunoglobulin domain crossover as a generic approach for the production of bispecific IgG antibodies. Proc Natl Acad Sci U S A. 2011;108(27):11187-92.
32. Carter P. Bispecific human IgG by design. J Immunol Methods. 2001;248(1-2):7-15.
33. Byrne H, Conroy PJ, Whisstock JC, O'Kennedy RJ. A tale of two specificities: bispecific antibodies for therapeutic and diagnostic applications. Trends Biotechnol. 2013;31(11):621-32.
34. Labrijn AF, Janmaat ML, Reichert JM, Parren PWHI. Bispecific antibodies: a mechanistic review of the pipeline. Nat Rev Drug Discov. 2019;18(8):585-608.
35. Yankelevich M, Thakur A, Modak S, Chu R, Taub J, Martin A, et al. Targeting refractory/recurrent neuroblastoma and osteosarcoma with anti-CD3×anti-GD2 bispecific antibody armed T cells. J Immunother Cancer. 2024;12(3):e008744.
36. Fadul CE, Thakur A, Kim J, Kassay-McAllister J, Schalk D, Lopes MB, et al. Phase I study targeting newly diagnosed grade 4 astrocytoma with bispecific antibody armed T cells (EGFR BATs) in combination with radiation and temozolomide. J Neurooncol. 2024;166(2):321-30.
37. Lum LG, Al-Kadhimi Z, Deol A, Kondadasula V, Schalk D,

Tomaszewski E, et al. Phase II clinical trial using anti-CD3 × anti-HER2 bispecific antibody armed activated T cells (HER2 BATs) consolidation therapy for HER2-negative (0-2+) metastatic breast cancer. J Immunother Cancer. 2021;9(6):e002194.
38. Vaishampayan UN, Thakur A, Chen W, Deol A, Patel M, Dobson K, et al. Phase II trial of pembrolizumab and anti-CD3 × anti-HER2 bispecific antibody armed activated T cells in metastatic castrate-resistant prostate cancer. Clin Cancer Res. 2023;29(1):122-32.
39. Lum LG, Thakur A, Choi M, Deol A, Kondadasula V, Schalk D, et al. Clinical and immune responses to anti-CD3 × anti-EGFR bispecific antibody armed activated T cells (EGFR BATs) in pancreatic cancer patients. Oncoimmunology. 2020;9(1):1773201.
40. Lum LG, Thakur A, Kondadasula SV, Al-Kadhimi Z, Deol A, Tomaszewski EN, et al. Targeting CD138-/CD20+ Clonogenic Myeloma Precursor Cells Decreases These Cells and Induces Transferable Antimyeloma Immunity. Biol Blood Marrow Transplant. 2016;22(5):869-78.
41. Goebeler ME, Bargou RC. Blinatumomab: a CD19/CD3 bispecific T cell engager (BiTE) with unique anti-tumor efficacy. Cancer Treat Rev. 2016;49:63-76.
42. Kantarjian H, Stein A, Gökbuget N, Fielding AK, Schuh AC, Ribera JM, et al. Blinatumomab versus chemotherapy for advanced acute lymphoblastic leukemia. N Engl J Med. 2017;376(9):836-47.
43. Jen EY, Xu Q, Schetter A, Przepiorka D, Shen YL, Roscoe D, et al. FDA approval: blinatumomab for patients with B-cell precursor acute lymphoblastic leukemia in morphologic remission with minimal residual disease. Clin Cancer Res. 2019;25(2):473-7.
44. U.S. Food and Drug Administration. FDA granted accelerated approval to blinatumomab (Blincyto, Amgen Inc.) for the treatment of adult and pediatric patients with B-cell precursor acute lymphoblastic leukemia. U.S. Food and Drug Administration; 2018.
45. Moreau P, Garfall AL, van de Donk NWCJ, Nahi H, San-Miguel J, Oriol A, et al. Teclistamab in relapsed or refractory multiple myeloma. N Engl J Med. 2022;387(6):495-505.
46. Lesokhin AM, Tomasson MH, Arnulf B, Mikhael JR, Minnema MC, Krishnan A, et al. Elranatamab in patients with relapsed or refractory multiple myeloma. Nat Med. 2023;29(9):2259-67.
47. Nathan P, Hassel JC, Rutkowski P, Baurain JF, Butler MO, Schlaak M, et al. Overall survival benefit with tebentafusp in metastatic uveal melanoma. N Engl J Med. 2021;385(13):1196-206.
48. Hassel JC, Piperno-Neumann S, Schankin C, Rutkowski P, Carvajal RD, Butler MO, et al. Three-year overall survival with tebentafusp in metastatic uveal melanoma. N Engl J Med. 2023;389(24):2256-66.
49. Luangwattananun P, Sangsuwannukul T, Supimon K, Thuwajit C, Chieochansin T, Sa-nguanraksa D, et al. Anti-PD-L1 × anti-CD3 bispecific T-cell engager-armed T cells can overcome immunosuppression and redirect T cells to kill breast cancer cells expressing PD-L1. Int Immunopharmacol. 2023;124:111012.
50. Supimon K, Sangsuwannukul T, Luangwattananun P, Yenchitsomanus PT. Enhanced cytotoxicity in multiple myeloma via T cells armed with bispecific T cell engager targeting B-cell maturation antigen on cancer cells and CD3 on T cells. Int Immunopharmacol. 2024;143(Pt 2):113480.
51. Songprakhon P, Luangwattananun P, Choomee K, Sawasdee N, Somboonpatarakun C, Chieochansin T, et al. CD138-targeted bispecific protein engager-armed T cells exhibit potent and selective cytotoxicity against multiple myeloma cells. Int Immunopharmacol. 2026;174:116295.
52. Suwanchiwasiri K, Somboonpatarakun C, Phanthaphol N, Yuti P, Chieochansin T, Junking M, et al. Bispecific T cell engager-armed T cells targeting integrin αvβ6 exhibit enhanced T cell redirection and antitumor activity in cholangiocarcinoma. Biomed Pharmacother. 2024;175:116718.
53. Dustin ML, Long EO. Cytotoxic immunological synapses. Immunol Rev. 2010;235(1):24-34.
54. Stinchcombe JC, Griffiths GM. Secretory mechanisms in cell-mediated cytotoxicity. Annu Rev Cell Dev Biol. 2007;23:495-517.
55. Huse M. Mechanical forces in the immune system. Nat Rev Immunol. 2017;17(11):679-90.
56. Dustin ML. The immunological synapse. Cancer Immunol Res. 2014;2(11):1023-33.
57. Voskoboinik I, Whisstock JC, Trapani JA. Perforin and granzymes: function, dysfunction and human pathology. Nat Rev Immunol. 2015;15(6):388-400.
58. Wathikthinnakon M, Sittithumcharee G, Chen S, Prasopporn S, Choomee K, Chieochansin T, et al. Gemcitabine and anti-PD-L1 × anti-CD3 bispecific T-cell engager synergistically enhance T-cell cytotoxicity against cholangiocarcinoma cells. Sci Rep. 2022;12(1):6154.
59. Sawasdee N, Songprakhon P, Luangwattananun P, Rujirachaivej P, Yuti P, Yenchitsomanus PT. Low-dose bortezomib enhances the cytotoxicity of anti-PD-L1 × anti-CD3 bispecific engager-armed T cells against multiple myeloma cells. Biomed Pharmacother. 2025;184:117878.
60. Wherry EJ, Kurachi M. Molecular and cellular insights into T cell exhaustion. Nat Rev Immunol. 2015;15(8):486-99.
61. Depil S, Duchateau P, Grupp SA, Mufti G, Poirot L. 'Off-the-shelf' allogeneic CAR T cells: development and challenges. Nat Rev Drug Discov. 2020;19(3):185-99.
62. Fesnak AD, June CH, Levine BL. Engineered T cells: the promise and challenges of cancer immunotherapy. Nat Rev Cancer. 2016;16(9):566-81.
63. Vivier E, Tomasello E, Baratin M, Walzer T, Ugolini S. Functions of natural killer cells. Nat Immunol. 2008;9(5):503-10.
64. Mackensen A, Müller F, Mougiakakos D, Böltz S, Wilhelm A, Aigner M, et al. Anti-CD19 CAR T cell therapy for refractory systemic lupus erythematosus. Nat Med. 2022;28(10):2124-32.
65. Vu T, Gwathmey K, Benatar M, Cutter G, Claussen G, Burns TM, et al. BCMA-directed mRNA CAR-T cell therapy for myasthenia gravis: a randomized, double-blind, placebo-controlled phase 2b trial. Nat Med. 2026 Jan 9. doi: 10.1038/s41591-025-04171-y.